

Washington University in St. Louis

Washington University Open Scholarship

Arts & Sciences Electronic Theses and
Dissertations

Arts & Sciences

Summer 8-15-2018

The Role of Mesenchymal Stromal Cells and Classical Dendritic Cells in the Maintenance and Regulation of the Bone Marrow Niche

Jingzhu Zhang

Washington University in St. Louis

Follow this and additional works at: https://openscholarship.wustl.edu/art_sci_etds



Part of the [Cell Biology Commons](#), [Genetics Commons](#), and the [Molecular Biology Commons](#)

Recommended Citation

Zhang, Jingzhu, "The Role of Mesenchymal Stromal Cells and Classical Dendritic Cells in the Maintenance and Regulation of the Bone Marrow Niche" (2018). *Arts & Sciences Electronic Theses and Dissertations*. 1664.

https://openscholarship.wustl.edu/art_sci_etds/1664

This Dissertation is brought to you for free and open access by the Arts & Sciences at Washington University Open Scholarship. It has been accepted for inclusion in Arts & Sciences Electronic Theses and Dissertations by an authorized administrator of Washington University Open Scholarship. For more information, please contact digital@wumail.wustl.edu.

WASHINGTON UNIVERSITY IN ST. LOUIS

Division of Biology and Biomedical Sciences
Molecular Genetics and Genomics

Dissertation Examination Committee:

Daniel Link, Chair

Grant Challen

Roberto Civitelli

Timothy Ley

Fanxin Long

Joshua Rubin

The Role of Mesenchymal Stromal Cells and Classical Dendritic Cells in the Maintenance and Regulation of the Bone Marrow Niche

By

Jingzhu Zhang

A dissertation presented to
The Graduate School
of Washington University in
partial fulfillment of the
requirements for the degree
of Doctor of Philosophy

August 2018
St. Louis, Missouri

© 2018, Jingzhu Zhang

TABLE OF CONTENTS

LIST OF FIGURES.....	vi
LIST OF TABLES.....	vii
ACKNOWLEDGEMENTS.....	viii
ABSTRACT.....	xi
CHAPTER 1: INTRODUCTION TO THE BONE MARROW NICHE, MESENCHYMAL STROMAL CELLS AND CLASSICAL DENDRITIC CELLS..	1
1.1. Components of the Bone Marrow Niche.....	5
1.1.1. Mesenchymal stem cells.....	5
1.1.2. Endothelial cells.....	6
1.1.3. Osteoblast lineage cells.....	7
1.1.4. Megakaryocytes.....	9
1.1.5. Macrophages.....	10
1.1.6. The sympathetic nervous system.....	12
1.2. Mesenchymal Stromal Cells.....	13
1.2.1. CAR cells.....	13
1.2.2. LepR ⁺ cells.....	15
1.2.3. Nestin-GFP ⁺ cells.....	15
1.3. B Lymphopoiesis.....	17
1.3.1. CXCL12.....	17
1.3.2. Memory plasma cells.....	19
1.3.3. Memory B cells.....	20
1.4. Dendritic Cells.....	22
1.4.1. cDC1.....	22
1.4.2. cDC2.....	23
1.4.3. pDC.....	25
1.5. Summary.....	26
CHAPTER 2: TARGETING OF MESENCHYMAL STROMAL CELLS BY CRE- RECOMBINASE TRANSGENES COMMONLY USED TO TARGET OSTEOBLAST LINEAGE CELLS.....	28
2.1. Introduction.....	28
2.2. Materials and Methods.....	29

2.2.1. Mouse strains.....	29
2.2.2. Flow cytometry.....	30
2.2.3. Immunostaining of bone sections.....	30
2.2.4. RNA expression profiling.....	32
2.2.5. Statistical analyses.....	32
2.3. Results.....	32
2.3.1. <i>Ocn-Cre</i> targets osteoblasts, a majority of CAR cells, and arteriolar pericytes.....	32
2.3.2. <i>Dmpl-Cre</i> targets osteoblasts and a subset of CAR cells.....	33
2.3.3. <i>Tagln-Cre</i> targets osteoblasts, a majority of CAR cells, and both arteriolar and venous sinusoidal pericytes.....	34
2.4. Discussion.....	35
2.5. Acknowledgements.....	37
2.6. Authorships Contributions.....	38
2.7. Figures.....	39
2.8. Supplementary Figures.....	45
2.9. Supplementary Table.....	52

CHAPTER 3: CXCL12 FROM *OCN-CRE* TARGETED BONE MARROW STROMAL CELLS REGULATES LATE-STAGE B CELL DEVELOPMENT.....53

3.1. Introduction.....	53
3.2. Materials and Methods.....	54
3.2.1. Mouse strains.....	54
3.2.2. Immunostaining of bone sections.....	55
3.2.3. Flow cytometry.....	55
3.2.4. Quantitative real-time PCR.....	56
3.2.5. Mature B cell homing assay.....	57
3.2.6. Primary and secondary immunization.....	57
3.2.7. Enzyme-linked immunosorbent assay (ELISA).....	57
3.2.8. Statistical analyses.....	58
3.3. Results.....	59
3.3.1. <i>Ocn-Cre</i> targeted stromal cells regulate mature naive B cells in the bone marrow...	59
3.3.2. CXCL12 expression in <i>Ocn-Cre</i> targeted stromal cells regulates the homing and/or retention of mature naive B cells in the bone marrow.....	60
3.3.3. Ablation of CXCL12 in <i>Ocn-Cre</i> targeted stromal cells did not affect bone marrow plasma cells and primary immune response.....	61
3.3.4. Ablation of CXCL12 in <i>Ocn-Cre</i> targeted stromal cells reduces the number of memory B cells in the bone marrow.....	62
3.4. Discussion.....	63
3.5. Acknowledgements.....	65

3.6. Authorships Contributions.....	65
3.7. Figures.....	66

**CHAPTER 4: CLASSICAL DENDERITIC CELLS IN BONE MARROW
REGULATE HEMATOPOIETIC STEM AND PROGENITOR CELL
TRAFFICKING THROUGH CXCR2 SIGNALING IN SINUSOIDAL
ENDOTHELIAL CELLS.....73**

4.1. Introduction.....	73
4.2. Materials and Methods.....	74
4.2.1. Mouse strains.....	74
4.2.2. Generation of bone marrow chimeras.....	74
4.2.3. Diphtheria toxin administration.....	75
4.2.4. CFU-C assays.....	75
4.2.5. Flow cytometry.....	75
4.2.6. Immunostaining of bone sections.....	76
4.2.7. Real-time quantitative RT-PCR.....	77
4.2.8. RNA expression profiling.....	77
4.2.9. In vitro permeability test and cell migration assay.....	77
4.2.10. Statistical analyses.....	78
4.3. Results.....	79
4.3.1. Classical dendritic cells (cDCs) are enriched in the perivascular region and may be functionally specific for the perivascular niche.....	79
4.3.2. BM cDC ablation induces a loss of macrophage and HSPC mobilization.....	81
4.3.3. BM cDC ablation affects bone marrow vascular endothelial cells.....	83
4.3.4. BM cDC ablation activates sinusoidal endothelial cells and sinusoidal CXCR2 Signaling.....	84
4.3.5. CXCR2 signaling pathway is important for BM cDC ablation induced HSPC Mobilization.....	85
4.4. Summary.....	87
4.5. Acknowledgements.....	88
4.6. Authorships Contributions.....	88
4.7. Figures.....	89
4.8. Supplemental Figures.....	98

CHAPTER 5: SUMMARY AND FUTURE DIRECTIONS.....102

5.1. Targeting mesenchymal stromal cells with different Cre-recombinase transgenes.....	103
5.1.1. Summary.....	103
5.1.2. Are <i>Dmp1-Cre</i> targeted stromal cells truly enriched for osteoprogenitors?.....	103

5.1.3. Further characterize the heterogeneity of CAR cells.....	104
5.2. CXCL12 from <i>Ocn-Cre</i> targeted mesenchymal stromal cells regulates late-stage B cell Development.....	105
5.2.1. Summary.....	105
5.2.2. Functionally characterize the role of bone marrow memory B cells in the regulation of humoral immunity.....	106
5.2.3. How does CXCL12 ablation in <i>Ocn-Cre</i> targeted stromal cells affect other cells in the bone marrow?.....	106
5.2.4. Do <i>Ocn-Cre</i> targeted stromal cells regulate mature naive B cells and memory B cells through other pathways?.....	107
5.3. Bone marrow cDCs regulate hematopoietic stem and progenitor cell trafficking.....	109
5.3.1. Summary.....	109
5.3.2. Further assess the role of CXCR2 in endothelial cells.....	110
5.3.3. How do BM cDCs regulate sinusoidal endothelial cells?.....	110
5.3.4. How do BM cDCs regulate BM macrophages?.....	111
5.3.5. Assess the effects of BM cDC ablation on osteoblasts.....	112
5.4. Conclusion.....	114
5.5. Figures.....	116
REFERENCE.....	120

LIST OF FIGURES

Figure 2.1. <i>Ocn-Cre</i> targets osteoblasts and a majority of CAR cells.....	39
Figure 2.2. <i>Ocn-Cre</i> targets the majority of arteriolar pericytes.....	40
Figure 2.3. <i>Dmp1-Cre</i> targets all the osteoblasts and a subset of CAR cells but no arteriolar pericytes.....	41
Figure 2.4. <i>Tagln-Cre</i> targets osteoblasts, a majority of CAR cells, and both venous sinusoidal and arteriolar pericytes.....	43
Supplementary Figure 2.1. Osteoblasts remain attached to bone following centrifugation of femurs.....	45
Supplementary Figure 2.2. <i>Ocn-Cre</i> efficiently targets osteoblasts.....	46
Supplementary Figure 2.3. Immunostaining of <i>Ocn-Cre Cxcl12^{gfp/+}</i> bone sections.....	47
Supplementary Figure 2.4. <i>Dmp1-Cre</i> efficiently targets osteoblasts.....	48
Supplementary Figure 2.5. Distribution of <i>Dmp1-Cre</i> targeted CAR cells.....	49
Supplementary Figure 2.6. RNA expression profiling of <i>Dmp1-Cre</i> targeted CAR cells.....	50
Supplementary Figure 2.7. <i>Tagln-Cre</i> efficiently targets osteoblasts.....	51
Figure 3.1 CXCL12 expression by stromal cells is important for B lymphopoiesis.....	66
Figure 3.2. CXCL12 expression in <i>Ocn-Cre</i> targeted stromal cells is important for the regulation of mature naive B cells.....	68
Figure 3.3. CXCL12 expression in <i>Ocn-Cre</i> targeted stromal cells regulates the homing and/or retention of mature naive B cells in the bone marrow.....	69
Figure 3.4. Ablation of CXCL12 in <i>Ocn-Cre</i> targeted stromal cells had no effects on plasma cells (PCs) and primary immune response.....	70
Figure 3.5. Ablation of CXCL12 in <i>Ocn-Cre</i> targeted stromal cells reduces the number of memory B cells in the bone marrow.....	71
Figure 4.1. Classical dendritic cells (cDCs) are enriched in the perivascular region and may be functionally specific for the perivascular niche.....	89
Figure 4.2. BM cDC ablation induces a loss of macrophage and HSPC mobilization.....	91
Figure 4.3. Ablation of BM cDCs affects bone marrow vascular endothelial cells (VECs).....	93
Figure 4.4. Ablation of BM cDCs activates sinusoidal endothelial cells and sinusoidal CXCR2 signaling.....	95

Figure 4.5. CXCR2 signaling pathway is important for BM cDC ablation induced HSPC mobilization.....	96
Supplemental Figure 4.1. BM cDC ablation induces a loss of macrophage and HSPC mobilization.....	98
Supplemental Figure 4.2. Ablation of BM cDCs activated sinusoidal endothelial cells and sinusoidal CXCR2 signaling.....	99
Supplemental Figure 4.3. CXCR2 signaling pathway is important for BM cDC ablation induced HSPC mobilization.....	101
Figure 5.1. CXCL12 expression in <i>Ocn-Cre</i> targeted stromal cells is important for the regulation of T cells.....	116
Figure 5.2. The effects of BM cDC ablation on bone marrow stromal cells (BMSCs).....	117
Figure 5.3. The effects of BM cDC ablation on osteoblasts.....	118

LIST OF TABLES

Supplementary Table 2.1. Primers for genotyping transgenic mice in this study.....	52
--	----

Acknowledgements

I would most like to acknowledge my mentor, Dr. Daniel Link, who has taught me how to conduct scientific research independently and more importantly set an extraordinary example of how to become a meticulous, rigorous and creative scientist. Dr. Link demonstrates great responsibility as a mentor. As a well-established principal investigator, Dr. Link tries really hard to make himself available for his trainees, despite his busy schedule. Instead of simply providing answers and telling his trainees what to do, he always encourages us to explore more deeply and independently about why and how, and sometimes challenges us with more thought-provoking and inspiring questions and suggestions. In addition, Dr. Link provides the freedom and flexibility for his trainees to design their own studies and to propose alternative experiments, and shows understanding at times of us making mistakes. Additionally, Dr. Link is very cordial and dispassionate, always trying to provide a collaborative, equal and pleasant research environment for his trainees, colleagues, collaborators and even competitors. What I respect the most of Dr. Link is his rigor and creativity in science, which will always guide, motivate and inspire me in my future career.

I would also like to thank the other members of the Link lab. Each and every one of them is an indispensable part of this greatly supportive, enjoyable and stimulating work environment. I sincerely appreciate them for kindly sharing their knowledge, giving advice and generously providing helpful extra pairs of hands when needed. Our lab manager, Amy Schmidt, always keeps the lab well-maintained and organized, which makes all the great ideas and executions possible in the first place. Jackie Tucker-Davis, staff in our animal facility, has made my work much easier with her conscientious management. Grazia Abou Ezzi, who sits beside me, has provided tremendous assistance and support to my projects, sharing knowledge about new

techniques and together brainstorming solutions to technical obstacles. More importantly, her wonderful whimsical sense of humor has made our lab an enjoyable workplace. Joseph Krambs has helped me analyze RNA microarray and sequencing data. My undergraduate trainee, Rachel Ye, has provided me with a pair of valuable and supportive hands, without which I could hardly achieve such efficient progress. Other members, including Jun Xia, Juo Chin (Robin) Yao, Terrence Wong, Wayne Warner and Megan Gauthier, although not directly involved in my projects, have all been generously helpful whenever I sought their help or advice. In addition, my appreciation also goes to previous members of the Link lab, including Ryan Day, my rotation mentor, Tim Supakorndej, and Bryan Antony, who contributed to developing necessary techniques and initiating my projects.

I would like to acknowledge my thesis committee members: Dr. Timothy Ley, who served as the chair of my thesis committee, Dr. Grant Challen, Dr. Fanxin Long, Dr. Roberto Civitelli and Dr. Joshua Rubin. I really appreciate their time and effort participating in my thesis committee, and for guiding me through my graduate study. I would also like to acknowledge Dr. John Dipersio and his staff, Dr. Darja Karpova and Dr. Mike Rettig, for their generous help and collaboration on my CXCR2 project. Dr. Laura Schuettpelz taught me how to analyze Genechip microarray data. Moreover, Dr. Deepta Bhattacharya and his postdoc, Dr. Arijita Jash, coached me on how to use the immunization method to generate memory B cells. Other faculty, staff and students on the 6th and 7th floors of the Southwest Tower and the members of our Monday lab meeting generously shared their equipment and materials, and provided valuable feedback at our regular meetings and journal clubs.

My thanks also go to the members of the Flow Cytometry Core at the Siteman Cancer Center for their help with my projects. Bill Eades, the director of the Flow Cytometry Core,

helped me understand flow cytometry and solved questions and challenges in my projects with his expertise. Angie Schrader of the RCAVS Microscopy and Digital Imaging Core provided support for confocal imaging. I would also like to thank my program, the Molecular Genetic and Genomics program in the Department of Biology and Biomedical Science. Melanie Relich, the program coordinator, and Dr. Jim Skeath, the program director, have been encouragingly supportive through my graduate study, especially during the critical moment when I was switching my thesis lab.

Very importantly, I would like to thank my family, who provided unconditionally support through my graduate study both emotionally and financially. Without them, I would not be able to acquire superior education in the United States. Besides my family, I also appreciate my friends in St. Louis for their help and company. Dongdong (Nathan) Han, in particular, helped me proofread my writings and provided constructive advice. Finally, I would like to thank my girlfriend, Li (Christina) Xu, for lightening up my life with her love, and for giving me the courage to face any challenges in my future career.

Jingzhu Zhang

Washington University

August 2018

ABSTRACT OF THE DISSERTATION

The Role of Mesenchymal Stromal Cells and Classical Dendritic Cells in the Maintenance and Regulation of the Bone Marrow Niche

by

Jingzhu Zhang

Doctor of Philosophy in Biology & Biomedical Sciences

Molecular Genetics and Genomics

Washington University in St. Louis, 2018

Professor Daniel Link, Chairperson

The bone marrow niche is an important microenvironment for the regulation of normal and malignant hematopoiesis. The first discovered niche component is mesenchymal stromal cells, which are the major source for the production and secretion of multiple niche factors. Mesenchymal stromal cells are heterogeneous and various transgenes have been used to target non-identical but overlapping subpopulations. To further characterize the heterogeneity of mesenchymal stromal cells, we tested the targeting specificity of three tissue-specific *Cre*-recombinase transgenes. We show that in addition to osteoblasts, *Ocn-Cre* targets a majority of Cxcl12-abundant reticular (CAR) cells and arteriolar pericytes. Surprisingly, *Dmp1-Cre* also targets a subset of CAR cells, in which expression of osteoblast-lineage genes is enriched. Moreover, a new tissue-specific *Cre*-recombinase, *Tagln-Cre* efficiently targets osteoblasts, a majority of CAR cells, and both venous sinusoidal and arteriolar pericytes. These observations

highlight the heterogeneity of mesenchymal stromal cells in the bone marrow and provide tools to interrogate this heterogeneity. To further analyze the functional heterogeneity of mesenchymal stromal cells, we assessed the function of CXCL12 from different subsets of mesenchymal stromal cells on B lymphopoiesis. We show that CXCL12 from *Ocn-Cre* targeted stromal cells is particularly important for the regulation of mature naive B cells and memory B cells, potentially through the regulation of their homing and/or retention. This suggests that B cell development requires distinct niches at different stages and *Ocn-Cre* targeted stromal cells may represent a specific niche for late-stage B cell development. Besides mesenchymal stromal cells, this thesis also assesses the function of a recently identified resident population of murine bone marrow classical dendritic cells (BM cDCs). We show that BM cDC ablation results in a secondary, non-cell autonomous loss of BM macrophages. And more importantly, BM cDCs regulate hematopoietic progenitor and stem cell (HSPC) trafficking through a macrophage independent pathway, at least in part, through its regulation of sinusoidal CXCR2 signaling and vascular permeability. These findings suggest BM cDCs may serve as a novel bone marrow niche component regulating HSPCs. Collectively, this thesis improves on the overall understanding of the bone marrow niche and provides insights with significant relevance to both basic and clinical research.

CHAPTER 1: INTRODUCTION TO THE BONE MARROW NICHE, MESENCHYMAL STROMAL CELLS AND CLASSICAL DENDRITIC CELLS

Hematopoiesis refers to the production of mature blood cells from hematopoietic stem cells (HSCs) in the bone marrow, which is tightly regulated by both intra- and extra-cellular signals. Hematopoietic differentiation proceeds through a hierarchical order. Uncommitted and quiescent HSCs may give rise to proliferative multipotent progenitors, which in turn differentiate into more restricted progenitors for the production of different hematopoietic lineages^{1,2}. Hematopoietic differentiation and proliferation are regulated by the bone marrow microenvironment or niche, which includes different types of niche cells, extracellular matrix, and secreted niche factors³⁻⁷. The concept of the niche was first hypothesized by Ray Schofield in 1978, where he proposed that a specialized bone marrow niche preserved the ability for stem cells to reconstitute the bone marrow⁸. Later, Michael Dexter showed that mesenchymal stromal cell enriched cultures could maintain primitive hematopoietic cells *ex vivo*⁹. Since then, extensive works have been done on the bone marrow niche, and recent studies have identified multiple niches to regulate different hematopoietic lineages or different stages during hematopoietic development¹⁰⁻¹³. Abnormal hematopoiesis has been associated with multiple diseases, including anemia, blood cancers, hemorrhagic disorders, infection-related diseases, and immune system regulation-related diseases¹⁴⁻¹⁷. Thus, it is important to study the components and functions of the bone marrow niche for its regulation of normal and abnormal hematopoiesis. Better understanding of the bone marrow niche will likely improve our knowledge about the initiation and progression of different diseases, and may advance the development of more effective treatments.

Prior studies on the bone marrow niche have identified multiple major niche components, including mesenchymal stem cells, endothelial cells, osteoblast lineage cells, megakaryocytes,

macrophages, the sympathetic nervous system, and the main focus of our lab, mesenchymal stromal cells^{4-7,10,12,13}. Although these components have been shown to regulate the development and maintenance of hematopoietic progenitor and stem cells (HSPCs), the regulatory mechanisms and the molecular pathways involved are not fully understood. Mesenchymal stromal cells are mainly found in the perivascular region, thus also referred to as perivascular stromal cells, and are the earliest niche component discovered^{3,9,10,12,18,19}. These stromal cells are the major source for the production and secretion of multiple niche factors, such as stromal derived factor-1 (SDF-1 or CXCL12) and stem cell factors (SCF or Kit ligand)^{3,10,11}. Mesenchymal stromal cells are heterogeneous and various markers have been used to characterize non-identical but overlapping subpopulations, including CXCL12 abundant reticular (CAR) cells, leptin receptor expressing (LepR⁺) cells, and Nestin-GFP⁺ cells^{3,10,20,21}. Collectively, these stromal cells are critical for maintaining quiescence and promoting proliferation of HSPCs, so it is important to further characterize its subpopulations for their potential specific functions and roles in the bone marrow niche.

B cells are an important component of the adaptive immune system whose functions include antigen presentation and secretion of cytokines and antibodies²². In mammals, B cells mature in the bone marrow, but also require input from peripheral lymphoid organs²³. B cells develop through a series of different stages which can be identified based on their surface marker expression²⁴. In the bone marrow, the common lymphoid progenitor (CLP) gives rise to the B lymphoid progenitor (BLP)²⁵. Dr. Hardy and colleagues have defined the later stages of B cell development using Hardy Fractions, referred as Fractions A through F^{26,27}. Pre-pro-B cells are defined as Fraction A cells, which are derived from BLPs and retain most gene expressions of germline immunoglobulin⁴³. Rearrangement of the heavy chain of immunoglobulin (IgH) starts

in early pro-B cells, or Fraction B cells, and is completed in late pro-B cells, or Fraction C cells⁴³. They then express pre-B cell receptor (pre-BCR), which leads to recombination of the immunoglobulin light chain, and these cells are defined as Fraction D cells, or pre-B cells^{26,27}. After light chain rearrangement, these cells are known as Fraction E cells, or immature B cells, and they express IgM on the surface⁴⁴. Most immature B cells enter the blood and migrate to the spleen for maturation into mature naive B cells, or Fraction F cells, expressing both IgM and IgD^{26,28-30}. Meanwhile, some immature B cells may mature in the bone marrow³¹. When exposed to recognized antigens, mature naive B cells further mature in the periphery to become anti-body secreting plasma cells or memory cells^{29,30,32}. Memory cells may include memory plasma cells and memory B cells, and studies have suggested the bone marrow as a potential microenvironment for their maintenance³²⁻³⁶. However, it remains unclear how these cells affect immune memory and how they are regulated in the bone marrow, which requires further research.

Dendritic cells (DCs) are found in different tissues with great heterogeneity and functional variations³⁷⁻³⁹. Classical or conventional DCs (cDCs) are generally defined as cells with dendritic morphology and outstanding capacity for presenting antigens and priming T cells^{40,41}. cDCs can be further divided into two subsets, type 1 cDCs (cDC1s) and type 2 cDCs (cDC2s). cDC1s are mainly responsible for immune responses against viruses, tumors and intracellular pathogens. cDC2s are mainly responsible for immune responses against parasites, allergens, extracellular bacteria, fungi and some intracellular pathogens⁴². Besides cDCs, studies have also discovered plasmacytoid DCs (pDCs), which are lymphocyte-like cells specialized in the production of type I interferons^{40,43}. DCs have a myeloid origin and their development consists of a branch of hematopoiesis that is different from lymphoid and granulocytic myeloid cell differentiation⁴⁴. A

cell population of clonogenic common DC progenitors (CDP) has been discovered in the bone marrow (BM), which may differentiate into both cDCs and pDCs^{45,46}. Although cDCs mature in the peripheral lymphoid organs, clonogenic cDC-restricted progenitors (pre-DCs) have been found in the spleen (Sp), BM and other tissues^{47,48}, suggesting the capability of cDCs to self-renew in their resident tissues. Recent studies have shown that BM cDCs mostly reside in the BM perivascular region, regulating B cells and neutrophils in the bone marrow⁴⁹⁻⁵¹, although it remains unknown whether BM cDCs may regulate HSPCs. BM cDCs and BM macrophages are both mononuclear phagocytes with a common myeloid origin, and recent studies have suggested BM macrophages may be important for the regulation of HSPCs^{7,52,53}. Thus, it would be interesting to test whether BM cDCs may function as a novel bone marrow niche component to regulate HSPCs.

1.1. Components of the Bone Marrow Niche

1.1.1. Mesenchymal stem cells

Mesenchymal stem cells (MSCs) are multipotent stromal cells with the capability to differentiate into osteogenic lineage cells, chondrocytes, and adipocytes⁴. To identify MSCs, *in vitro* colony forming assays can be performed to test whether the cells of interest may form all three lineages. However, a prior study has identified a population of proliferative osteoblastic progenitors, MX-1 positive bone marrow stromal cells, which could differentiate into osteolineage cells, chondrocytes, and adipocytes *in vitro* yet only differentiate into osteoblasts *in vivo*⁵⁴. Other studies have proposed various markers to identify MSCs in mouse bone marrow, including platelet-derived growth factor receptor-alpha and -beta (PDGFR α and PDGFR β), CD51, Sca1 and alpha smooth muscle actin⁵⁵⁻⁵⁸. But until now, no precise and universal definition of MSCs exists due to a lack of consensus in defining markers⁴. Recent studies have identified Nestin-GFP⁺ cells that are enriched for MSC activity and express high levels of key niche factors, such as SCF, CXCL12, PDGFR α , and fibroblast activation protein (FAP)^{58,59}. Follow-up studies showed that HSCs localize near Nestin-GFP⁺ cells, and ablation of Nestin-GFP⁺ cells leads to bone marrow hypocellularity, anemia, and depletion of osteogenic cells^{60,61}. Our lab and others have discovered that the *Prx1-Cre* targeted PDGFR α ⁺ Sca1⁺ (PaS) cells are highly enriched for MSCs³. To our surprise, these *Prx1-Cre* targeted PaS cells did not express nestin, one possible explanation being that Nestin-GFP transgene does not accurately reflect the nestin expression *in vivo*³. Despite the recent research emphasis, the complex population heterogeneity remains an obstacle for precisely defining the MSC population and studying them in greater detail.

1.1.2. Endothelial cells

HSPCs preferentially localize to the perivascular regions in the bone marrow^{4,5,62}. Prior studies have shown that BM endothelial cells (ECs) promote HSPC maintenance, and sinusoidal endothelial cells promote long-term HSC reconstituting capability^{10,63-66}. In addition, BM ECs have been illustrated to release soluble niche factors, referred as angiocrine function⁶⁷. CXCL12 and SCF are important niche factors that have been widely investigated in the regulation of HSPCs in the bone marrow^{10,68-70}. A recent study shows that deletion of *Kitl* in ECs results in decreased HSC numbers and reduces the repopulating capability of HSCs after bone marrow transplantation¹⁰. In contrast, later studies using similar models to delete CXCL12 in BM ECs show minimal decrease in HSPCs and only a modest loss of long-term repopulating capacity of HSCs after transplantation^{3,11}. Other than secreted niche factors, an EC-specific adhesion molecule, E-selectin, is shown to activate HSC proliferation⁷¹. More recent data suggests that activation of endothelial CXCR2 by Gro- β (CXCL2) could induce bone marrow vascular permeability and promote HSPC mobilization⁷². Another recent study showed that activation of Notch signaling in ECs results in the up-regulation of cellular SCF level and the expansion of PDGFR β ⁺ perivascular mesenchymal cells⁷³. Collectively, these studies provide evidences to implicate BM ECs as an important component of the bone marrow niche.

BM ECs are heterogeneous, and prior studies have revealed different types of ECs in the bone marrow⁷⁴. Sinusoidal capillaries, highly branched small vessels found throughout the marrow cavity, are the most abundant blood vessels in the bone marrow⁷⁴. Sinusoidal ECs express vascular endothelial cadherin (VEcad) and vascular endothelial growth factor receptor-3 (VEGFR3), and are laminin⁺ or low Sca-1⁻ or low, while arteriolar ECs are mainly laminin⁺ Sca-1⁺ VEcad⁺ Vegfr-3⁻^{75,76}. A recent study on the murine postnatal development reveals a novel

subtype of blood vessel, type H vessel. These blood vessels express higher levels of endomucin (Emcn) and CD31 (Pecam1) compared to sinusoidal vessels, and are found in more proliferative regions of the bone marrow^{77,78}. Distinct bone marrow niches have been proposed around both arteriolar and sinusoidal vessels^{12,13,18,79}. The arteriolar niche consists of arteriolar ECs and Nestin-GFP^{high} NG2^{high} mesenchymal stromal cells, which are demonstrated to maintain HSC quiescence¹². Arteriolar vessels are less permeable compared to sinusoidal vessels and were shown to maintain a low level of reactive oxygen species (ROS) in HSCs, while sinusoidal vessels were shown to be important for regulating HSC trafficking and homing^{73,79}. In comparison, the sinusoidal niche consisting of sinusoidal ECs and LepR⁺ (leptin receptor) mesenchymal stromal cells, was illustrated to regulate both quiescent HSCs and more proliferative progenitor cells¹⁸. So far, it remains unclear whether quiescent HSCs are regulated by the arteriolar or sinusoidal niche, and it is also possible that both niches may play important roles to maintain quiescent HSCs. Although the existence and the exact function of arteriolar and sinusoidal niches are still controversial, it is clear that BM ECs and their surrounding perivascular niches are critical for the maintenance and development of HSPCs.

1.1.3. Osteoblast lineage cells

Osteoblast lineage cells include osteoblasts, osteocytes and osteoblastic progenitors^{19,80}. Osteoblasts produce bone matrix proteins and have the potential to differentiate into osteocytes⁸¹. Osteocytes are abundant in bones and are important for bone remodeling, regulating both osteoblast and osteoclast functions^{81,82}. Osteoblastic progenitors or immature osteoblasts are bone marrow stromal cells that are likely to differentiate into mature

osteoblasts¹⁹. A recent study showed that transgenic mouse models used previously to study osteoblasts or osteocytes in fact target other osteoblast lineage cells or mesenchymal stromal cells¹⁹. Thus, it would be more accurate to discuss the roles and functions of osteoblast lineage cells, instead of each individual, in the bone marrow niche.

Early studies done by Taichman and colleagues show that osteoblast lineage cells support hematopoietic development and HSC maintenance^{83,84}. Later experiments show that osteoblast lineage cells are necessary for normal hematopoiesis and HSC activities^{85,86}. In addition, activation of osteoblast lineage cells has been shown to promote the expansion of phenotypic and functional HSCs *in vivo*^{21,87-89}. However, another study suggests that the expansion of osteoblasts is not sufficient to increase HSC number⁹⁰. Moreover, a later study shows that defects in osteoblast function in a murine inflammatory arthritis model are insufficient to impair HSCs⁹¹. While the roles and functions of osteoblast lineage cells on HSPCs remain controversial, recent study suggests that they may play more important roles for the regulation of lymphoid progenitors, but not HSPCs¹¹. The differences among these studies may be caused by the heterogeneity of osteoblast lineage cells, and that different subsets may play different roles in hematopoiesis⁹². For example, immature osteoblasts marked by high expression of a transcription factor, *Runx2*, may have a greater potential in HSC maintenance and enhancement⁹³. In contrast, mature osteoblasts and osteocytes that are activated by constitutive parathyroid hormone (PTH) signaling have a decreased ability to support HSCs, compared to immature osteoblasts⁹³. Since the common transgenic models used for studying osteoblast lineage cells lack specificity for a certain cell subset¹⁹, it is necessary to develop better markers or models to further dissect this heterogeneous population and to more accurately study its function.

1.1.4. Megakaryocytes

Megakaryocytes (MKs) are hematopoietic lineage cells recognized by their unique morphology, especially their large size⁹⁴⁻⁹⁶. MKs have been reported to mainly reside in proximity to bone marrow sinusoids during hematopoietic homeostasis⁹⁷. Interestingly, after irradiation, MKs may relocate from the central marrow space to the endosteal surface⁹⁸. The same study shows that MKs promote the expansion of the endosteal niche through its production and release of platelet-derived growth factor-BB (PDGF-BB), thus to increase HSC engraftment after irradiation⁹⁸. In fact, one major function of MKs is to release different soluble factors in the bone marrow⁹⁹. MKs are the main source of thrombopoietin (TPO) which is important for the maintenance of quiescent HSCs, and depletion of MKs results in a decrease of intra-BM TPO concentration and a decrease in HSC number^{100,101}. In addition, MKs are the main source of platelet factor 4 (PF4 or CXCL4) in the bone marrow that regulates the cell cycle activity to maintain HSC quiescence¹⁰². In contrast, another group has reported an *in vitro* study in which MKs release insulin-like growth factor-1 and insulin-like growth factor binding protein-3 to increase HSC proliferation¹⁰³. To explain the dual functions of MKs for both maintaining HSC quiescence and promoting HSC proliferation, Li's group reported that MKs are the main source of transforming growth factor β 1 (TGF- β 1) and fibroblast growth factor-1 (FGF1). While TGF- β 1 regulates the quiescence of HSCs during homeostatic conditions, MKs switch to promote HSC expansion by releasing FGF1 under chemotherapeutic stress⁶. Collectively, prior studies have demonstrated that MKs release different soluble niche factors under homeostatic and stressful conditions, and they serve as an important bone marrow niche component to regulate both quiescence and proliferation of HSCs.

1.1.5. Macrophages

Macrophages are professional phagocytic cells with great heterogeneity, found in both lymphoid and non-lymphoid tissues^{38,44,104}. Most macrophages are capable of engulfing and degrading large particles, which allow them to clear foreign and damaged cells^{23,88,105}.

Macrophages are equipped with a broad-range of pattern-recognition receptors (PRRs), which are required for engulfing cellular debris and pathogenic particles that leads to the production of inflammatory or immunosuppressive cytokines^{38,44,104,106}. Macrophages are also highly plastic and can shift their physiology rapidly in response to injury or infection^{104,107}. The phenotypes and functions of macrophages are largely dependent on the surrounding microenvironment¹⁰⁴.

In general, macrophages can be simply classified into two different types: classically activated, or M1, macrophages (CAMs), and alternatively activated, or M2, macrophages (AAMs)¹⁰⁸.

CAMs are more specialized for antigen presentation, production of nitric oxide (NO), secretion of chemokines and cytokines, and promoting T-helper 1 (Th1) lymphocytes expansion^{104,107,108}.

Therefore, CAMs play a critical role in the defense against bacteria, although their defense mechanisms may also damage the host^{104,108}. In contrast, AAMs are involved in the defense against parasites and fungi^{109,110}. AAMs express large amounts of cytosolic arginase and

extracellular matrix related proteins, allowing them to regulate inflammation and promote tissue repair, thus they are also referred to as wound-healing macrophages^{107,109-111}.

Additionally, unique subsets of resident macrophages exist in different tissues, such as brain microglia, lung alveolar macrophages, and liver Kupffer cells^{107,109}. Early studies have suggested that most resident macrophages are derived from circulating monocytes with bone marrow origin^{38,104,105,112,113}. However, recent studies provide clear evidence that resident

macrophages can proliferate locally in both steady state and stressful conditions, and it remains

to be determined whether circulating monocytic precursors or self-renewal is more important for resident macrophage homeostasis^{105,114,115}. Meanwhile, resident macrophages may also be classified into CAMs or AAMs, although their response to a given stimulus can be different from regular CAMs or AAMs^{116,117}.

Bone marrow macrophages were first discovered in 1958 by ultrastructural study, which serve as the central component for the erythroblastic island, surrounded by erythroblasts at different stages of maturation^{118,119,120}. Erythroblastic island macrophages (EIMs) are essential for the maturation and survival of erythroblasts¹¹⁹. EIMs produce principal growth factors to regulate erythropoiesis, such as erythropoietin (EPO)¹²¹⁻¹²³, insulin-like growth factor-1 (IGF1)^{124,125} and bone morphogenetic protein-4 (BMP4)¹²⁶. EIMs also contribute to the synthesis of hemoglobin by incorporating iron into ferritin¹²⁷. Moreover, EIMs aid in the enucleation process by phagocytosis and degradation of extruded nuclei^{128,129}. Another subset of BM macrophages resides in the endosteal niche and is referred as osteomacs^{119,130}. On resting bone surfaces, bone lining cells are interspersed by osteomacs, which are in direct contact with the bone surface^{119,131}. Osteomacs play an important role in osteoblast formation and maturation^{103,115}, and can express a wide array of pro-anabolic molecules that are essential for parathyroid hormone anabolic actions¹³². Osteomacs may also contribute to injury response and tissue regeneration through production of growth factors, inflammatory cytokines and chemokines^{133,134}.

In addition, recent studies reveal that macrophages also localize to the bone marrow hematopoietic niche and may support other bone marrow niche components *in vitro*^{52,131,135}. Prior studies have used different *in vivo* macrophage depletion models to assess their function and have shown that macrophage depletion results in the suppression of osteoblast lineage

cells, reduced expression of important niche factors, HSPC mobilization and marked decrease of erythroblasts^{7,52,53,131}. In these studies, macrophages regulate HSPCs indirectly through regulation of osteoblast lineage cells and Nestin⁺ mesenchymal stem cells^{7,135}. Interestingly, a more recent study suggests that these macrophages may also regulate HSPCs directly, as CD234 on macrophages stabilizes CD82 on long term (LT)-HSCs to promote quiescence¹³⁶. Moreover, BM macrophages express high levels of granulocyte colony stimulating factor (G-CSF) receptor^{137,138}, and exposure to the pro-inflammatory factor G-CSF, a commonly used HSPC mobilizing reagent, substantially reduces BM macrophages^{52,139}. The loss of BM macrophages then promotes HSCs to proliferate and mobilize, both directly and indirectly^{7,135,136,140}. Collectively, evidence suggests BM macrophages serve as an important bone marrow niche component, regulating the quiescence, proliferation and mobilization of HSPCs under homeostatic and stressful conditions.

1.1.6. The Sympathetic Nervous System

The sympathetic nervous system (SNS) is another important bone marrow niche component. Prior studies have shown that the SNS regulates HSC mobilization through its modulation of granulocyte colony stimulating factor (G-CSF) and/or CXCL12 signaling^{141,142}. Another study suggests that the SNS stimulates Nestin⁺ mesenchymal cells to send adrenergic signals to HSPCs¹⁴³. Meanwhile, non-myelinating Schwann cells are a major source of activated transforming growth factor β (TGF β) in the bone marrow¹⁴⁴, and TGF β induces HSC quiescence *ex vivo*¹⁴⁵. There is evidence that ablation of Schwann cells results in decreased HSC dormancy

and HSC number¹⁴⁶. Therefore, the SNS has been proposed as a major component of the bone marrow niche.

Collectively, all the components discussed above, as well as mesenchymal stromal cells, make the bone marrow niche a complicated but critical microenvironment to study.

Understanding the bone marrow niche will not only enhance our knowledge on hematopoiesis, but it will also help us improve treatments for bone marrow related diseases.

1.2. Mesenchymal Stromal Cells

1.2.1. CAR cells

CXCL12-abundant reticular (CAR) cells are identified by the expression of GFP which is knocked into the *cxcl12* locus¹⁴⁷. They have a characteristic reticular morphology, with long processes extending throughout the bone marrow, and are predominantly perivascular¹⁴⁸. In mouse bone marrow, CAR cells can be defined as Lineage⁻ (CD45, CD31, Ter119 and Gr-1) stromal cells expressing high levels of GFP¹⁹. CAR cells are the main source of bone marrow CXCL12, and they also express high levels of SCF^{10,149}. A prior study used CXCL12-diphtheria toxin receptor (DTR) mice to deplete CAR cells, which resulted in HSC reduction in the bone marrow¹⁴⁹. Since CAR cells express both CXCL12 and SCF, CXCL12 from CAR cells may not be necessary for HSC maintenance in the bone marrow. To test this possibility, a later study used *Osterix-Cre (Osx-Cre)* and *Cxcl12^{fllox}* models to ablate CXCL12 from CAR cells and found that CXCL12 expression from CAR cells, while essential for efficient retention of HSPCs in the bone marrow, was not required for HSC maintenance³.

CAR cells were originally described as adipo-osteoprogenic mesenchymal progenitors¹⁴⁹. Lineage mapping using *Osterix-Cre* to target CAR cells shows that both osteoblasts and CAR cells are targeted, suggesting the osteoprogenic potential of CAR cells³. Meanwhile, *Leptin-receptor-Cre (LepR-Cre)* targets both CAR cells and adipocytes, which suggests the adipogenic potential of CAR cells¹¹. While both models target CAR cells efficiently, they target adipocytes and osteoblasts differently, which brings doubts on CAR cell's adipo-osteoprogenic potentials. One possible explanation is that CAR cells may have different adipo-osteoprogenic potentials at different time points during development, *Osx-Cre* and *LepR-Cre* may be turned on at different stages, thus target adipocytes and osteoblasts differently.

CAR cells have also been reported to affect B lymphopoiesis. A prior study using the diphtheria toxin-ablation model has shown that CAR cells are important for early B cell development, as CAR cell ablation results in a loss of CLP, decreased proliferation and increased apoptosis of pro-B cells¹⁴⁸. CXCL12 produced by CAR cells likely plays an important role during B cell development, as a recent study has demonstrated the effects of ablating CXCL12 from different subsets of CAR cells on B cell development³. In addition, interleukin 7 (IL-7) has been reported to play an essential role in early B lymphopoiesis¹⁵⁰. Deletion of either IL-7 or IL-7 receptor has been shown to cause reductions in pro-B and pre-B lymphocytes with no change to pre-pro-B lymphocytes¹⁵¹⁻¹⁵³. A recent study crossed *IL7-Cre* transgenic mice with *Rosa26^{EYFP}* mice and illustrated that the IL-7 expressing cells in the bone marrow were predominantly bipotent CAR cells¹⁵⁴.

1.2.2. LepR⁺ Cells

LepR⁺ cells are stromal cells expressing leptin receptor which were originally identified as *Lepr-Cre* targeted stromal cells by the Morrison group¹⁰. LepR⁺ cells include more than 90% of cells expressing high levels of *Scf-GFP* or *Cxcl12-DsRed* in young-adult mouse bone marrow^{155,156}. LepR⁺ cells are mostly perivascular and especially enriched around sinusoids and small-diameter arterioles^{156,157}. In normal young-adult mouse bone marrow, LepR⁺ cells and CAR cells almost completely overlap with each other^{155,156}. Consistent with this observation, a later study used *Lepr-Cre* to conditionally delete *Foxc1*, a transcription factor that is required by CAR cells, which resulted into substantial depletion of HSCs and reduced bone marrow cellularity¹⁵⁸. Therefore, LepR⁺ cells and CAR cells may be considered as the same cell population, at least in young-adult mice¹⁵⁶. Although LepR⁺/CAR cells only represent approximately 0.3% of bone marrow cells, their long processes are present throughout the bone marrow, providing them the capability to affect most bone marrow cells¹⁵⁶. LepR⁺/CAR cells express both SCF and CXCL12, and are also closely associated with HSCs, thus making them an important component of the perivascular bone marrow niche^{3,11,76,155,159}.

1.2.3. Nestin-GFP⁺ Cells

Nestin-GFP⁺ (Nes-GFP⁺) cells are bone marrow mesenchymal stromal cells expressing GFP under the regulatory element of the nestin promoter^{21,160}. Histomorphometry analysis of whole bone marrow shows two different subsets of Nes-GFP⁺ cells, according to their expression levels of GFP and their locations: Nes-GFP^{dim} cells that are perisinusoidal and heavily overlap with CAR/LepR⁺ cells; and Nes-GFP^{bright} cells that are periarteriolar and express NG2^{156,157}. A prior

study done by Frenette's group used confocal imaging and spatial modeling to reveal that about 35% of HSCs are closely associated with arterioles¹². The same study also suggests that these arteriolar Nes-GFP⁺ stromal cells and arteriolar niches are indispensable for maintaining HSC quiescence¹². This is in contrast to a later study which shows non-dividing HSCs are mainly perisinusoidal¹⁵⁹.

The concept of the periarteriolar niche was initially based on the suggestion that Nes-GFP⁺ cells, especially the *Nes-CreER* and *NG2-CreER* targeted periarteriolar Nes-GFP^{bright} cells, were an important source of SCF and CXCL12^{12,21}. Since Nes-GFP⁺ cells include two distinct subsets, it is not clear whether the SCF and CXCL12 expressed by Nes-GFP⁺ cells reflect the expression by perisinusoidal Nes-GFP^{dim} CAR/LepR⁺ cells or the expression by periarteriolar Nes-GFP^{bright} NG2⁺ cells¹⁵⁶. Moreover, inconsistent with the original studies^{12,21}, other groups revealed that conditional deletion of *Cxcl12* and *Scf* in *Nes-CreER* and *NG2-CreER* targeted cells showed no significant effects on HSC frequency or HSC functions in adult bone marrow^{10,11,18,155}. Different observations between these groups may be due to the age of mice used in their experiments. Studies supporting the arteriolar niche administered tamoxifen to deplete *Cxcl12* from *NG2-CreER* or *Nes-CreER* targeted cells within 3 weeks after birth^{161,162}, when these *Cre* alleles are more broadly expressed in the bone marrow¹⁶³. Other studies administered tamoxifen 6 weeks after birth, when *NG2-CreER* and *Nes-CreER* are more restricted to periarteriolar cells^{11,159}. While the function of Nes-GFP^{bright} NG2⁺ stromal cells and the concept of the periarteriolar niche still remain debatable, Nestin-GFP⁺ stromal cells do represent an important stromal population in the bone marrow niche.

1.3. B Lymphopoiesis

1.3.1. CXCL12

CXCL12, also known as stromal-derived factor 1 (SDF-1) was originally discovered as a chemokine stimulating pre-B cell development *in vitro*¹⁶⁴. CXCL12 is an important chemokine for hematopoiesis and B lymphopoiesis²⁰, and mice lacking CXCL12 are perinatal lethal with significant defects in B cell development¹⁶⁵. CXCR4 is the primary receptor of CXCL12, and mice lacking CXCR4 have a defect in early B cell development, with reductions in pre-pro B cells, CLPs and BLPs¹⁶⁶⁻¹⁶⁸. CXCL12 interacts with CXCR4 to activate mitogen-activated protein kinase (MAPK), PI3 kinase (PI3K), extracellular-signal-regulated kinases (ERK1/2) and P38¹⁶⁹. MAPK activation leads to actin polymerization and the regulation of cytoskeletal change, and PI3K activation induces polarization of adhesion molecules; both are responsible for the control of chemotaxis¹⁶⁹. In addition, PI3K and ERK1/2 activate the NF κ B pathway for gene transcription to promote cell proliferation, while P38 and PI3K down-regulate pro-apoptotic factors to inhibit apoptosis and up-regulate anti-apoptotic factors to promote cell survival^{20,170}.

A prior study used transgenic mice to express an intracellular form of CXCL12 to inhibit CXCL12/CXCR4 signaling by sequestering CXCR4 intracellularly and found defects in B cell development starting from pro-B cell stage¹⁷¹. The same study showed that extracellular overexpression of CXCL12 could increase B cell number, further suggesting extracellular CXCL12/CXCR4 signaling is important for normal B cell development¹⁷¹. In another study, after being transplanted into irradiated wild type recipients, fetal liver cells from *Cxcl12*^{-/-} or wild type mice showed indistinguishable capability to reconstitute the hematopoietic system including B lymphopoiesis, demonstrating extracellular CXCL12 from the microenvironment, but not from

hematopoietic cells, is required for B cell development¹⁷². In contrast, serial transplantation from mice reconstituted with *Cxcr4*^{-/-} fetal liver cells shows a reduction of B cell progenitors in the bone marrow, illustrating the importance of CXCR4 signaling for efficient B cell development¹⁷². In addition to promoting B cell proliferation, CXCL12/CXCR4 signaling may also play an important role in regulating B cell retention and trafficking. Transplantation of *Cxcr4*^{-/-} fetal liver cells into wild type recipients results in a decrease of B cells in the bone marrow, but an increase of IgM⁻ B cells in the peripheral blood, indicating a retention defect of B cell progenitors in the bone marrow¹⁷³.

In the bone marrow, mesenchymal stromal cells, especially CAR cells, are the main source of CXCL12^{3,10}. However, these stromal cells are heterogeneous and may include different subsets with more specific functions. The Link lab has used several stromal-specific transgenic *Cre* models to delete *Cxcl12* from the bone marrow, including *Prx1-Cre*, *Osx-Cre* and *Ocn-Cre*³. *Prx1-Cre* and *Osx-Cre* models, crossed with *Cxcl12*^{fllox/-} mice, induced significant ablation of CXCL12 in the bone marrow, but *Ocn-Cre:Cxcl12*^{fllox/-} mice did not ablate CXCL12 significantly, compared to *Cxcl12*^{fllox/-} control mice³. Interestingly, *Prx1-Cre:Cxcl12*^{fllox/-}, but not *Osx-Cre:Cxcl12*^{fllox/-} mice, induced significant reductions in CLPs and BLPs, while both models had significant reduction in pre-pro B cells³. These observations might be explained by the more robust ablation of CXCL12 in *Prx1-Cre:Cxcl12*^{fllox/-} mice, compared to *Osx-Cre:Cxcl12*^{fllox/-} mice³, suggesting B cell progenitors at different stages may be sensitive to different concentrations of CXCL12. Another possibility is that the expression of CXCL12 by mesenchymal stem cells, targeted by *Prx1-Cre*, but not *Osx-Cre*, is required for the development and maintenance of CLPs and BLPs. Collectively, further studies are required to understand the role of bone marrow stromal CXCL12 in the regulation of B cell development.

1.3.2. Memory plasma cells

B cells can develop into two major types of memory cells, and they are memory plasma cells (PCs) and memory B cells. PCs were initially described in 1948¹⁷⁴, and were originally considered as short-lived cells that secrete either IgM or downstream isotypes³². A later study identified long-lived PCs in the bone marrow, which are resting in terms of proliferation and migration, but may produce antibodies of humoral memory^{32,175}. Thus, these cells may also be referred to as memory PCs. Human PCs generally express high levels of CD38 and CD27, and low levels of CD20. In mice, the comparable markers are CD138 and B220. To distinguish memory PCs from short-lived PCs, genes or markers labeling cell cycle and proliferation may be used, such as Ki67. The bone marrow is the major reservoir for memory PCs, and studies have suggested that PC progenitors from different lymphoid organs may migrate to the bone marrow and differentiate into memory PCs³². A prior study has provided some evidence that the longevity of memory PCs is an intrinsic feature, but extrinsic signals from the surrounding microenvironment are also required for the survival of memory PCs and the prevention from apoptosis^{32,176}. In the bone marrow, stromal cells have been strongly suggested to constitute an important part of the survival niche for memory PCs, either by directly supporting memory PC survival, or by recruiting and supporting other important niche components. In both human and mouse, PCs express CXCR4, and CXCL12 produced by stromal cells play a critical role for the maintenance of memory PCs in the bone marrow³². Disruption of CXCL12/CXCR4 signaling in the bone marrow may result in a significant loss of bone marrow PCs¹⁴⁸. In addition, IL-6 produced by stromal cells has been identified as another important survival factor for memory PCs. Therefore, it is important to further dissect the stromal cell population and study their regulation of PCs, especially memory PCs in the bone marrow.

1.3.3. Memory B cells

Memory B cells are defined as cells that participate in a primary response and persist in the host after acute immune response. Memory B cells are normally in a resting state and do not express any effector functions, but upon secondary exposure to the memorized antigen, they quickly recognize them and produce a faster and stronger immune response³². Memory B cells differentiate into antibody-secreting PCs upon reactivation, and they are more likely to undergo PC differentiation compared to naive B cells. Thus, chronic antigen exposure may persistently reactivate memory B cells to generate more antibody-secreting PCs, which is critical for the maintenance of long-lived humoral immunity³².

Memory B cells are highly diverse and multiple subsets have been discovered that may potentially carry different functions for the immune memory³². In humans, memory B cells were historically identified as immunoglobulin D⁻ (IgD⁻) B cells, as they had undergone class-switch recombination^{177,178}. However, a later study identified another subset of IgD⁺ memory B cells¹⁷⁹. To identify both types of human memory B cells, the same study provides a novel marker, the tumor necrosis factor (TNF) receptor family member CD27, which is also used nowadays to mark human memory B cells¹⁷⁹. Being a general marker for memory B cells, CD27 cross-links CD70 to enhance B cell activation *in vivo* and to favor differentiation towards PCs, resulting in stronger antibody secretion¹⁸⁰⁻¹⁸³. CD27⁺ memory B cells can be further divided into IgM⁻ IgD⁻, IgM⁺ IgD⁺ and IgM⁺ IgD⁻ cells, and IgM⁺ memory cells respond faster to stimulation than naive cells^{179,184,185}. In addition, more recent studies identify a new subset of memory B cells that are CD27⁻, and they are similar to CD27⁺ memory B cells for carrying somatically mutated immunoglobulin genes^{186,187}. The identification of murine memory B cells is more complicated, as CD27 is not a marker for memory B cells in mice¹⁸⁸. Due to the heterogeneity of memory B

cells, simply using surface markers may not provide an accurate method to identify them. A recent study used the immunization method to induce the production of memory B cells against a specific antigen, which can be identified by their capability to recognize the specific antigen and their expressions of conventional memory B cell markers¹⁸⁹.

Memory B cells specific for vaccinia virus antigens (smallpox) have been discovered in humans even 50 years after immunization¹⁹⁰. Multiple mechanisms have been shown or discussed for the maintenance of memory B cells³². A prior study suggests the requirement of an antigen for the maintenance of the antigen-specific memory B cells¹⁹¹. However, another study shows that phycoerythrin (PE) specific memory B cells are well persisted in nitrophenyl-chicken gamma globulin (NP-CGG) immunized mice that have not been exposed to PE¹⁹². Other than antigen dependency, survival and proliferation are other important mechanisms for memory B cell maintenance³². The spleen has been shown as a major reservoir of memory B cells against vaccinia virus¹⁹³. In patients, circulating IgM⁺ IgD⁺ CD27⁺ memory B cells rapidly decline and finally disappear after splenectomy¹⁹⁴. Splenectomy also results in reduced, but not abrogated circulation of IgD⁻CD27⁺ memory B cells after 2 years, suggesting that while the spleen is an important reservoir for these memory B cells, other organs may also serve as their reservoirs³². Prior studies have also proposed the bone marrow as a reservoir for memory B cells^{35,36}. Although a recent study suggests that only a small fraction of memory B cells are BM resident³⁴, it is possible that these cells may carry unique functions. The bone marrow niche provides a microenvironment for the maintenance of long-term quiescent HSCs, thus it would be interesting to test whether these BM memory B cells are more quiescent and may survive in long term, and to study the potential mechanisms involved in the regulation of these memory B cells by the bone marrow niche.

1.4 Dendritic Cells

1.4.1. cDC1

Classical DCs type 1 (cDC1s), also known as CD8 α ⁺ cDCs or CD103⁺ cDCs, were originally described as a subset of DCs in blood that express high levels of CD141 (thrombomodulin, BDCA-3)¹⁹⁵⁻¹⁹⁷. Human cDC1s are a rare population among all cDCs, as they are only about one-tenth of cDC2s in steady-state blood and tissues^{42,198-201}. cDC1s are found in both lymphoid and non-lymphoid tissues, and there are suggestions that they are more abundant in tissues compared to blood, although this idea may need further validation⁴². While sharing similar phenotypic markers with cDC2s, cDC1s may be distinguished by their low expression of CD11c, little expression of CD11b and SIRP α ⁴². Besides, cDC1s express high levels of CLEC9A, CADM1 and BTLA⁴². Several gene expression studies have also identified XCR1 as a conserved marker for cDC1s in many species²⁰². In addition, intracellular IRF8 expression may be used as a standard marker for identifying cDC1s, as unopposed expression of IRF8 (without IRF4) defines the lineage¹⁹⁸. IRF8 is a transcription factor that play an important role to regulate the differentiation of DCs, especially cDC1s, at several stages during hematopoiesis through direct or indirect competition with transcription factors promoting other lineages^{42,203}. IRF8 may limit granulocytic differentiation, balance DC to monocyte differentiation, compete with IRF4 to control cDC1:cDC2 output, and maintain cDC1 maturation^{27,156}. Gene dosage of IRF8 is a critical determinant during DC development. Homozygous deletion of *Irf8* causes loss of monocytes and all DCs, but excessive production of neutrophils^{204,205}. Interestingly, subtle losses of IRF8 activity in mice only reduces the production of cDC1s²⁰⁶.

Functionally, cDC1s have been characterized as a subset of DCs with a high intrinsic capacity to cross-present antigens via MHC I to activate CD8⁺ T cells and to release IL-12 to promote T helper type 1 (Th1) and natural killer responses²⁰⁷⁻²¹⁰. Expression of XCR1 chemokine receptor by cDC1s enables close interaction with XCL-producing activated T cells and nature killer (NK) cells²⁷. Human cDC1s efficiently recognize viral and intracellular antigens, and transport antigens to the appropriate endosomal compartments through several conserved mechanisms^{27,211}. For example, cDC1s express high levels of CLEC9A, a unique receptor that recognizes bare actin filaments exposed upon necrotic cell death, thus directs cell-associated antigens into the cross-presentation pathway²¹²⁻²¹⁵. cDC1s are also a major source of type III interferons (IFN), and the production and accumulation of these interferons during hepatitis C virus infection have been proposed to benefit viral clearance²¹⁶. In mice, cDC1s have also been characterized as cross-priming tolerogenic cells, but this potential has not been well characterized in human^{217,218}.

1.4.2. cDC2

The majority of myeloid cDCs in different tissues and organs are characterized as classical DCs type 2 (cDC2s), also referred as CD11b⁺ cDCs, expressing CD1c, CD2, SIRP α and Fc ϵ R1^{42,197}. Similar to cDC1s, cDC2s also express myeloid surface markers CD13 and CD33, but high levels of CD11b and CD11c²⁷. A prior transcriptional profiling study has also revealed CLEC10A, VEGFA and FCGR2A as surface markers of cDC2s¹⁹⁹. There is great heterogeneity among cDC2s found in different tissues, and different subsets of cDC2s may be further characterized²⁷. Recent studies have characterized human blood cDC2s into two subsets: one

subset being DC-like with higher expression of CD5, CD1c, HLA-DQ and IRF4; the other subset being monocyte-like expressing CD14, CD32, CD36 and proportionately higher MAFB^{219,220}. The development of cDC2s may depend on multiple transcription factors, but unlike cDC1s or pDCs, no single transcription factor plays an exclusive role to regulate this process^{197,221-223}. In mice, recent studies have identified ZEB2 as a factor influencing the fate of pre-DCs towards the cDC2 lineage and IRF4 as a cDC2 lineage defining factor^{198,222}. Subsets of murine cDC2s exist in different tissues and may depend on variable factors, such as RELB, NOTCH2 and KLF4¹⁹⁷. In contrast, the regulation of cDC2 development in humans is different from mice, and is less understood. In humans, heterozygous GATA2 deficiency leads to eventual loss of all cDC2s²²¹. Deletion of IRF8 in humans abrogates entire DC development including cDC2s^{204,205}, while cDC2s are IRF8-independent in mice²²⁴.

cDC2s express a wide range of lectins, TLRs, NOD-like receptors and RIG-I-like receptors, and may respond to intracellular pathogens, parasites, allergens, fungi and extracellular bacteria²⁷. CD1a and CD1c expressed by cDC2s may present the glycolipid antigens of mycobacteria and other pathogens²²⁵. Dectin-1 and Dectin-2 are also highly expressed in tissue cDC2s, which are important for fungal recognition^{226,227}. cDC2s may secrete IL-1, IL-8, IL-10, IL-12, IL-23 and tumor necrosis factor- α (TNF- α), but little type III interferons, which are mainly secreted by cDC1s^{228,229}. In addition, *in vitro* studies have shown that human cDC2s could activate Type I T helper (Th1), Th2, Th17 and CD8⁺ T cells¹⁸²⁻²³⁰. Thus, cDC2s have great potential to induce a wide range of immune responses in human.

1.4.3. pDC

Plasmacytoid DCs (pDCs) were first discovered in human tonsil and blood^{231,232}. Different from myeloid cDCs, pDCs do not express CD11c, CD11b, CD13 or CD33^{195,196,233}. Well-known markers for human pDCs include CD303 (CLEC4C or BDCA-2), CD304 (BDCA-4), CD85k (ILT3) and CD85g (ILT7), together with more recently characterized antigens FcεRI, BTLA, CD358 and CD300A^{234,235}. Transcriptional profiling studies have also identified additional markers, FAM129C, CUX2 and GZMB¹⁹⁹. Development of pDCs depend on the coordinated process of multiple transcription factors⁴². The key factors regulating the balance between pDC and cDC development are E2-2 (TCF4), a basic hemophagocytic lymphohistiocytosis protein, and its antagonist ID2, a DNA binding inhibitor^{197,236}. TCF4 is the lineage-determining factor for pDCs and is negatively regulated by ID2²³⁷. Recent studies have described multiple transcription factors to regulate the relative production of pDCs and cDCs, through their interactions with the TCF4/ID2 signaling pathway⁴². In humans, heterozygous loss of *Tcf4* results in Pitt–Hopkins syndrome with a pDC deficiency⁴².

Functionally, pDCs are specialized DCs that detect and respond to viral infections through the rapid production of large quantities of type I and type III interferons, and the secretion of cytokines^{235,238}. Toll-like receptor 7 (TLR7) and TLR9 are key receptors for pDCs sensing single-stranded RNA and double-stranded DNA, respectively²³⁵. Interestingly, a prior study has revealed the potential of pDCs to sense self-nucleic acids²³⁹. Together with their prominent role in the production of type I interferon, pDCs have been implicated in the pathogenesis of autoimmune diseases including psoriasis and systemic lupus erythematosus^{240,241}. Multiple studies have also suggested that pDCs are capable of priming CD4⁺ T cells and CD8⁺ T cells, although further studies may be necessary to evaluate their antigen-presenting capacity⁴².

Moreover, pDCs have been reported to play conflicting roles in allergy^{242,243}. In addition, tolerogenic pDCs may be affected by granulocyte-macrophage colony-stimulating factor (GM-CSF) to contribute to tumor progression²⁴⁴.

1.5. Summary

The bone marrow niche is a complicated microenvironment that regulates HSPC maintenance and B lymphopoiesis. Prior studies have identified multiple cellular components of the bone marrow niche, including mesenchymal stem cells, endothelial cells, osteoblast lineage cells, megakaryocytes, macrophages, the sympathetic nervous system and mesenchymal stromal cells. Among these cellular components, mesenchymal stromal cells are particularly of our interest, which are heterogeneous and serve as the main source of multiple important soluble niche factors, such as CXCL12, SCF and IL-7. Prior studies in our lab have shown the importance of stromal CXCL12 expression on regulating B cell development in the bone marrow. Moreover, BM cDCs have been discovered in the bone marrow that may be important for the regulation of B cells, suggesting their potential involvement in the bone marrow niche. Further characterization of the heterogeneity of stromal cells, the role of CXCL12 expression in different stromal subsets and the role of BM cDCs in the regulation of HSPCs, will improve the overall understanding on the bone marrow niche and may provide potential targets for future clinical applications.

In Chapter 2, the heterogeneity of mesenchymal stromal cells will be studied by using different transgenic *Cre* models. In Chapter 3, the role of CXCL12 produced by different subsets of stromal cells will be assessed for their effects on B cell development, especially on the

maintenance of memory PCs and B cells. In Chapter 4, BM cDCs will be assessed for their effects on HSPCs by using ablation models, and the potential molecular mechanisms involved in their regulation of HSPCs will also be studied. Finally, in Chapter 5, these findings on the bone marrow niche and its regulation of HSPCs or B cells will be summarized and future directions will be outlined.

CHAPTER 2: TARGETING OF MESENCHYMAL STROMAL CELLS BY CRE-RECOMBINASE TRANSGENES COMMONLY USED TO TARGET OSTEOBLAST LINEAGE CELLS

2.1. Introduction

The bone marrow microenvironment contains a heterogeneous population of stromal cells that contribute to the regulation of hematopoiesis. Identifying these stromal cells and the signals they generate has important clinical implications for a number of hematopoietic diseases^{5,11}. Mesenchymal stromal cells implicated in the maintenance of hematopoietic stem cells (HSCs) include endothelial cells, osteoblasts, CXCL12-abundant reticular (CAR) cells, mesenchymal stem cells (MSCs), and arteriolar pericytes^{3,4,10,12}. The use of tissue-specific *Cre*-recombinase transgenes to delete genes of interest from defined stromal cell populations is an established and important technique in the field. Rigorously defining the targeting specificity of the *Cre*-recombinase transgenes is a key to the interpretation of such experiments.

Two *Cre*-recombinase transgenes that are commonly used to target osteolineage cells are *Ocn-Cre* and *Dmp1-Cre*. Osteocalcin (*Ocn*, *Bglap*) is a secreted protein implicated in bone and glucose metabolism²⁴⁵. Cell culture and in situ expression studies show that OCN expression is mostly limited to osteoblasts and osteocytes^{245,246}. This has led to the widespread use of *Ocn-Cre* transgenes to specifically target osteoblasts and osteocytes^{247,248}. Dentin matrix acidic phosphoprotein 1 (*Dmp1*) is expressed in odontoblasts, preosteocytes and osteocytes^{249,250}. Indeed, a transgene containing an 8 kb regulatory region of *Dmp1* linked to GFP results in osteocyte-specific GFP expression in the bone marrow²⁵¹. These data have led to the widespread use of *Dmp1-Cre* transgenes to specifically target osteocytes, although targeting of some

osteoblasts also has been observed^{250,252,253}. Furthermore, a study by Kalajzic et al showed that a 10 kb *Dmp1-Cre* transgene targeted both osteoblasts and osteocytes, as well as a small population of undefined cells in the bone marrow²⁵⁰.

In the present study, we used high-resolution microscopy of bone sections and flow cytometry to carefully define the targeting specificity of *Ocn-Cre* and *Dmp1-Cre* in the bone marrow. We showed that both the *Ocn-Cre* and *Dmp1-Cre* transgenes target a much broader population of bone marrow stromal cells than previously appreciated. We also characterized for the first time the spectrum of bone marrow stromal cells targeted by a *Tagln-Cre* transgene. We show that *Tagln-Cre* efficiently targets osteoblasts and perivascular stromal cells, but not endothelial cells.

2.2. Materials and Methods

2.2.1. Mouse strains

Ai9 (B6.Cg-Gt(ROSA)26Sor^{tm9(CAG-tdTomato)Hze/J})²⁵⁴ mice and *Tagln-Cre* (B6.129S6-*Tagln*^{tm2(cre)Yec/J}) mice were obtained from The Jackson Laboratory²⁵⁵. *Ocn-Cre* mice were a gift from Thomas Clemens (Johns Hopkins University, Maryland)²⁵⁶. *Cxcl12^{gfp}* mice were a gift from Takashi Nagasawa (Kyoto University, Japan)²⁵⁷, and *Dmp1-Cre* mice (containing the 9.6 kb murine *Dmp1* promoter) were a gift from Roberto Civitelli (Washington University, MO)²⁵⁸. All mice used in this study were 8-10 weeks old. Both male and female mice were used equally in these studies. Genotyping primers are listed in Suppl. Table 2.1. Mice were maintained under SPF conditions, and all experimental procedures were performed according to methods approved by the Animal Studies Committee at Washington University.

2.2.2. Flow cytometry

Bone marrow cells were harvested from mouse femurs by first uncapping the ends of the bone and then centrifuging at 3300 x g for 5 minutes to expel the bone marrow contents. These cells were then digested with 1.67 mg/ml of type II collagenase (Worthington) in phosphate-buffered saline (PBS) for 12 minutes at 37 °C. Of note, the majority of osteoblasts are not recovered using this procedure (Suppl. Fig 2.1). The following antibodies were used: CD45 (30-F11), CD31 (390), and Ter119 (TER-119). Cells were analyzed on a Gallios flow cytometer (Beckman Coulter), and data analysis was done using FloJo version 10.0.7 software (TreeStar).

To sort *Dmp1-Cre* targeted or non-targeted CAR cells, we first isolated platelet-derived growth factor receptor-beta (PDGFR β)-positive stromal cells from the bone marrow of *Dmp1-Cre ROSA26^{Ai9/+} Cxcl12^{gfp/+}* mice using the AutoMacs Pro Separator system (Miltenyi Biotec) and a biotinylated anti-PDGFR β antibody (APB5). Cells were incubated with antibodies against Gr-1 (RB6-8C5), PDGFR β (APB5), CD45 (30-F11), CD31 (390), and Ter119 (TER-119) and then incubated with brilliant violet 421-conjugated Streptavidin (405225, BioLegend). CAR cells were identified as *Cxcl12-GFP^{bright} PDGFR β ⁺ Gr1⁻ CD45⁻ CD31⁻ Ter119⁻* cells. *Dmp1-Cre* targeted CAR cells were tdTomato^{high}. Cells were sorted using a MoFlo high-speed flow cytometer (Dako Cytomation). All antibodies were obtained from eBioscience, unless otherwise noted.

2.2.3. Immunostaining of bone sections

Mouse hindlimbs were fixed in PBS containing 4% paraformaldehyde, pH 7.4, for 24 hours at 4 °C. Bones were then decalcified in PBS containing 14% EDTA, pH 7.4, for 7 days at 4 °C. Following incubation in PBS containing 30% sucrose for 24 hours at 4 °C, bones were

embedded in Optimal Cutting Temperature Compound (Sakura Finetek). These tissue blocks were cut into 12 μm sections using a Leica Cryo-Jane system (Leica Biosystems). For immunostaining, the slides were blocked with 10% donkey serum, diluted in 0.1M Tris-Cl pH 7.5, 150 mM NaCl, and 0.1% Tween 20 (TNT) buffer for 1 hour at room temperature. Following blocking using the Avidin/Biotin Blocking Kit (SP-2001, Vector Laboratories), slides were then incubated in primary antibody overnight at 4 $^{\circ}\text{C}$ and, where applicable, they were incubated with secondary antibody for 1 hour at room temperature. The following antibodies were used: rabbit anti-NG2 (AB5320, EMD Millipore), rat anti-Sca1 (557403, BD Biosciences), goat anti-VECadherin (AF1002, R&D Systems), mouse anti- αSMA (1A4, Sigma Aldrich); AlexaFluor 488-conjugated donkey anti-rat IgG (Jackson ImmunoResearch); DyLight649-conjugated donkey anti-rat IgG (Jackson ImmunoResearch); and biotin-conjugated donkey anti-goat IgG (Jackson ImmunoResearch). In some cases, slides were then incubated with streptavidin-DyLight 649 (Jackson ImmunoResearch) for 1 hour at room temperature. Finally, slides were mounted with ProLong Gold antifade reagent with DAPI (Life Technologies). Images were acquired with a LSM 700 microscope (Carl Zeiss) and processed using Volocity software (PerkinElmer).

For Hematoxylin & Eosin (H&E) staining, bone sections were air dried for 1 hour and then incubated with Hematoxylin Gill #3 (GHS316, Sigma-Aldrich) for 5 minutes followed by incubation with Eosin (HT110132, Sigma-Aldrich) for 3 minutes. Sections were then fixed by serial five-minute incubations in 50%, 70%, 95%, and 100% ethanol, followed by a five-minute incubation in xylene. Finally, slides were mounted with Permount mounting medium (Fisher Chemical). Images were acquired with a LSM 700 microscope (Carl Zeiss).

2.2.4. RNA expression profiling

RNA was purified from sorted CAR cells using the Qiagen RNeasy Micro Kit (74004, Qiagen). Libraries were generated using the NuGen Pico SL kit (NuGEN Technologies, San Carlos, CA) and then hybridized to Affymetrix Mouse Gene 1.0 ST arrays (Affymetrix, Santa Clara, CA). Gene set enrichment was performed using the GSEA software (Broad Institute). Differences in gene expression were determined using Significance Analysis of Microarrays (SAM; Stanford University, Stanford, CA). Expression data has been submitted to Gene Expression Omnibus, record number GSE81399.

2.2.5. Statistical analyses

Unpaired t-test was used to evaluate the significance of differences between two groups. All data are presented as mean \pm S.D.

2.3. Results

2.3.1. *Ocn-Cre* targets osteoblasts, a majority of CAR cells, and arteriolar pericytes

To characterize the targeting specificity of *Ocn-Cre* in postnatal mouse bones, we generated *Ocn-Cre ROSA26^{Ai9/+}* mice and *Ocn-Cre ROSA26^{Ai9/+} Cxcl12^{gfp/+}* mice. The *Cxcl12^{gfp/+}* transgene allows for the identification of CXCL12-GFP^{bright} (CAR) cells, which are perivascular stromal cells in the bone marrow implicated in HSC maintenance⁴. The *ROSA26^{Ai9/+}* transgene allows for the identification of *Ocn-Cre* targeted tdTomato⁺ cells. Immunostaining of the bone sections confirmed that the *Ocn-Cre* transgene efficiently targets osteoblasts (Fig. 2.1A & B, Suppl. Fig. 2.2)²⁵⁶. Surprisingly, we also observed that *Ocn-Cre* targets a substantial fraction of CXCL12-GFP^{bright} cells (Fig. 2.1A & C). Of note, as expected, no tdTomato⁺ CAR cells were

detected in control (*Cxcl12^{gfp/+}*) mice (Suppl. Fig. 2.3). Flow cytometry showed that *Ocn-Cre* targets $72.2 \pm 4.0\%$ ($n = 3$ mice) of CXCL12-GFP^{bright} cells (Fig. 2.1D). To assess targeting of arteriolar pericytes, we stained bone sections from wild type mice with antibodies against alpha-smooth muscle actin (α SMA) and NG2 (Fig. 2.2A & B). In these assays, arteriolar endothelial cells were identified by Sca1¹², which is also expressed on hematopoietic stem/progenitor cells but not on CAR cells³. Whereas α SMA staining was limited to a subset of arteriolar pericytes, NG2 staining was observed in all arteriolar pericytes (Fig. 2.2A & B). Accordingly, all α SMA-positive arteriolar pericytes co-expressed NG2, while only $56.9 \pm 11.1\%$ ($n = 3$ mice) of NG2-positive arteriolar pericytes co-expressed α SMA. Immunostaining of bone sections from *Ocn-Cre ROSA26^{Ai9/+}* mice showed that *Ocn-Cre* targets $72.2 \pm 13.3\%$ ($n = 3$ mice) of NG2-positive arteriolar pericytes (Fig. 2.2C). Thus, in addition to osteoblasts, *Ocn-Cre* targets the majority of CAR cells and arteriolar pericytes in mice.

2.3.2. *Dmp1-Cre* targets osteoblasts and a subset of CAR cells

To characterize the targeting specificity of *Dmp1-Cre* in postnatal mouse bones, we generated *Dmp1-Cre ROSA26^{Ai9/+}* mice and *Dmp1-Cre ROSA26^{Ai9/+} Cxcl12^{gfp/+}* mice. As reported previously^{253,258}, the *Dmp1-Cre* transgene efficiently targets all osteoblasts (Fig. 2.3A & B, Suppl. Fig. 2.4). Surprisingly, *Dmp1-Cre* also targets a subset of CAR cells (Fig. 2.3A & C). Interestingly, *Dmp1-Cre* targeted CAR cells were not enriched near the endosteum or osteoblasts, but were distributed throughout the bone marrow (Suppl. Fig. 2.5A & B). By flow cytometry $29.2 \pm 1.7\%$ ($n = 3$ mice) of CAR cells are targeted by *Dmp1-Cre* (Fig. 2.3D). In contrast to *Ocn-Cre*, NG2⁺ arteriolar pericytes were rarely targeted by *Dmp1-Cre* (Fig. 2.3 E). Thus, *Dmp1-Cre* targets all osteoblasts and a subset of CAR cells but few arteriolar pericytes.

To characterize the *Dmp1-Cre* targeted subset of CAR cells, we sorted tdTomato⁺ (*Dmp1-Cre* targeted) and tdTomato⁻ CAR cells (non-targeted) and performed RNA expression profiling. Gene set enrichment analysis showed that *Dmp1-Cre* targeted CAR cells were highly enriched for a previously identified group of genes involved in osteoblast maturation or bone development (Suppl. Fig. 2.6A). Indeed, expression of genes associated with mature osteoblasts such as *Bglap2* (*Ocn*) and *Postn* (periostin) are increased nearly 4-fold compared to non-targeted CAR cells (Fig. 2.3F). In contrast, expression of early osteoblast lineage genes, including *Sp7* (osterix) and *Runx2* were normal or only minimally elevated (Fig. 2.3F). Expression of key HSC maintenance genes (*Cxcl12*, *Kitl*, and *Angpt1*) or key B lymphoid factor genes (*Igfl1*, *Flt3l*, or *BAFF*) was similar in *Dmp1-Cre* targeted and non-targeted CAR cells (Suppl. Fig. 2.6B & C). However, expression of interleukin-7, which is required for pro-B cell maintenance, was significantly reduced in *Dmp1-Cre* targeted CAR cells.

2.3.3. *Tagln-Cre* targets osteoblasts, a majority of CAR cells, and both arteriolar and venous sinusoidal pericytes

Arteriolar pericytes have been implicated in HSC maintenance and can be readily identified in the bone marrow as Nestin-GFP^{bright} or NG2⁺ periarteriolar cells¹². However, a recent study reported that a substantial number of functional HSCs localize to venous sinusoids in the central bone marrow¹⁵⁹. In an effort to better visualize and isolate sinusoidal pericytes, we tested targeting by the *Tagln-Cre* transgene. *Tagln* encodes for transgelin (SM22a) and is expressed in smooth muscle cells and cardiomyocytes²⁵⁹⁻²⁶¹. *Tagln* is also expressed in osteoblasts²⁶². Accordingly, *Tagln-Cre* targets all osteoblasts (Fig. 2.4A & B, Suppl. Fig. 2.7). Analyzing *Tagln-Cre ROSA26^{Ai9/+} Cxcl12^{gfp/+}* mice, we observed that *Tagln-Cre* and CXCL12-GFP mark

overlapping, but distinct, bone marrow stromal cell populations (Fig. 2.4B & C). Whereas *Tagln-Cre* targets the great majority of CXCL12-GFP⁺ CAR cells that line venous sinusoids which are marked by VE-cadherin^{12,13}, it does not efficiently target those CXCL12-GFP⁺ CAR cells that are not in direct contact with sinusoids (Fig. 2.4D, yellow arrows). Conversely, *Tagln-Cre* targets a population of perisinusoidal cells that are CXCL12-GFP^{dim}/negative (Fig. 2.4D, red arrows), presumably representing non-CAR venous pericytes. Moreover, *Tagln-Cre*, but not CXCL12-GFP, marks periarteriolar pericytes (Fig. 2.4E). Indeed, *Tagln-Cre* targeted nearly all NG2⁺ arteriolar pericytes (Fig. 2.4E & F). Flow cytometry showed that *Tagln-Cre* targets 74.9 ± 5.2% (n = 3 mice) of CAR cells (Fig. 2.4G). Conversely, 16.6 ± 2.3% (n = 3 mice) of *Tagln-Cre* targeted stromal cells were CXCL12-GFP^{dim}/negative. Collectively, these data show that *Tagln-Cre* efficiently targets all osteoblasts, a majority of CAR cells and both venous and arteriolar pericytes.

2.4. Discussion

Ocn-Cre has been widely used to target osteoblasts in past studies^{245,247,248}. Our data show that *Ocn-Cre* targets not only osteoblasts, but also more than 70% of CAR cells and arteriolar pericytes. CAR cells are mesenchymal progenitors that have adipogenic and osteogenic capacity in vitro²⁶³. However, only a small subset of CAR cells contributes to osteoblast development in vivo⁴. Whether the *Ocn-Cre* targeted subset of CAR cells is fated to osteoblast differentiation is unclear. Of note, we did not observe preferential localization of *Ocn-Cre* targeted CAR cells to the endosteal region. CAR cells constitutively produce high levels of multiple cytokines and chemokines that regulate hematopoiesis, including CXCL12 and stem cell factor²⁶³. Indeed, CAR cells have been implicated in the maintenance of HSCs and B lymphoid progenitors^{264,265}.

Thus, phenotypes reported using *Ocn-Cre* need to be interpreted in light of our data showing targeting of CAR cells and arteriolar pericytes, in addition to osteoblasts.

Dmp1-Cre has been widely used to target osteocytes^{250,252,266}. Several *Dmp1-Cre* transgenes have been described. In this study, we show that the 10 kb *Dmp1-Cre* transgene, not only efficiently targets osteoblasts, but also a subset of CAR cells. The results are consistent with a prior study by Kalajzic et. al. showing that the 10 kb *Dmp1-Cre* transgene targets a small population of undefined cell in the bone marrow, in addition to osteoblasts and osteocytes²⁵⁰. Of note, the same group also reported that an 8 kb *Dmp1-Cre* transgene, which is thought to be more osteocyte restricted, targets, at least a subset of, osteoblasts²⁵⁰. Whether the 8 kb *Dmp1-Cre* transgene targets a subset of CAR cells will require further study. Our data show that the 10 kb *Dmp1-Cre* transgene targets approximately 30% of CAR cells. Expression profiling of this subset of CAR cells shows higher expression of genes associated with mature osteoblasts, suggesting that *Dmp1-Cre* targeted CAR cells may be enriched for osteoprogenitors. Functional studies are needed to confirm this possibility.

We report for the first time the spectrum of bone marrow stromal cells that are targeted by a *Tagln-Cre* transgene. Prior studies in non-bone tissues had shown transgelin expression in cardiomyocytes and vascular smooth muscle cells²⁵⁹⁻²⁶¹. Consistent with its expression in osteoblasts²⁶², *Tagln-Cre* efficiently targets osteoblasts. Interestingly, *Tagln-Cre* appears to target a majority of CAR cells. Specifically, it targets those CAR cells that are closely associated with venous sinusoids (i.e., venous sinusoidal pericytes). Conversely, *Tagln-Cre* does not efficiently target CAR cells that are more distant from sinusoids. Finally, *Tagln-Cre* efficiently targets arteriolar pericytes, which, despite evidence for high CXCL12 expression¹², do not express high-level GFP in *Cxcl12^{gfp}* mice. Thus, the *Tagln-Cre* represents an important new tool

for investigators to efficiently target both venous sinusoidal and arteriolar pericytes in the bone marrow.

This study highlights the complexity and heterogeneity of mesenchymal stromal cells in the bone marrow. Nestin-GFP⁺, LepR⁺, and CAR cells represent overlapping but not identical populations of perivascular mesenchymal stromal cells^{4,10,21,265}. Bulk cell analysis of each of these populations shows high-level expression of genes that regulate hematopoiesis, including factors that regulate HSCs (e.g., kit ligand) and B lymphopoiesis (e.g., interleukin-7)^{4,21,264,265}. Our study suggests that there is considerable heterogeneity within the CAR cell population. For example, the *Dmp1-Cre* targeted subset of CAR cells, in addition to being enriched for osteoblast genes, expresses a lower level of interleukin-7 (IL-7). IL-7 producing stromal cells in the bone marrow are required for the maintenance of Pro-B cells²⁶⁴, suggesting that *Dmp1-Cre* targeted CAR cells likely don't contribute this specific stage of B cell development.

In summary, we have rigorously defined the targeting specificities in the bone marrow for the three *Cre*-recombinase transgenes. *Ocn-Cre* and *Dmp1-Cre* target broader stromal cell populations than previously appreciated, and this data should be incorporated in the design of future studies. These data further highlight the heterogeneity of mesenchymal stromal cells in the bone marrow, and suggest that the *Cre*-recombinase transgenes used in this study could be used to interrogate this heterogeneity.

2.5. Acknowledgements

We thank Amy Schmidt for technical assistance and Jackie Tucker-Davis for animal care. This work was supported by RO1 HL60772 (DCL) and P50 CA171963 (DCL).

2.6. Author Contributions

JZ and DCL conceived and designed the experiments, analyzed the data, and wrote the manuscript. JZ performed the experiments.

2.7. Figures

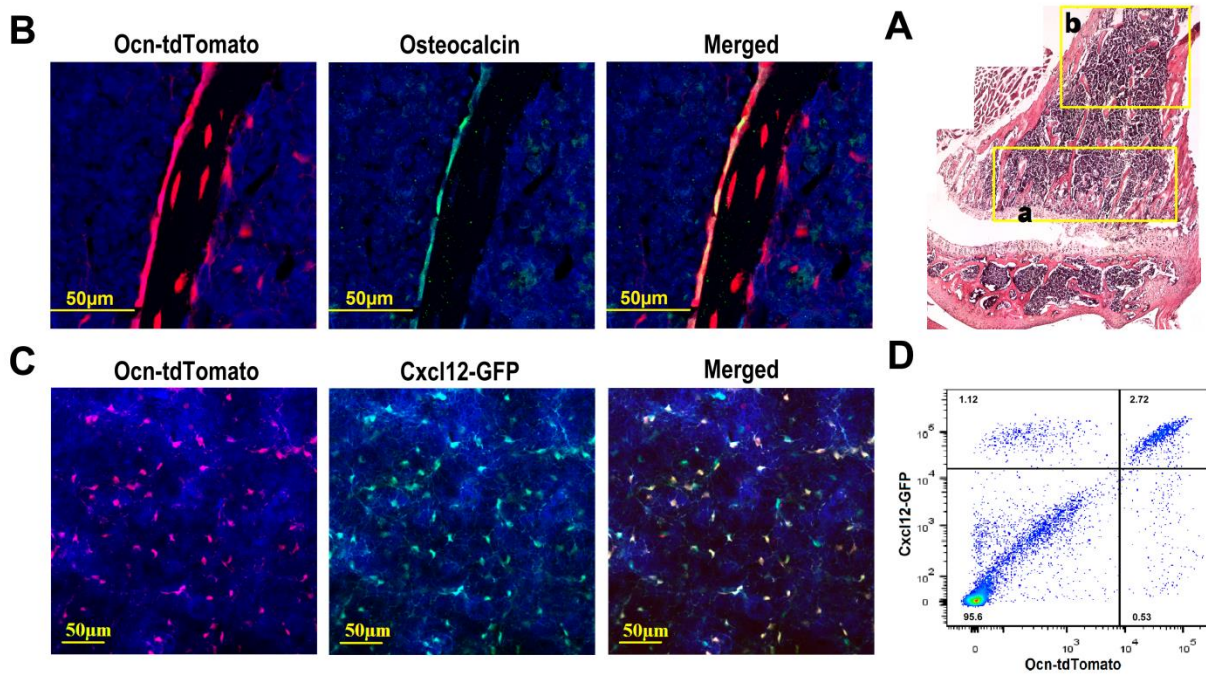


Figure 2.1. *Ocn-Cre* targets osteoblasts and a majority of CAR cells. (A) Composite image of H & E stained sections from the femur of an *Ocn-Cre ROSA26^{Ai9/+}* mouse. (B) Representative photomicrographs of the metaphyseal region (region “a” in panel A) of a femur section stained for osteocalcin (green) to mark osteoblasts and DAPI (blue) to highlight nuclei; cells that had undergone Cre-mediated recombination express tdTomato (red). (C) Representative photomicrographs taken from the diaphyseal region (similar to region “b” in panel A) of a femur section from an *Ocn-Cre ROSA26^{Ai9/+} Cxcl12^{gfp/+}* mouse. Cells that express CXCL12 also express GFP (green). Counterstaining with DAPI highlights nuclei (blue). (D) Representative dot plots showing GFP and tdTomato expression in lineage (CD45, CD31 and Ter119) negative stromal cells harvested from *Ocn-Cre ROSA26^{Ai9/+} Cxcl12^{gfp/+}* mice. Original magnification, 200X except for panel A, which is 100X.

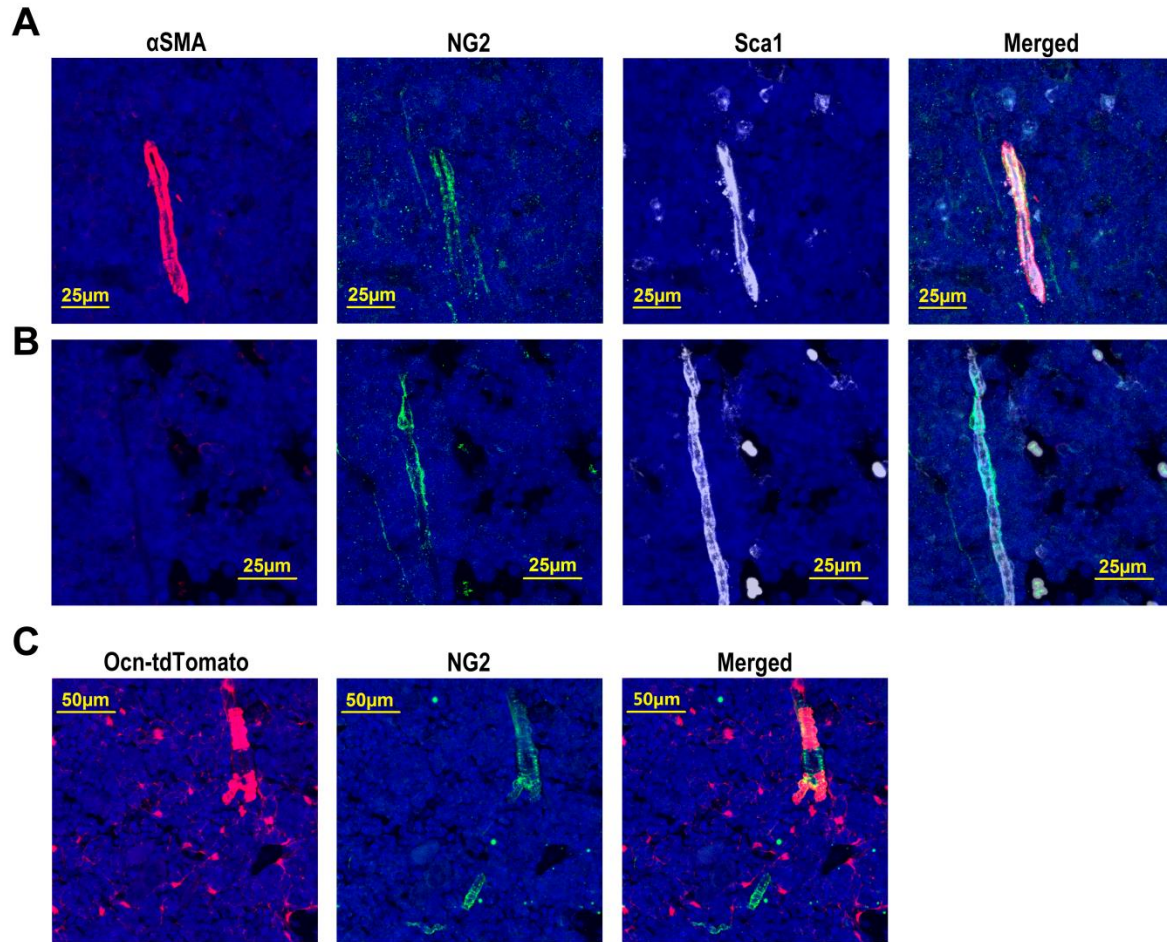


Figure 2.2. *Ocn-Cre* targets the majority of arteriolar pericytes. Representative photomicrographs of the diaphyseal region (similar to region “b” in Fig. 1A) of a femur section from a wild type mouse stained for α SMA (red), NG2 (green), Sca1 (white) and DAPI (blue). (A) Images showing α SMA⁺ NG2⁺ arteriolar pericytes around Sca1⁺ arteriolar endothelial cells. (B) Images showing α SMA⁻ NG2⁺ arteriolar pericytes around Sca1⁺ arteriolar endothelial cells. (C) Representative photomicrographs of the diaphyseal region of a femur section from an *Ocn-Cre ROSA26^{Ai9/+}* mouse stained for NG2 (green) and DAPI (blue). TdTomato (red) represents cells targeted by *Ocn-Cre*. Original magnification, 200X.

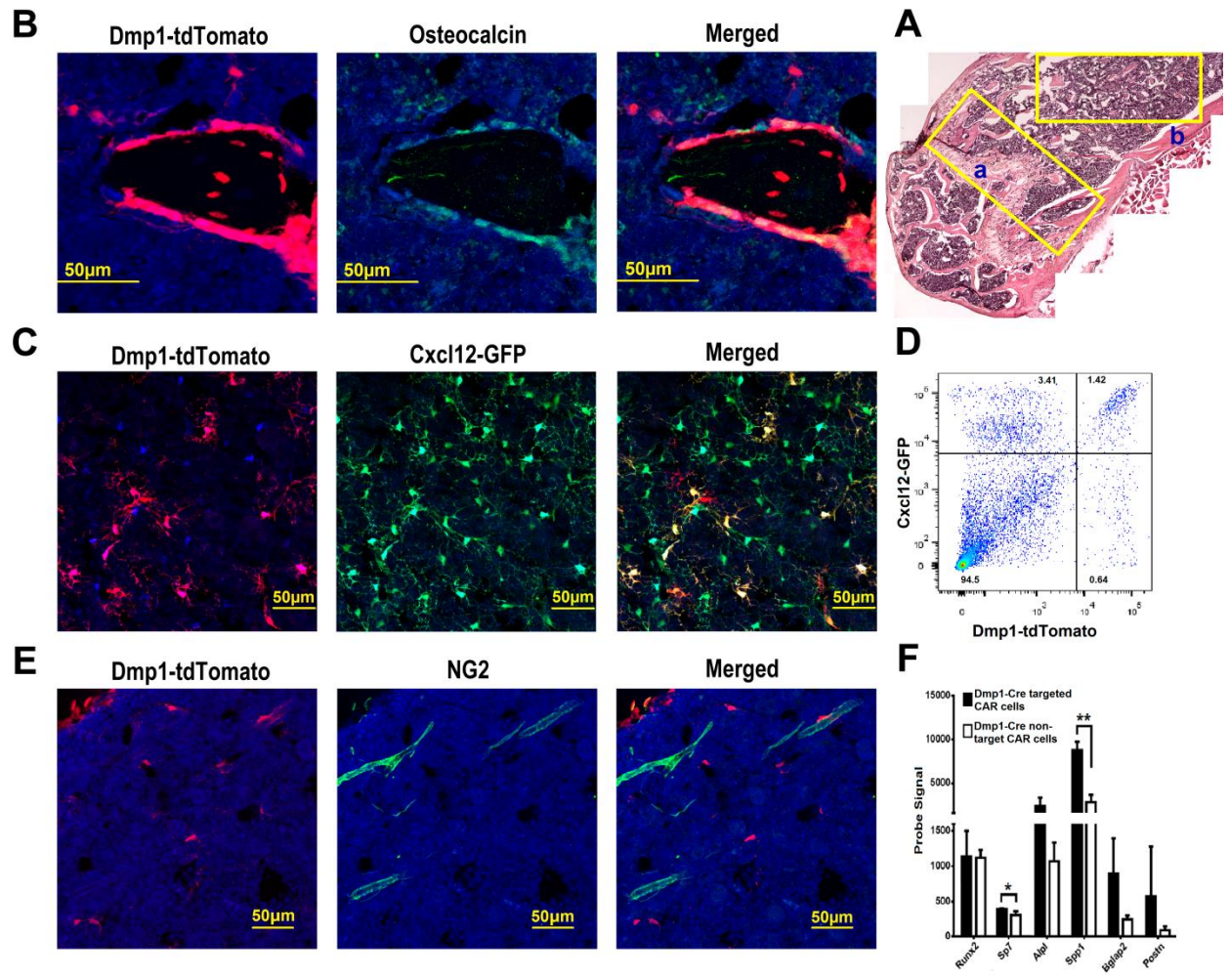


Figure 2.3. *Dmp1-Cre* targets all the osteoblasts and a subset of CAR cells but no arteriolar pericytes. (A) Composite image of H & E stained sections from the femur of a *Dmp1-Cre ROSA26^{Ai9/+}* mouse. (B) Representative photomicrographs of the metaphyseal region (region “a” in panel A) of a femur section that was stained for osteocalcin (green) and DAPI (blue). *Dmp1-Cre* targeted cells express tdTomato (red). (C) Representative photomicrographs taken from the diaphyseal region (similar to region “b” in panel A) of a femur section from a *Dmp1-Cre ROSA26^{Ai9/+} Cxcl12^{gfp/+}* mouse; cells that express CXCL12 also express GFP (green). (D) Representative dot plot showing GFP and tdTomato expression in lineage (CD45, CD31 and Ter119) negative stromal cells harvested from *Dmp1-Cre ROSA26^{Ai9/+} Cxcl12^{gfp/+}* mice. (E) Representative photomicrographs taken from the diaphyseal region of a femur section from a *Dmp1-Cre ROSA26^{Ai9/+} Cxcl12^{gfp/+}* mouse stained for NG2 (green) and DAPI (blue). (F) RNA expression profiling of sorted *Dmp1-Cre* targeted (tdTomato⁺) or non-targeted (tdTomato⁻) CAR cells was performed. Shown are probe signals for the indicated genes (n = 3 mice). All data represent the mean ± S.D. *P < 0.05; **P < 0.01 (unpaired t-test). Original magnification, 200X except for panel A, which is 100X.

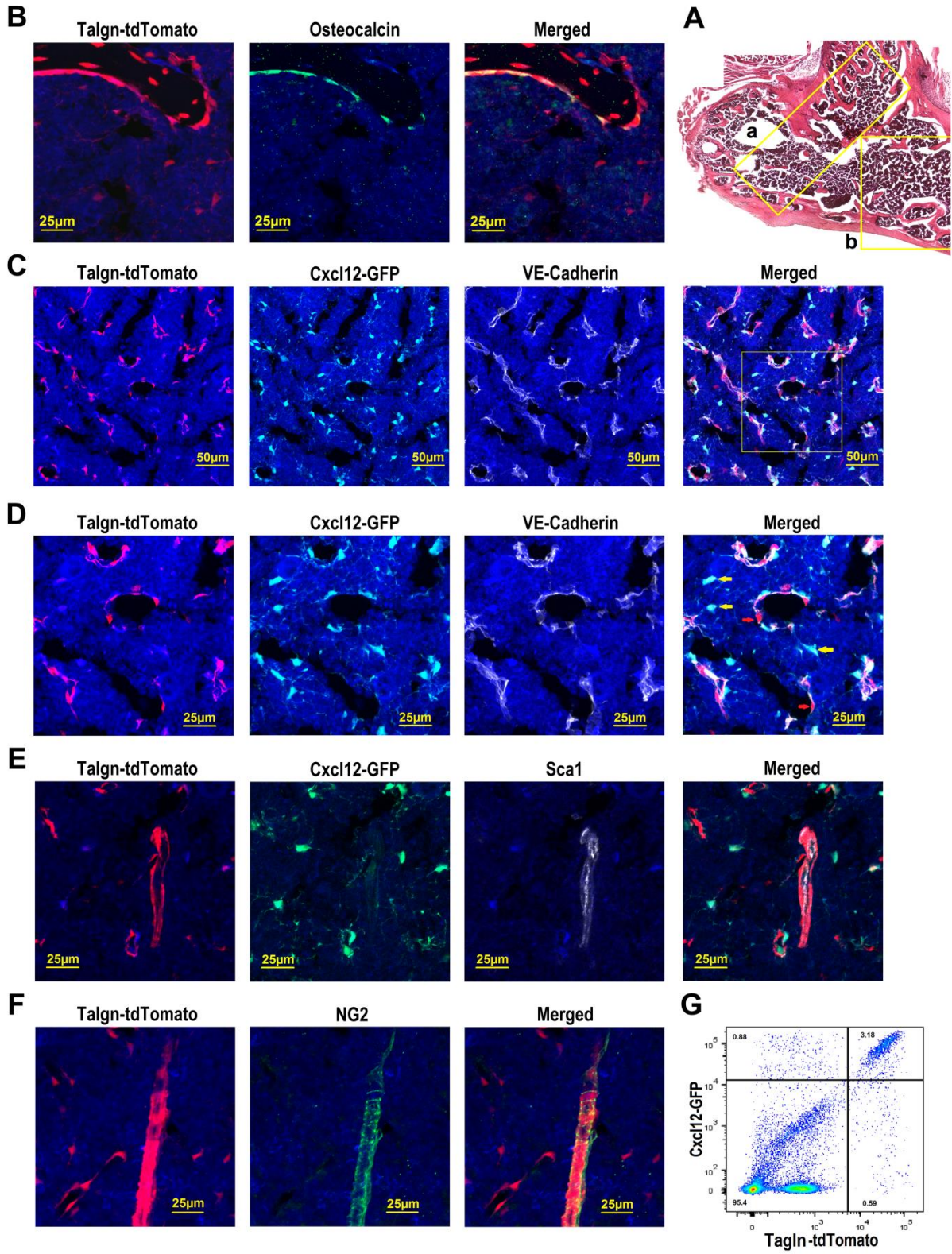
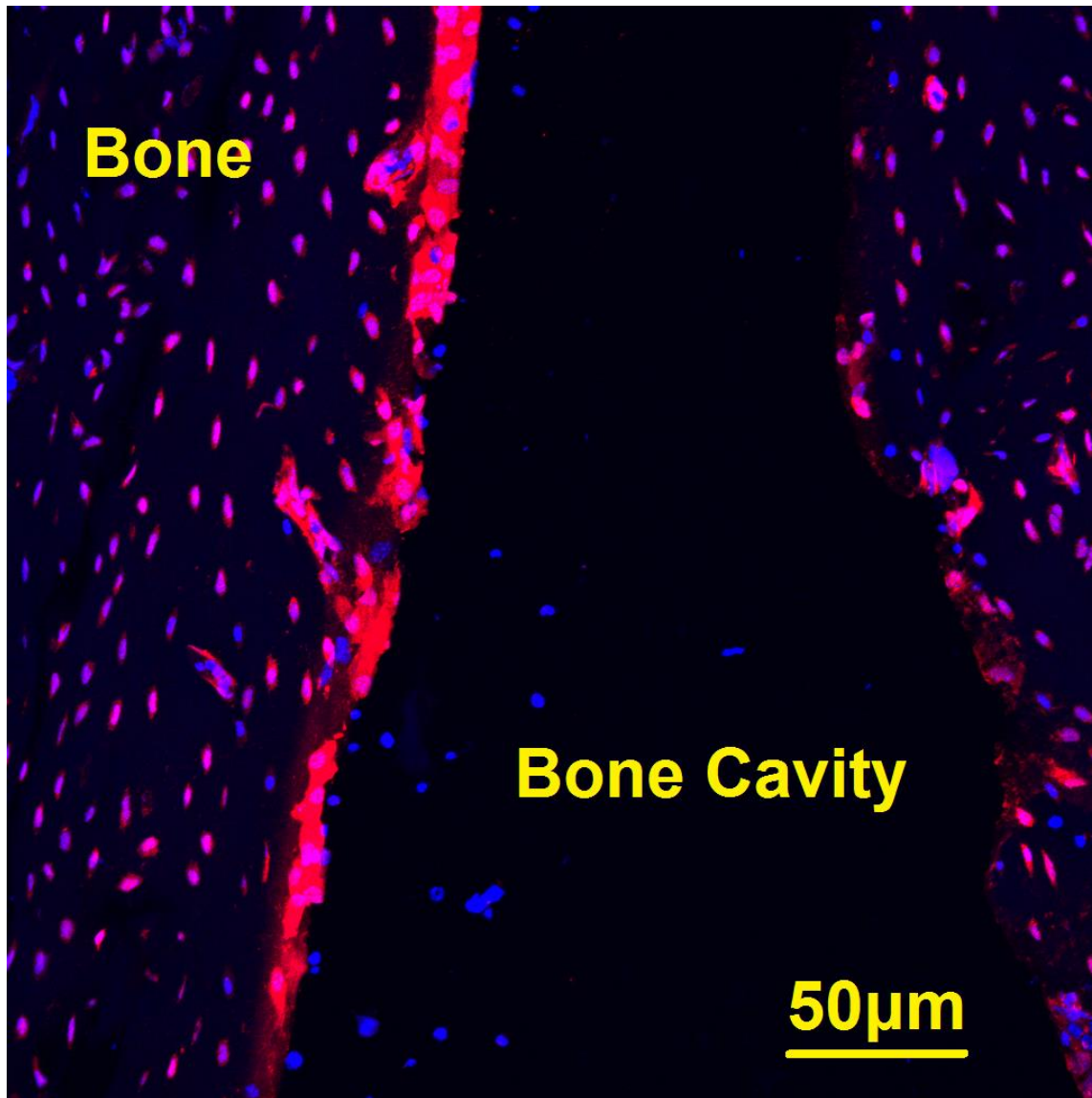
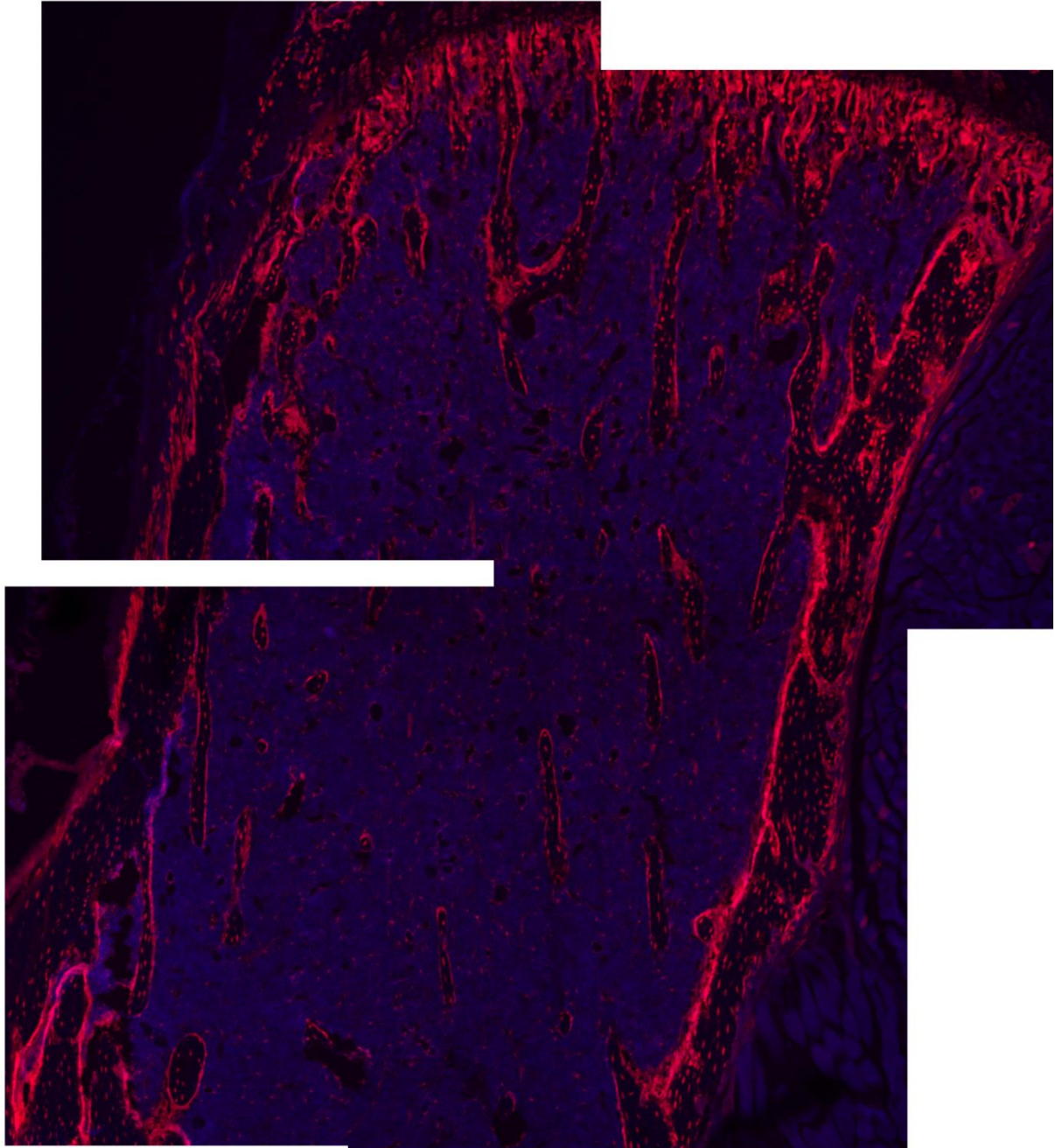


Figure 2.4. *Tagln-Cre* targets osteoblasts, a majority of CAR cells, and both venous sinusoidal and arteriolar pericytes. (A) Composite image of H & E stained sections from the femur of a *Tagln-Cre ROSA26^{Ai9/+}* mouse. (B) Representative photomicrographs of the metaphyseal region (region “a” in panel A) of a femur section that was stained for osteocalcin (green) and DAPI (blue). (C) Representative photomicrographs taken from the diaphyseal region (similar to region “b” in panel A) of a femur section from a *Tagln-Cre ROSA26^{Ai9/+} Cxcl12^{gfp/+}* mouse stained for VE-cadherin (white) to mark all endothelial cells; cells that express CXCL12 also express GFP (green). (D) Enlarged images of the boxed region in panel C. (E) Representative photomicrographs taken from the diaphyseal region of a femur section from a *Tagln-Cre ROSA26^{Ai9/+} Cxcl12^{gfp/+}* mouse stained for Sca1 (white) to mark arteriolar endothelial cells. (F) Representative photomicrographs taken from the diaphyseal region of a femur section from *Tagln-Cre ROSA26^{Ai9/+}* mouse stained for NG2 (green) to mark arteriolar pericytes. (G) Representative dot plot of lineage (CD45, CD31 and Ter119) negative stromal cells from a *Tagln-Cre ROSA26^{Ai9/+} Cxcl12^{gfp/+}* mouse showing GFP and tdTomato expression. Original magnification, 200X except for panel A, which is 100X.

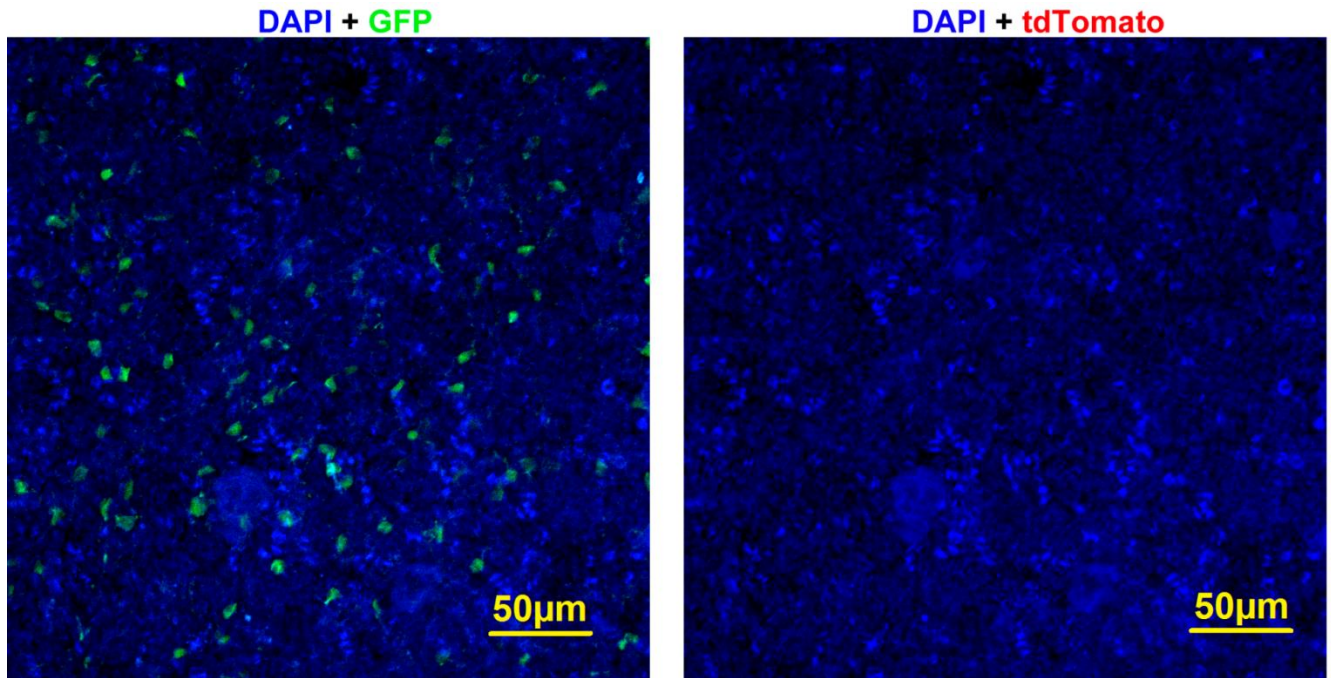
2.8. Supplementary Figures



Supplementary Figure 2.1. Osteoblasts remain attached to bone following centrifugation of femurs. Representative photomicrographs of a femur section from an *Ocn-Cre ROSA26^{Ai9/+}* mouse obtained after centrifugation to expel bone marrow contents. *Ocn-Cre* targeted cells express tdTomato (red). TdTomato⁺ cells lining bone are identified as osteoblasts. Nuclei are highlighted with DAPI (blue). Original magnification, 200X.

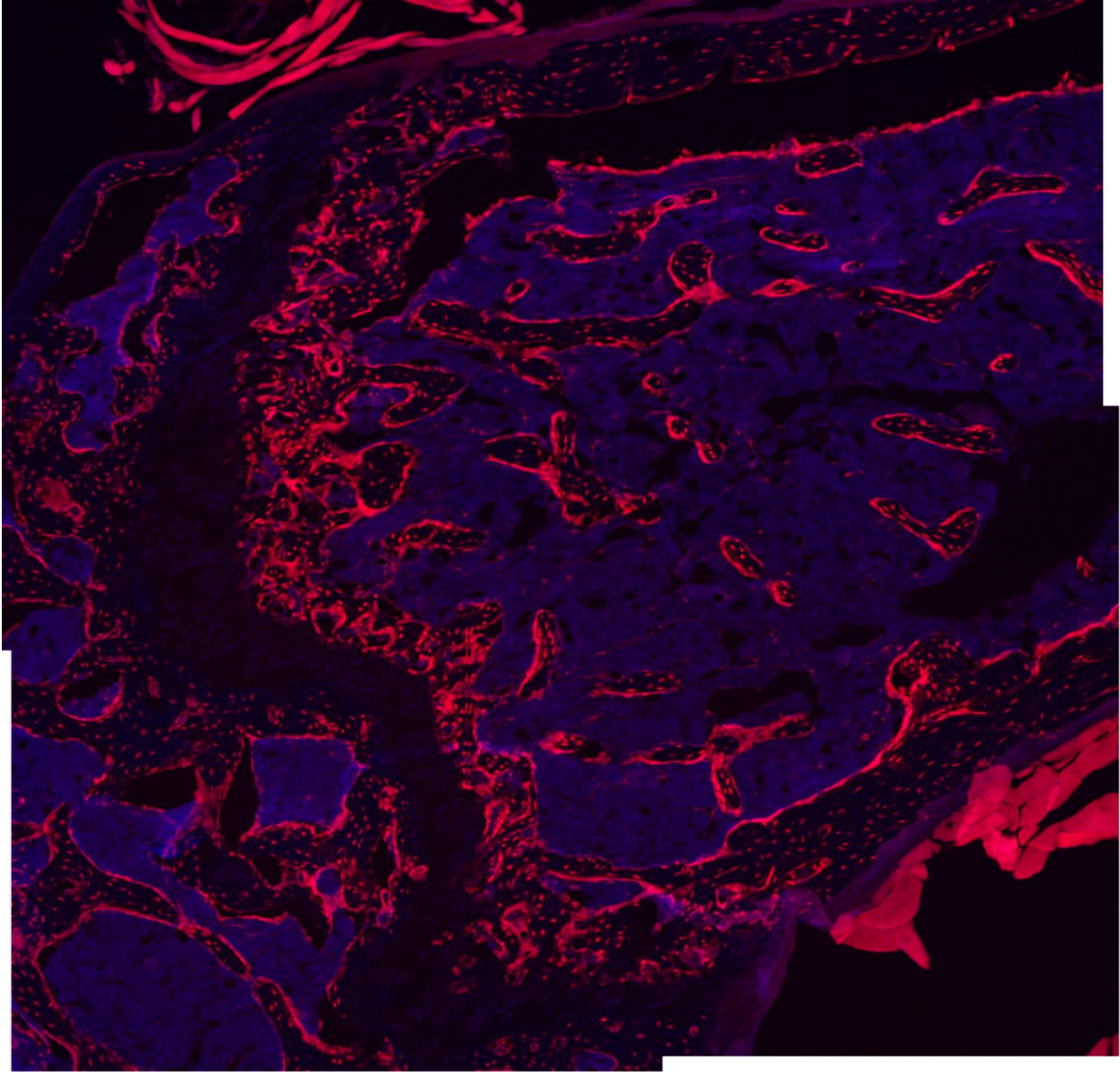


Supplementary Figure 2.2. *Ocn-Cre* efficiently targets osteoblasts. Composite image of representative photomicrographs from an *Ocn-Cre ROSA26^{Ai9/+}* mouse. Cells that have undergone *Cre*-mediated recombination express tdTomato (red); DAPI (blue) highlights nuclei. Tdtomato⁺ cells lining bone are identified as osteoblasts. Original magnification, 100X for all images.

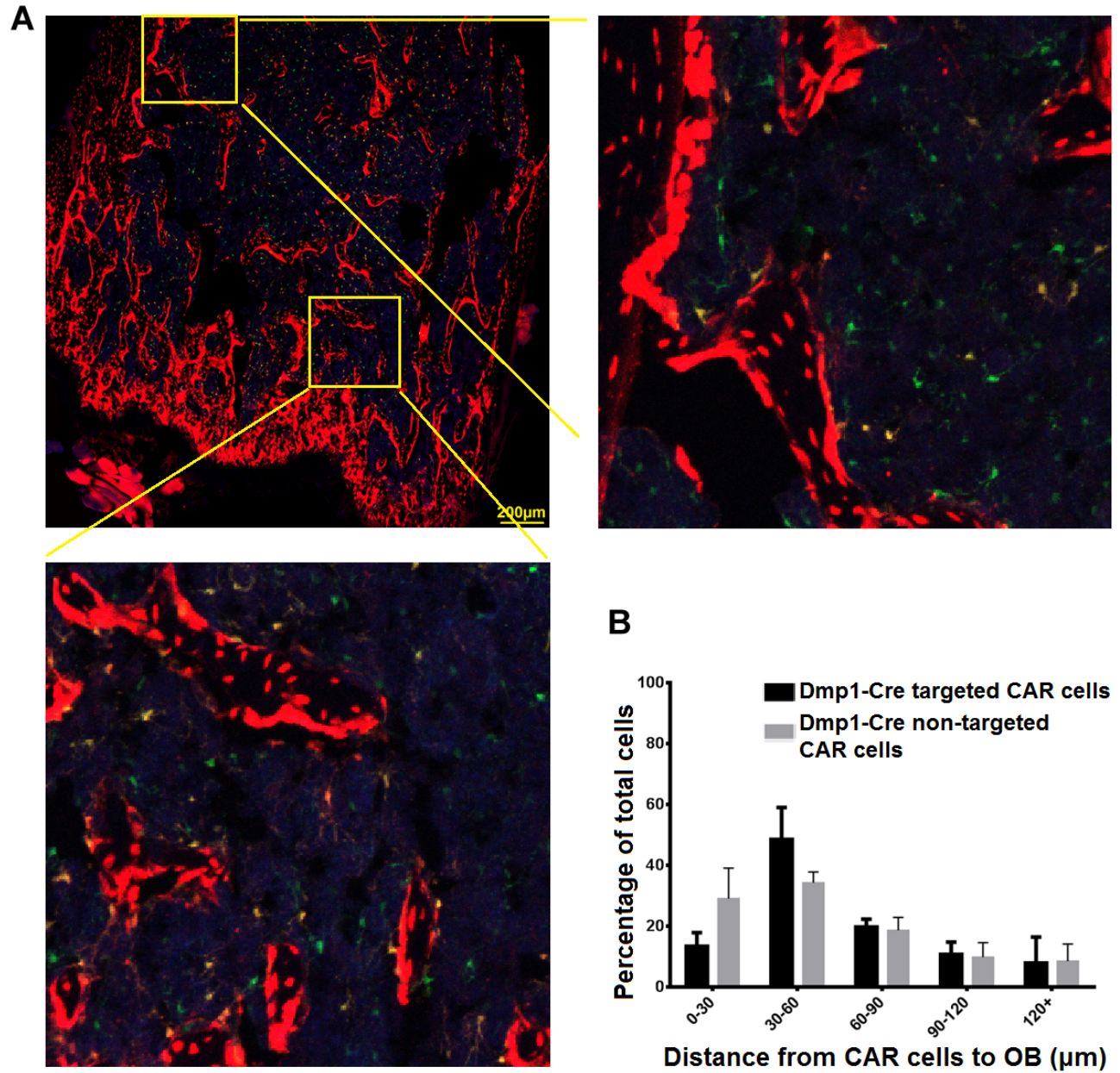


Supplementary Figure 2.3. Immunostaining of *Ocn-Cre Cxcl12^{gfp/+}* bone sections.

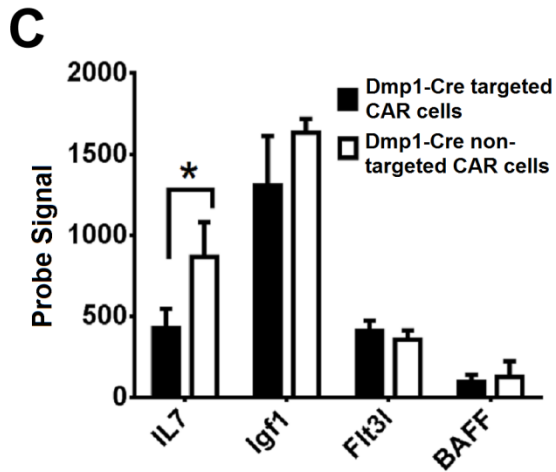
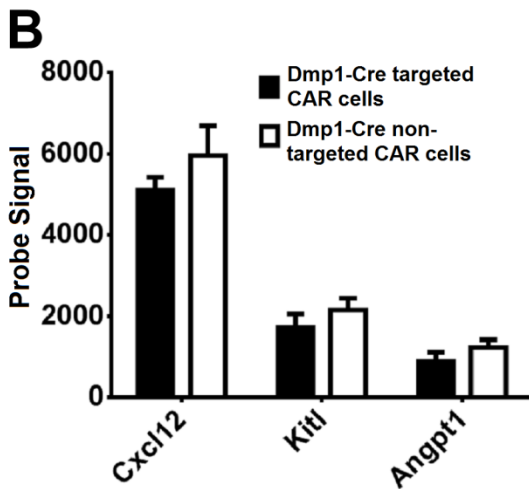
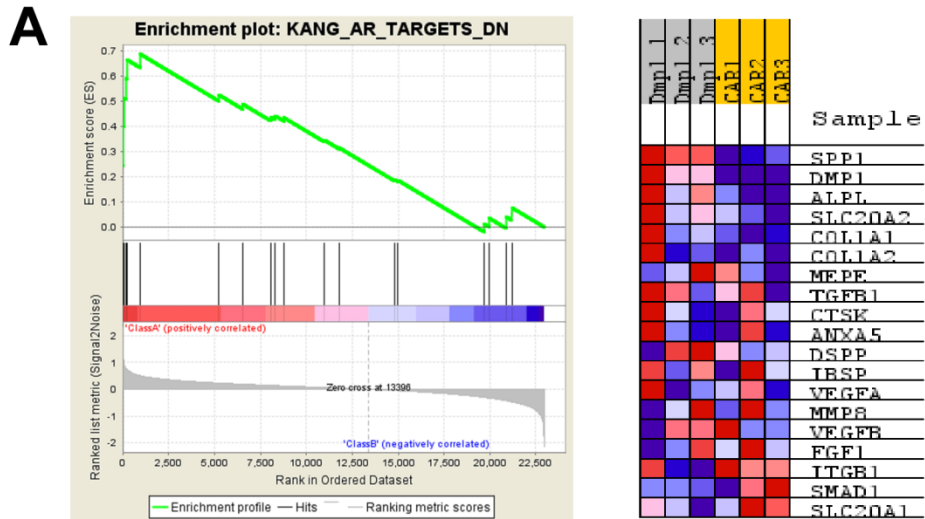
Representative photomicrographs taken from the diaphysis of a femur section from an *Ocn-Cre Cxcl12^{gfp/+}* mouse. GFP (left panel) and tdTomato (right panel) fluorescent signals are shown. Note, as expected, no tdTomato⁺ CAR cells are seen in these mice. Original magnification, 200X for all images.



Supplementary Figure 2.4. *Dmp1-Cre* efficiently targets osteoblasts. Composite image of representative photomicrographs from a *Dmp1-Cre ROSA26^{Ai9/+}* mouse. Cells that had undergone *Cre*-mediated recombination express tdTomato (red); DAPI (blue) highlights nuclei. Tdtomato⁺ cells lining bone are identified as osteoblasts. Original magnification, 100X for all images.

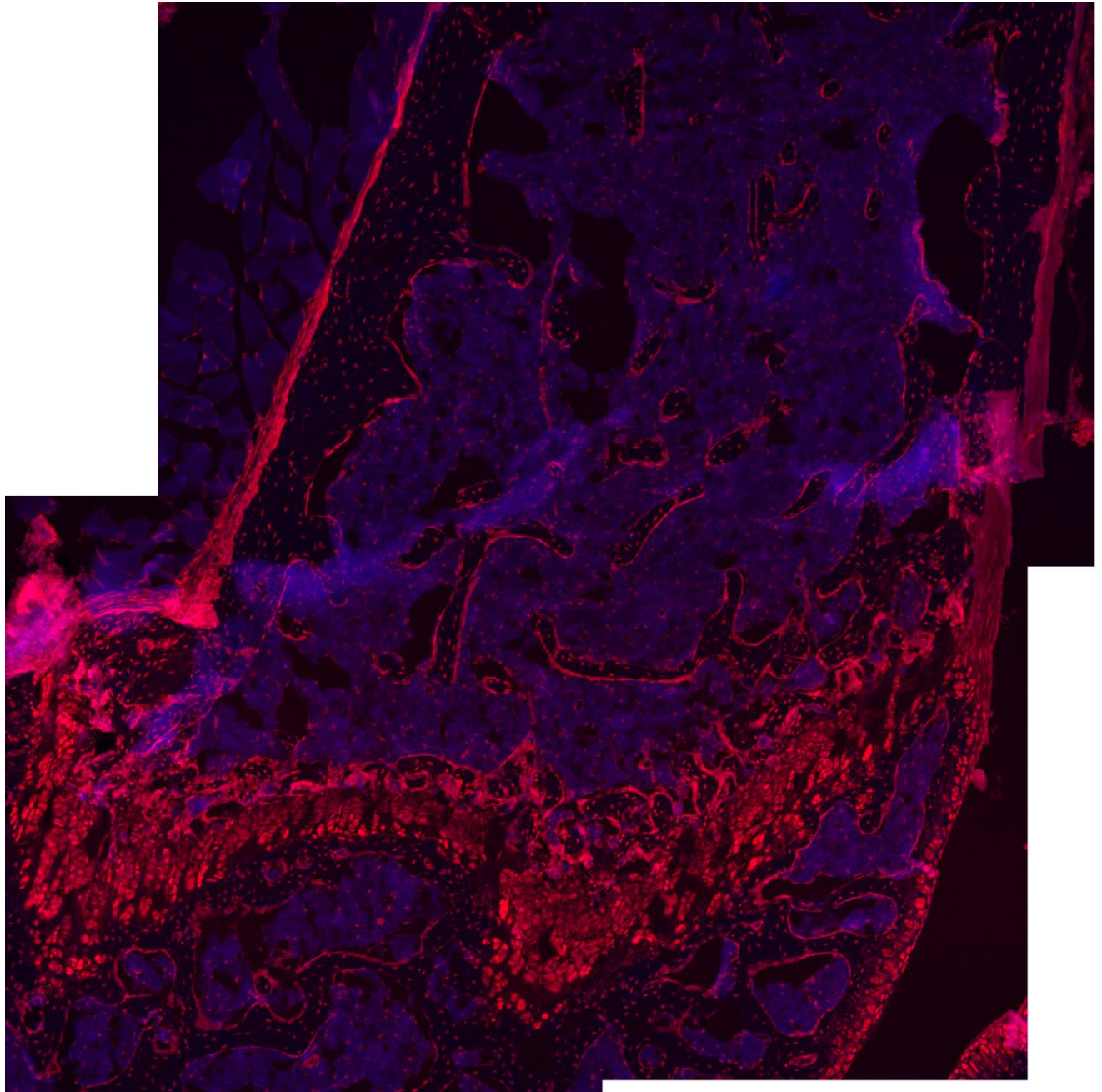


Supplementary Figure 2.5. Distribution of *Dmp1-Cre* targeted CAR cells. (A) Composite image of representative photomicrographs of a femur section from a *Dmp1-Cre ROSA26^{Ai9/+} Cxcl12^{gfp/+}* mouse (upper left panel). *Dmp1-Cre* targeted cells express tdTomato (red). Cells that express CXCL12 also express GFP (green). Counterstaining with DAPI highlights nuclei (blue). Higher magnifications of the highlighted regions are shown in the upper right and lower left panels. Original magnification, 100X for all images. (B) Percentage of *Dmp1-Cre* targeted and non-targeted CAR cells within a specified distance from the closest osteoblast (OB). Data represent the mean \pm S.D. n = 3 mice.



Supplementary Figure 2.6. RNA expression profiling of *Dmp1-Cre* targeted CAR cells.

Dmp1-Cre targeted (tdTomato⁺) and non-targeted CAR cells (tdTomato⁻) were sorted from *Dmp1-Cre ROSA26^{At9/+} Cxcl12^{gfp/+}* mice and RNA expression profiling was performed (n=3 mice). (A) Left panel is the gene set enrichment analysis (GSEA) plot showing enrichment for a previously identified group of osteoblast-lineage genes (p<0.001, FDR = 0.009). The right panel is a heat map for each gene in this group; red represents higher and blue represents lower expression. Samples “Dmp1 1, 2 and 3” represent *Dmp1-Cre* targeted CAR cell samples, while “CAR 1, 2 and 3” represent non-targeted CAR cell samples. (B) Expression of key genes associated with HSC maintenance. (C) Expression of key genes that support B lymphopoiesis. All data are presented as mean ± S.D. *, p-value < 0.05 (unpaired t-test).



Supplementary Figure 2.7. *Tagln-Cre* efficiently targets osteoblasts. Composite image of representative photomicrographs from a *Tagln-Cre ROSA26^{Ai9/+}* mouse. Cells that have undergone *Cre*-mediated recombination express tdTomato (red); DAPI (blue) highlights nuclei. Tdtomato⁺ cells lining bone are identified as osteoblasts. Original magnification, 100X for all images.

2.9. Supplementary Table

Primers for the detection of generic *Cre* transgene in *Ocn-Cre* and *Dmp1-Cre* mice.

Primer Name	Primer Sequence (5' -> 3')
Cre FOR	GCATTACCGGTCGATGCAACGAGTGATGAG
Cre REV	GAGTGAACGAACCTGGTCGAAATCAGTGCG

Primers for the detection of *Cxcl12^{sfp}* transgene.

Primer Name	Primer Sequence (5' -> 3')
CXCL12-GFP FOR	GGACTGGGAAGATCAAAGGTC
CXCL12-GFP mutant REV	GAACTTCAGGGTCAGCTTGC
CXCL12-GFP wt REV	GGTGGACCGAGAGTGAAAGT

Primers for the detection of *ROSA26^{Ai9}* transgene.

Primer Name	Primer Sequence (5' -> 3')
Ai9 wt FOR	AAGGGAGCTGCAGTGGAGTA
Ai9 wt REV	CCGAAAATCTGTGGGAAGTC
Ai9 mutant REV	GGCATTAAAGCAGCGTATCC
Ai9 mutant FOR	CTGTTCTGTACGGCATGG

Primers for the detection of the *Tagln-Cre* transgene.

Primer Name	Primer Sequence (5' -> 3')
Tagln-Cre FOR	GGCCCAGGGGTTGTCAAATAGTC
Tagln-Cre wt REV	CTCCTCCAGCTCCTCGTCATACTTC
Tagln-Cre mutant REV	CGCCGCATAACCAGTGAAACAG

Supplementary Table 2.1. Primers for genotyping transgenic mice in this study. “FOR” means forward primer and “REV” means reverse primer. “mutant” represents the primers used for the detection of a transgene and “wt” represents the primers used for the detection of the wild type allele at the corresponding locus for that transgene.

CHAPTER 3: CXCL12 FROM *OCN-CRE* TARGETED BONE MARROW STROMAL CELLS REGULATES LATE-STAGE B CELL DEVELOPMENT

3.1. Introduction

CXCL12 is a common chemokine found in the bone marrow that is important for the regulation of B lymphopoiesis. CXCL12 interacts with its main receptor, CXCR4, to activate multiple signaling pathways responsible for the control of chemotaxis, cell proliferation and cell survival^{20,169,170}. In the bone marrow, mesenchymal stromal cells, especially CAR cells are the main source of CXCL12^{3,10}. CAR cells are a heterogeneous population and previous studies have tested multiple transgenic Cre mouse models for targeting different subsets of CAR cells^{3,19}. Among these Cre models, *Prx1-Cre* and *Osx-Cre* target nearly all CAR cells, while *Prx1-Cre* targets additional mesenchymal stem cells³. In contrast, *Ocn-Cre* and *Dmp1-Cre* targets around 70% and 30% of CAR cells, respectively¹⁹. A prior study has suggested the specific role of *Dmp1-Cre* targeted CAR cells as being enriched for potential osteoprogenitors, but the specific functions of *Ocn-Cre* targeted CAR cells have not yet been discussed¹⁹.

In humans and mice, B lymphopoiesis mainly occurs in the bone marrow, with the additional requirement of peripheral lymphoid organs²³. B cell development undergoes a stepwise progression of stages which can be identified based on surface marker expression²⁴. Hardy Fractions have been extensively used to identify different stages of B cells, and Fraction F describes the last stage of B cell development before maturation, the mature naive B cells that express IgD^{26,28-30}. In response to stimulation, such as antigen exposure, mature B cells will further differentiate into anti-body secreting plasma cells (PCs) or memory cells³². Memory cells may include memory B cells and memory PCs, also known as long-lived PCs, both have been

suggested to potentially reside in the bone marrow³²⁻³⁶. So far, only limited research has been done to study the functions and regulations of mature naive B cells, memory B cells and memory PCs in the bone marrow.

In the present study, we used different transgenic Cre models to test the regulation of B cell development by CXCL12 from different subsets of stromal cells. We show that CXCL12 expressed by *Ocn-Cre* targeted stromal cells may be specifically important for the regulation of mature naive B cells and memory B cells in bone marrow. Collectively, data from this study may provide insight into the complex relationships between different stromal cell populations and may improve our understanding of the regulation of B lymphopoiesis and immune memory in the bone marrow by CXCL12.

3.2. Materials and Methods

3.2.1. Mouse strains

Cxcl12^{fllox} mice were generated as previously described³. *Prx1-Cre* (B6.Cg-Tg(Prrx1-cre)1Cjt/J) mice, *Osx-Cre* (B6.Cg-Tg(Sp7-tTA,tetO-EGFP/cre)1Amc/J) mice, *CAG-GFP* (Tg(CAG-GFP*)1Hadj/J) mice, *IgHa/J* (B6.Cg-Gpi1^a Thy1^a Igh^a/J) mice and *Ai9* (B6.Cg-Gt(ROSA)26Sor^{tm9(CAG-tdTomato)Hze/J})²⁵⁴ mice were obtained from The Jackson Laboratory²⁵⁵. *Ocn-Cre* mice were a gift from Thomas Clemens (Johns Hopkins University, Maryland)²⁵⁶. *Cxcl12*^{gfp} mice were a gift from Takashi Nagasawa (Kyoto University, Japan)²⁵⁷, and *Dmp1-Cre* mice (containing the 9.6 kb murine *Dmp1* promoter) were a gift from Roberto Civitelli (Washington University, MO)²⁵⁸. *Cxcl12*^{+/-} mice were obtained through the RIKEN BioResource Center (Ibaraki, Japan). All mice used in this study were 8-10 weeks old. Both male and female mice were used equally in these studies. Mice were maintained under SPF

conditions, and all experimental procedures were performed according to methods approved by the Animal Studies Committee at Washington University.

3.2.2. Immunostaining of bone sections

Femurs and tibias were harvested from mice and fixed overnight in 10% formalin (Sigma-Aldrich) at 4°C. Fixed bones were then washed twice in PBS, followed by decalcification in 14% ethylenediaminetetraacetic acid (EDTA) pH 7.4 solution for 7 days. Decalcified bones were then incubated in 30% sucrose in PBS overnight at 4°C. These bones were then snap frozen in optimum cutting temperature (OCT) medium (Tissue-Tek) in Cryomold (Tissue-Tek). Frozen blocks were sectioned using the Cryostat system (Leica Biosystems). Sections were then processed using standard immunofluorescent staining protocol. Antibodies used for immunofluorescent staining included: goat anti-mouse VE-Cadherin (R&D Systems AF1002), rat anti-mouse IgD (BD Biosciences clone 11-26c.2a), rat anti-mouse B220 (BD-Biosciences, RA3-6B2), and rat anti-mouse IgM (eBioscience II/4). In the end, slides were mounted with Prolong Gold Antifade Reagent (Invitrogen) and were sealed with nail polish. Slides were imaged using a LSM 700 confocal microscope and ZEN imaging software (Zeiss).

3.2.3. Flow Cytometry

Bone marrow cells were harvested from mouse femurs by first uncapping the ends of the bone and then centrifuging at 3300 x g for 5 minutes to expel the bone marrow contents. Spleen cells were harvested from mouse spleen by crushing spleen and filter the cells through a 22um strainer. Cells were stained by standard protocols with the following antibodies (eBiosciences unless otherwise noted): CD3e (145-2C11), CD4 (L3T4), CD8a (53-6.7), CD11b (M1/70),

CD45R (RA3-6B2, B220), CD11c (N418), Flk2 (A2F10), CD27 (LG.7F9), Gr-1 (RB6-8C5, BioLegend), IL-7Ra (gift of Deepta Bhattacharya, Washington University), Ly6D (49-H4, BD Biosciences), NK1.1 (PK136), IgM (II/4), IgD (11-26c), CD19 (eBio1D3), CD43 (S7, BD Biosciences), TER-119, CD45 (30-F11), CD31 (390), CD80 (16-10A1, BioLegend), CCR6 (29-2L17, BioLegend). NP (4-Hydroxy-3-nitrophenylacetyl hapten) (Biosearch Technologies) was conjugated with Allophycocyanin (APC) to form NP-APC (gift of Deepta Bhattacharya, Washington University). Cells were analyzed on a Gallios flow cytometer (Beckman Coulter), and data analysis was done using FloJo version 10.0.7 software (TreeStar).

3.2.4. Quantitative real-time PCR

To collect total bone marrow RNA, tibias from mice were flushed with 1 mL of Trizol (Invitrogen) and RNA was extracted following the manufacturer's instructions. cDNA was prepared using iScript cDNA Synthesis Kit (Bio-Rad). Quantitative real-time PCR (qRT-PCR) was then performed using the TaqMan Universal RT Master Mix (Applied Biosystems), with no template and no RT controls. Data was collected on a OneStep Real-Time PCR System (Applied Biosystems). Primers were:

CXCL12 forward, 5'-GAGCCAACGTCAAGCATCTG-3';

CXCL12 reverse, 5'-CGGGTCAATGCACACTTGTC-3';

CXCL12 dT-FAM/TAMRA probe, 5'-TCCAAACTGTGCCCTTCAGATTGTTGC-3';

β -actin forward, 5'-ACCAACTGGGACGATATGGAGAAGA-3';

β -actin dT-VIC/TAMRA probe, 5'-AGCCATGTACGTAGCCATCCAGGCTG-3'.

3.2.5. Mature B cell homing assay

Spleens were harvested from 8-12 week old *CAG-GFP* mice, and were then crushed and filtered through a 22um cell strainer. 5 million splenocytes were injected into *Cxcl12^{flox/-}* or *Ocn-Cre: Cxcl12^{flox/-}* mice, through retro-orbital injection. Recipient mice were then harvested 24 hours after transplantation to collect bone marrow and spleen using the same method as described earlier. GFP⁺ mature naive B cell number was quantified via flow cytometry.

3.2.6. Primary and secondary immunization

Ocn-Cre:Cxcl12^{flox/flox} or *Cxcl12^{flox/flox}* mice were immunized with a mixture of 100 µg NP-CGG (Chicken Gamma Globulin) (Biosearch Technologies) and 100 µl of aluminium hydroxide gel adjuvant (Alhydrogel) (InvivoGen), through intraperitoneal injection. The enzyme-linked immunosorbent assay (ELISA) was then performed to test primary immune response. Immune memory was measured 2 weeks after primary immunization. For secondary immunization, 20 million donor cells from NP-CGG immunized *Ocn-Cre:Cxcl12^{flox/flox}* or *Cxcl12^{flox/flox}* mice were transplanted into *IgHa/J* recipient mice without irradiation, through retro-orbital injection. One day after transplantation, 50 µg of NP-CGG was injected into these recipient mice, through retro-orbital injection. Secondary immune response was then measured with ELISA.

3.2.7. Enzyme-linked immunosorbent assay (ELISA)

ELISA plates were coated with 5 µg/ml NP (18)-BSA protein, or 5 µg/ml BSA as control, overnight at 4 °C. Then, block the ELISA plates with ELISA blocking buffer (PBS + 2% BSA + 0.05% Tween20) at 37 °C for 1 hour. Wash plates, add diluted serum samples, serially diluted

standard controls or negative controls into ELISA plates, incubate at room temperature for 2 hours. For primary immune response, add anti-mouse IgM antibody (Life Technologies) and incubate at room temperature for 1 hour. Wash plates, then add HRP-goat anti-mouse IgM (Life Technologies) and incubate at room temperature for 1 hour. Then, develop the plate in TMB solution (eBioscience) and stop the reaction with stop buffer (eBioscience). Read the plates at 450nm wavelength, using an Epoch Microplate Spectrophotometer (BioTek).

For measuring secondary immune response, after incubating the plate with serially diluted serum samples, add biotinylated anti-IgG1b (BD Pharmingen) or biotinylated anti-IgG1a (BD Pharmingen) antibodies into the plates, incubate at room temperature for 1 hour. Wash plates, add streptavidin-HRP (BD Pharmingen), incubate at room temperature for 1 hour. Then, use the same protocol as for measuring primary immune response to develop the plates.

3.2.8. Statistical analyses

Statistical significance was determined using Prism software (GraphPad). Unless otherwise indicated, unpaired t-test or 1/2-way ANOVA analyses were used to evaluate the significance of differences between two or multiple groups. All data are presented as mean \pm SEM.

3.3. Results

3.3.1. *Ocn-Cre* targeted stromal cells regulate mature naive B cells in bone marrow

To assess the role of CXCL12 expressed by different subsets of bone marrow stromal cells in B cell lymphopoiesis, we previously crossed different transgenic Cre models with *Cxcl12^{fllox/-}* mice (experiments done by Ryan Day). *Prx1-Cre* was used to ablate CXCL12 from nearly all bone marrow stromal cells as it targets mesenchymal stem cells and their downstream progeny, including CAR cells, osteoblasts and osteocytes³. As expected, ablation of CXCL12 in *Prx1-Cre* targeted stromal cells significantly reduced the mRNA level of CXCL12 to a minimal level in the bone marrow (Fig. 3.1A). Meanwhile, we observed significant decrease in white blood cells (WBCs) and all stages of B cells during B lymphopoiesis in the bone marrow (Fig. 3.1B-J). *Osx-Cre* was used to target CAR cells and their downstream progeny, including osteoblasts and osteocytes³. Ablation of CXCL12 in *Osx-Cre* targeted stromal cells resulted in a significant reduction of CXCL12 mRNA level, but to a lesser extent compared to *Prx1-Cre:Cxcl12^{fllox/-}* model (Fig. 3.1A). Similar to *Prx1-Cre:Cxcl12^{fllox/-}* mice, we observed significant decrease in WBCs and total B cells, as well as in other stages during B cell development, except in common lymphoid progenitors (CLPs) and B lymphoid restricted progenitors (BLPs) (Fig. 3.1B-J). This is consistent with our previous finding that CXCL12 expressed by *Prx1-Cre* targeted mesenchymal stem cells is important for the development and maintenance of CLPs and BLPs³. *Ocn-Cre* targets ~70% of CAR cells, all osteoblasts and arteriolar pericytes¹⁹. Interestingly, ablation of CXCL12 in *Ocn-Cre* targeted cells resulted in a mild, but non-significant reduction of CXCL12 mRNA level (Fig. 3.1A). Moreover, *Ocn-Cre:Cxcl12^{fllox/-}* mice showed no significant decrease of WBCs, total B cells and most stages of B cell development, except mature naive B cell or Fraction F cells (Fig. 3.1B-J). To address the question whether the mild decrease of CXCL12 in

Ocn-Cre:Cxcl12^{fllox/-} mice may affect mature naive B cells, we further examined *Prx1-Cre:Cxcl12^{fllox/+}* mice. Our data shows that the two models have nearly the same expression levels of CXCL12, but *Ocn-Cre:Cxcl12^{fllox/-}* mice have a significantly lower number of mature naive B cells (Fig. 3.1K&L). Collectively, these data suggests that CXCL12 from *Ocn-Cre* targeted cells may play a specific role in the regulation of mature naive B cells in the bone marrow.

To more specifically assess the role of CXCL12 expressed by *Ocn-Cre* targeted cells, we further generated *Ocn-Cre:Cxcl12^{fllox/fllox}* mice. In these mice, we observed a significant, but mild reduction of CXCL12 mRNA level, compared to *Cxcl12^{fllox/fllox}* control mice (Fig. 3.2A). Meanwhile, we observed significant decrease of mature naive B cells, while other stages of B cell development remain unchanged (Fig. 3.2B). *Dmp1-Cre* targets ~30% of CAR cells, all osteoblasts and few arteriolar pericytes¹⁹. In *Dmp1-Cre:Cxcl12^{fllox/fllox}* mice, we observed no significant decrease in CXCL12 mRNA level and all stages of B cell development (Fig. 3.2C&D). Comparing data from *Dmp1-Cre:Cxcl12^{fllox/fllox}* and *Ocn-Cre:Cxcl12^{fllox/fllox}* mice, it suggests that the expression of CXCL12 by osteoblasts plays little role in the regulation of mature naive B cells, and *Ocn-Cre* targeted stromal cells specifically regulate mature naive B cells through their expression of CXCL12.

3.3.2. CXCL12 expression in *Ocn-Cre* targeted stromal cells regulates the homing and/or retention of mature naive B cells in the bone marrow

Mature naive B cells were mostly developed in the spleen and some of them home back to the bone marrow^{26,28-30}. In *Ocn-Cre:Cxcl12^{fllox/-}* mice, the number of mature naive B cells in the

spleen was comparable to the *Cxcl12^{flox/-}* control mice (Fig. 3.3A). This observation suggests that the loss of mature naive B cells in the bone marrow of *Ocn-Cre:Cxcl12^{flox/-}* mice is not likely due to a defect in peripheral maturation. To examine the homing and/or retention of mature naive B cells in the bone marrow, we transplanted splenocytes from *CAG-GFP* donor mice that ubiquitously express GFP into *Ocn-Cre:Cxcl12^{flox/-}* mice or *Cxcl12^{flox/-}* control mice (Fig. 3.3B). After 24 hours, the recipient mice were harvested and the number of GFP⁺ mature naive B cells was quantified in both bone marrow and spleen, using flow cytometry (Fig. 3.3C&D). While there was no significant difference in spleen (Fig. 3.3C), the number of GFP⁺ mature naive B cells was significantly reduced in the bone marrow of *Ocn-Cre:Cxcl12^{flox/-}* mice (Fig. 3.3D). Collectively, these data demonstrate that CXCL12 expression in *Ocn-Cre* targeted stromal cells plays an important role in the regulation of homing and/or retention of mature naive B cells in the bone marrow.

3.3.3. Ablation of CXCL12 in *Ocn-Cre* targeted stromal cells did not affect bone marrow plasma cells and primary immune response

Other than Hardy fractions of B cells during different developmental stages, plasma cells (PCs) and memory B cells, two terminal stage B cells have also been found in the bone marrow^{32,35,36}. To assess the effects of stromal CXCL12 ablation on plasma cells in the bone marrow, femurs from *Ocn-Cre:Cxcl12^{flox/flox}* mice and *Cxcl12^{flox/flox}* control mice were harvested and analyzed. Using flow cytometry, we discovered no significant difference after stromal CXCL12 ablation, for the numbers of IgM⁺ or IgG⁺ PCs, defined as B220⁺ CD138⁺ cells (Fig. 3.4A&B). To functionally assess the effects of stromal CXCL12 ablation on PCs, we examined

the humoral immunity after antigen exposure in the two groups of mice. *Ocn-Cre:Cxcl12^{flx/flx}* mice and *Cxcl12^{flx/flx}* control mice were immunized with NP-CGG (1:19 ratio), and we quantified the humoral immune response by measuring the amount of NP-specific IgM antibodies in blood serum using ELISA. At different time points, we found no significant change on the NP-specific IgM levels in blood serum after stromal CXCL12 ablation (Fig. 3.4C). Collectively, these data suggests that the ablation of CXCL12 in *Ocn-Cre* targeted stromal cells does not affect the number of PCs in the bone marrow and the humoral immunity.

3.3.4. Ablation of CXCL12 in *Ocn-Cre* targeted stromal cells reduces the number of memory B cells in the bone marrow

To assess the effects of CXCL12 ablation in *Ocn-Cre* targeted stromal cells on memory B cells, we immunized *Ocn-Cre:Cxcl12^{flx/flx}* mice and *Cxcl12^{flx/flx}* control mice with NP-CGG (1:19 ratio). Two months after immunization, we quantified the number of NP-specific memory B cells in the bone marrow using flow cytometry. NP-specific memory B cells were defined as NP⁺ Lin⁻ B220⁺ IgM⁻ IgD⁻ CCR6⁺ CD80⁺ cells, and we observed a significant reduction of the memory B cells when CXCL12 was ablated in the bone marrow (Fig. 3.5A). In addition, we quantified the number of NP-specific memory B cells in the spleen from the same mice and found no significant differences (Fig. 3.5B). Collectively, these data demonstrates the importance of CXCL12 expressed by *Ocn-Cre* targeted stromal cells in the regulation of memory B cells in the bone marrow.

To our surprise, a population of NP⁺ Lin⁻ B220⁺ IgM⁺ IgD⁺ CCR6⁺ CD80⁺ cells was found in the bone marrow whose number was decreased in *Ocn-Cre:Cxcl12^{flx/flx}* mice, compared to

Cxcl12^{flx/flx} control mice (Fig. 3.5C). Same population was also found in the spleen, but had no decrease when stromal CXCL12 was ablated (Fig. 3.5D). The potential existence of IgM⁺ IgD⁺ memory B cells was previously discussed by other studies^{179,184,185}. To test whether these cells may carry similar functions as the conventional memory B cells that are IgM⁻ IgD⁻, we assessed the secondary immune response generated from these cells. Wildtype mice were immunized with NP-CGG to generate memory B cells and we collected unenriched cells, IgM⁺ and IgD⁺ enriched cells (including IgM⁺ IgD⁺ cells), and IgM⁻ IgD⁻ enriched cells from these mice at 2 months post immunization. All three samples of cells were then transferred into IgHa/J recipient mice through retro-orbital injection, followed by secondary immunization of NP-CGG one day after transplant. IgHa/J mice only express IgG1a but not IgG1b which is the only isotype expressed by the donor mice. One week after secondary immunization, ELISA was used to quantify the amount of NP-specific IgG1b in these recipient mice to estimate the secondary immune response generated from the donor memory cells. Our preliminary data showed that IgM⁺ and IgD⁺ enriched cells from both bone marrow and spleen could not generate significant secondary immune response, suggesting IgM⁺ IgD⁺ cells play little role in the B cell immune memory (Fig. 3.5E).

3.4. Discussion

We have previously shown the importance of CXCL12 in the regulation of B lymphopoiesis in the bone marrow³. We have demonstrated the requirement of CXCL12 expression from mesenchymal stem cells for the maintenance of CLPs and BLPs, while CXCL12 expression from CAR cells are not required for early B lymphopoiesis until pre-pro-B cell stage³. This study further characterizes the role of CXCL12 expression from different subsets of stromal cells on B

lymphopoiesis. Our data shows that CXCL12 expression from *Ocn-Cre* targeted cells are specifically important for the maintenance of mature naive B cells. We also ablated CXCL12 in *Dmp1-Cre* targeted cells and found no effects on mature naive B cells or other B cell compartments. A prior study has shown that both *Ocn-Cre* and *Dmp1-Cre* targets nearly all osteoblasts, and about 70% or 30% of CAR cells, respectively¹⁹. Moreover, *Ocn-Cre*, but not *Dmp1-Cre*, targets arteriolar pericytes¹⁹. Thus, CXCL12 expression by *Ocn-Cre* targeted stromal cells, but not osteoblasts, regulates mature naive B cells. To further understand this regulation, we examined the homing and/or retention of mature naive B cells in *Ocn-Cre:Cxcl12^{flox/-}* mice, and observed a significant defect, compared to the control mice.

In addition, we also examined the effects of CXCL12 ablation in *Ocn-Cre* targeted stromal cells on two end-stage B cells, plasma cells and memory B cells in the bone marrow. We observed no significant decrease of plasma cells in *Ocn-Cre:Cxcl12^{flox/flox}* mice, while IgM⁻ IgD⁻ NP-specific memory B cells were significantly reduced. To confirm this finding, further experiments will be performed to test whether there is a functional defect of NP-specific immune memory in the bone marrow. Interestingly, we also discovered an IgM⁺ IgD⁺ NP-specific B cell population in the bone marrow, expressing similar markers as the conventional memory B cells. To test the function of these cells, we performed secondary immunization and assessed the secondary immune response generated by these cells. Our data suggests that these cells play little role in the generation of secondary immune response, and their functions remain unclear.

In conclusion, our data show that CXCL12 expression by *Ocn-Cre* targeted stromal cells may specifically regulate mature naive B cells and memory B cells. This study provides further evidence to support the functional heterogeneity of bone marrow mesenchymal stromal cells, which may improve our knowledge on the regulation of the bone marrow niche. Meanwhile,

better understanding of the regulation of B lymphopoiesis and B cell derived immune memory may provide targets with clinical relevance, contributing to the development of potential therapies against different diseases involved in the bone marrow.

3.5. Acknowledgements

We thank Amy Schmidt and Rachel Ye for technical assistance, and Jackie Tucker-Davis for animal care. This work was supported by RO1 HL60772 (DCL) and P50 CA171963 (DCL).

3.6. Author Contributions

Jingzhu Zhang, Ryan Day and Daniel C. Link conceived and designed the experiments, and analyzed the data. RD performed the experiments using *Ocn-Cre:Cxcl12^{flox/-}* and *Cxcl12^{flox/-}* mice. JZ performed all the rest experiments. DCL supervised all of the research.

3.7. Figures

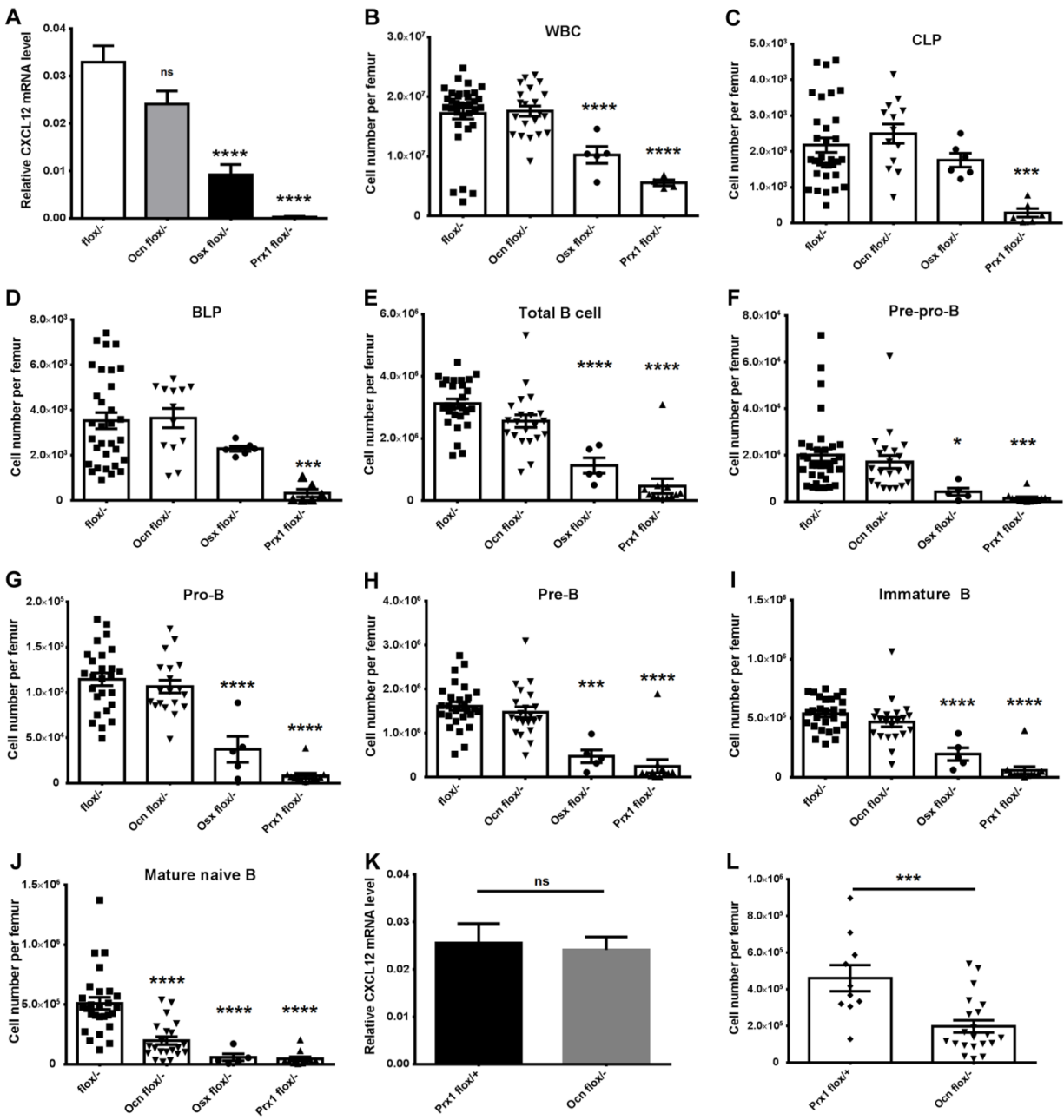


Figure 3.1 CXCL12 expression by stromal cells is important for B lymphopoiesis. A.

Cxcl12^{fllox/-} (floxx/-), *Ocn-Cre:Cxcl12^{fllox/-}* (Ocn floxx/-), *Osx-Cre:Cxcl12^{fllox/-}* (Osx floxx/-) and *Prx1-Cre:Cxcl12^{fllox/-}* (Prx1 floxx/-) mice were flushed with Trizol to extract total bone marrow RNA, which was then used for RT-qPCR. mRNA level of CXCL12 was normalized to β -actin. **B-J.** Femurs from four groups of transgenic mice were harvested and analyzed for different cells populations using flow cytometry. Cell populations include: white blood cell (WBC) (**B**), common lymphoid progenitor (CLP) (**C**), B lineage restricted progenitor (BLP) (**D**), total B cell (**E**), pre-pro B cell (**F**), pro-B cell (**G**), pre-B cell (**H**), immature B cell (**I**) and mature naive B cell (**J**). Sample size, n = 5-37 mice per group in all experiments. **K&L.** *Prx1-Cre:Cxcl12^{fllox/+}* (Prx1 floxx/+) mice were also examined and compared with Ocn floxx/- group for CXCL12 expression (**K**) (n = 7 or 12 mice, respectively) and the number of mature naive B cells (**L**) (n = 10 or 21 mice, respectively). Data represent the mean \pm SEM, *P < 0.05; **P < 0.01; ***P < 0.001; ****P < 0.0001; “ns” means non-significant, compared to *Cxcl12^{fllox/-}* control mice unless otherwise indicated.

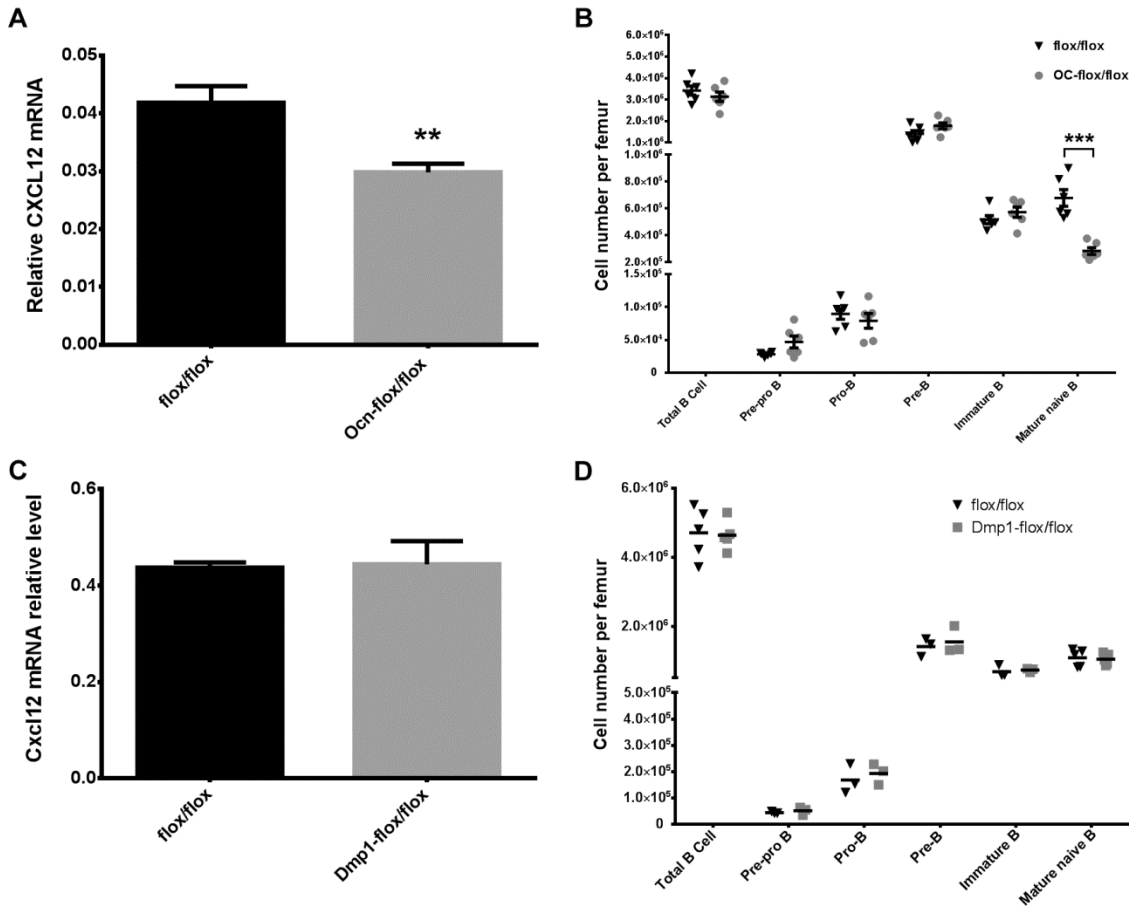


Figure 3.2. CXCL12 expression in *Ocn-Cre* targeted stromal cells is important for the regulation of mature naive B cells. **A&C.** Tibias from **A.** *Ocn-Cre:Cxcl12^{flox/flox}* (*Ocn-flox/flox*), **C.** *Dmp1-Cre:Cxcl12^{flox/flox}* (*Dmp1-flox/flox*), and *Cxcl12^{flox/flox}* (*flox/flox*) mice were flushed with Trizol to extract total bone marrow RNA, which was then used for RT-qPCR. mRNA level of CXCL12 was normalized to β -actin. **B&D.** Femurs were harvested from *Ocn-Cre:Cxcl12^{flox/flox}* mice (**B**), *Dmp1-Cre:Cxcl12^{flox/flox}* mice (**D**), and *Cxcl12^{flox/flox}* control mice (**B&D**). Bone marrow from the femurs were then analyzed using flow cytometry to quantify the number of B cells during different developmental stages. Sample size, n = 3-6 mice per group in all experiments. Data represent the mean \pm SEM, **P < 0.01; ***P < 0.001, compared to *Cxcl12^{flox/flox}* control mice unless otherwise indicated.

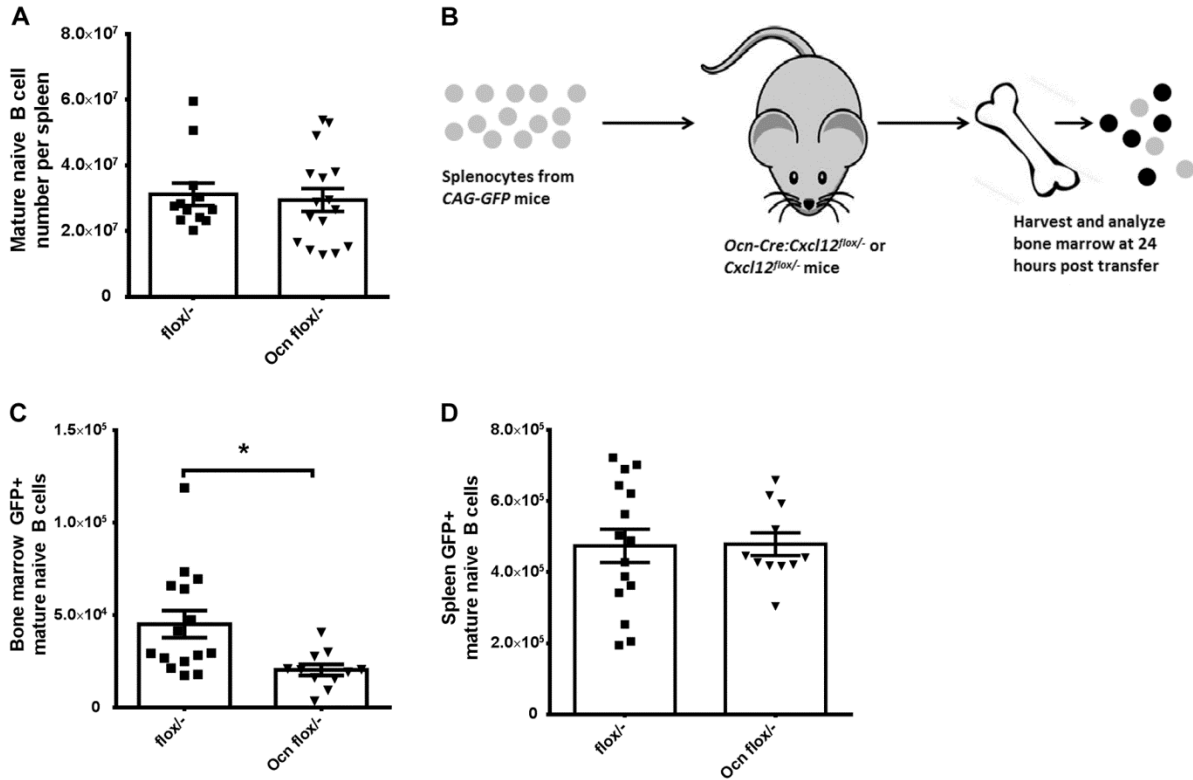


Figure 3.3. CXCL12 expression in *Ocn-Cre* targeted stromal cells regulates the homing and/or retention of mature naive B cells in the bone marrow. **A.** The number of mature naive B cells in the spleen from *Cxcl12^{flox/-}* (*flox^{-/-}*) and *Ocn-Cre:Cxcl12^{flox/-}* (*Ocn flox^{-/-}*) mice, were quantified using flow cytometry. **B.** 5×10^6 splenocytes from *CAG-GFP* mice were transplanted into *Cxcl12^{flox/-}* and *Ocn-Cre:Cxcl12^{flox/-}* recipient mice through retro-orbital injection, and the bone marrow from femurs were harvested and analyzed at 24 hours after injection. **C&D.** The numbers of GFP⁺ mature naive B cells in the bone marrow (**C**) and spleen (**D**) were quantified using flow cytometry. Sample size, n = 11-16 mice per group in all experiments. Data represent the mean ± SEM, *P < 0.05, compared to *Cxcl12^{flox/-}* control mice unless otherwise indicated.

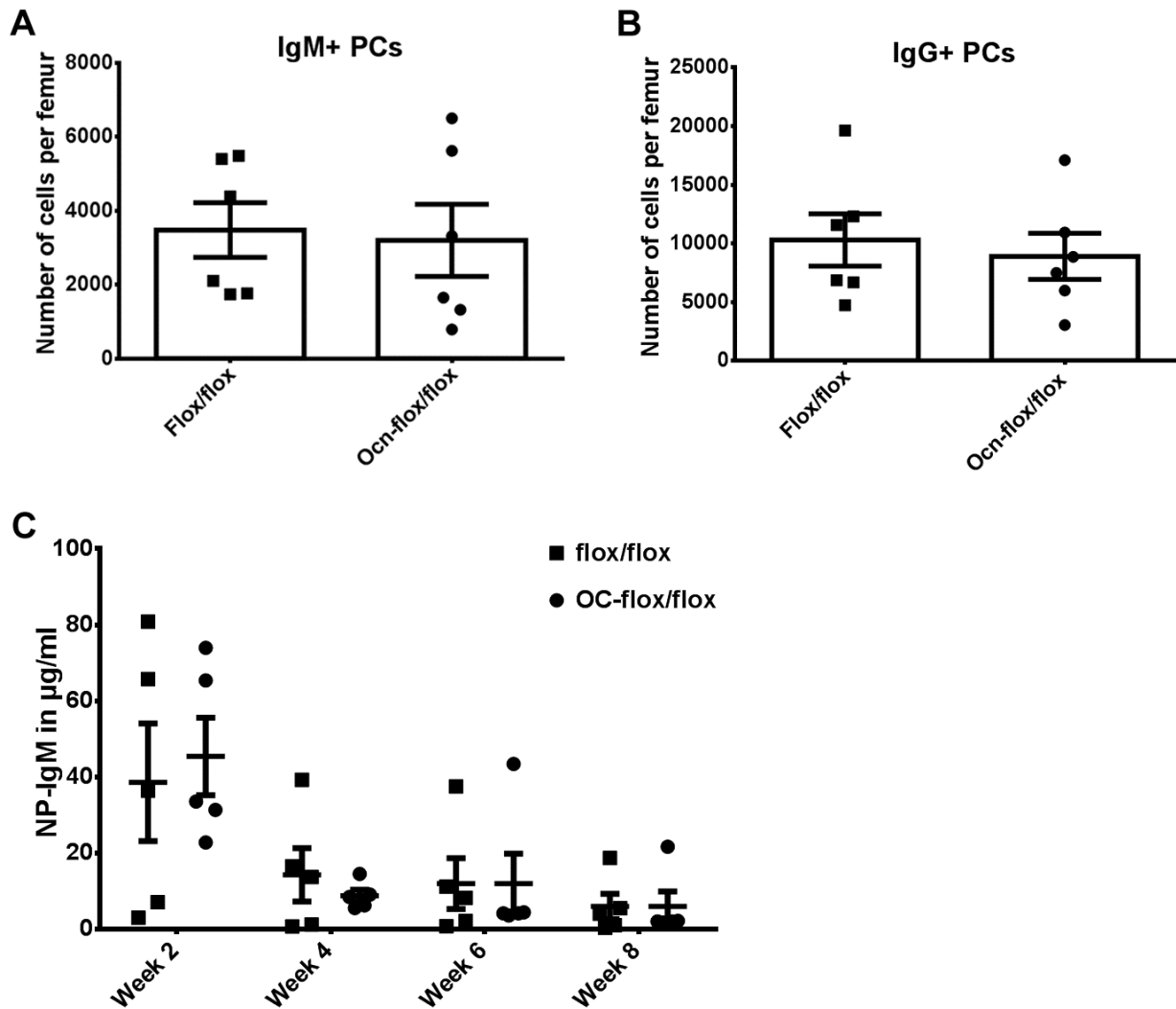


Figure 3.4. Ablation of CXCL12 in *Ocn-Cre* targeted stromal cells had no effects on plasma cells (PCs) and primary immune response. **A&B.** The number of IgM⁺ PCs (**A**) and IgG⁺ PCs (**B**) were quantified by flow cytometry in *Ocn-Cre:Cxcl12^{flox/flox}* and *Cxcl12^{flox/flox}* mice (n = 6 mice per cohort). **C.** *Ocn-Cre:Cxcl12^{flox/flox}* and *Cxcl12^{flox/flox}* mice were immunized with NP-CGG and the amount of NP-specific IgM antibodies were quantified at different time points (n = 5 mice per cohort). Data represent the mean ± SEM.

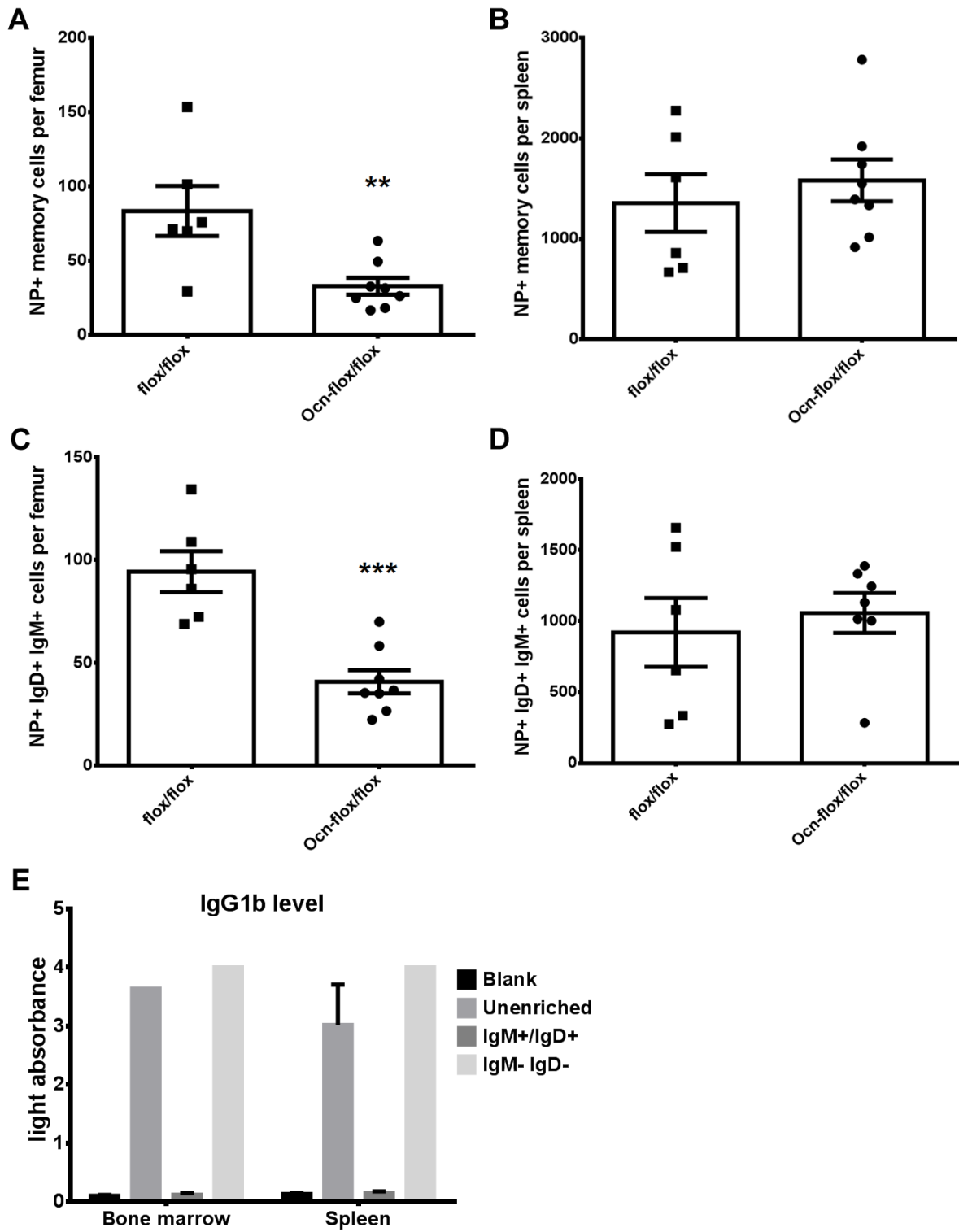


Figure 3.5. Ablation of CXCL12 in *Ocn-Cre* targeted stromal cells reduces the number of memory B cells in the bone marrow. *Ocn-Cre:Cxcl12^{flox/flox}* and *Cxcl12^{flox/flox}* mice were immunized with NP-CGG. **A&B.** Two months later, Np-specific IgM⁻ IgD⁻ conventional memory B cells were quantified in the bone marrow (**A**) and the spleen (**B**) of these mice by flow cytometry. **C&D.** Np-specific IgM⁺ IgD⁺ memory-like B cells were quantified in the bone marrow (**C**) and the spleen (**D**) of the same mice (n = 6 or 8 mice per cohort). Wildtype mice were immunized with NP-CGG. Two months later, unenriched cells, IgM⁺ and IgD⁺ enriched cells, and IgM⁻ IgD⁻ enriched cells were collected from both the bone marrow and the spleen of these mice. All of these cells were separately transferred into IgHa/J recipient mice through retro-orbital injection, followed by secondary NP-CGG immunization one day after transplant. **E.** The amount of NP-specific IgG1b in blood serum was quantified one week later using ELISA, which was represented by light absorbance. Data represent the mean ± SEM, **P < 0.01; ***P < 0.001, compared to *Cxcl12^{flox/flox}* control mice unless otherwise indicated.

CHAPTER 4: CLASSICAL DENDRITIC CELLS IN BONE MARROW REGULATE HEMATOPOIETIC STEM AND PROGENITOR CELL TRAFFICKING THROUGH CXCR2 SIGNALING IN SINUSOIDAL ENDOTHELIAL CELLS

4.1. Introduction

A resident population of classical dendritic cells (cDCs) has been identified in murine bone marrow, but its contribution to the regulation of hematopoiesis and establishment of the stem cell niche is largely unknown⁴⁹. Here, we show that murine bone marrow cDCs are perivascular and have a cDC2-like immunophenotype. A similar population of cDCs is present in human bone marrow. RNA expression analysis of sorted BM cDCs showed that expression of many chemokines and chemokines receptors is distinct from that observed in splenic cDC2s, suggesting that BM cDCs may represent a unique DC population. Ablation of cDCs results in hematopoietic stem/progenitor cell (HSPC) mobilization that is greater than that seen with ablation of bone marrow macrophages. Ablation of cDCs is associated with an expansion of bone marrow endothelial cells and increased vascular permeability. CXCR2 expression in sinusoidal endothelial cells and the expression of two CXCR2 ligands, CXCL1 and CXCL2, in the bone marrow are markedly increased following BM cDC ablation. Treatment of endothelial cells *in vitro* with CXCL1 induced increased permeability and transmigration of HSPCs. Finally, we show that HSPC mobilization after BM cDC ablation is attenuated in mice lacking CXCR2 expression. Collectively, these data suggest that BM cDCs play an important role in regulating HSPC trafficking, at least in part, through its regulation of sinusoidal CXCR2 signaling and vascular permeability.

4.2. Material and Methods

4.2.1. Mouse strains

The *CX3CR1^{gfp/+}* mice were a gift from D. Littmann²⁶⁷ (New York University School of Medicine). *Zbtb46^{dtr}* (*B6(Cg)-Zbtb46^{tm1(HBEGF)Mnz/J}*), *Zbtb46^{gfp}* (*129S-Zbtb46^{tm1Kmm/J}*), *Col2.3-GFP* (*B6.Cg-Tg(Coll1a1*2.3-GFP)1Rowe/J*) and *CXCR2^{-/-}* (*C.129S2(B6)-Cxcr2^{tm1Mwm/J}*) mice were obtained from The Jackson Laboratory. *CD169^{dtr}* mice were a gift from Y. Obata^{268,269} (Riken BioResource Center, Ibaraki, Japan). *CD169^{dtr}* mice were bred with *Zbtb46^{dtr}* mice to generate *CD169^{dtr}:Zbtb46^{dtr}* mice. Sex- and age-matched mice were used in all experiments. All mice were inbred on a C57BL/6 background except *Zbtb46^{gfp}* mice, which were on a mixed C57BL/6 and 129 SvEv background. The numbers of animals used per experiment are stated in the figure legends. Mice were maintained under SPF conditions, and all experimental procedures were performed according to methods approved by the Animal Studies Committee at Washington University.

4.2.2. Generation of bone marrow chimeras

Six to eight weeks old wild-type Ly5.1/Ly5.2 recipient mice were irradiated with two 550 cGy doses, 6 hours apart. Two million donor bone marrow cells were then injected retro-orbitally. Mice were placed on prophylactic antibiotics (trimethoprim-sulfamethoxazole) for 2 weeks following the first dose of irradiation. Mice were analyzed eight weeks after transplantation.

4.2.3. Diphtheria toxin administration

Diphtheria toxin (D0564, Sigma) was diluted in PBS containing 0.1% low-endotoxin bovine serum albumin and administered intraperitoneally at a dose of 200 ng/day for up to 6 days.

4.2.4. CFU-C assays

Cells obtained from the bone marrow, peripheral blood, and spleen were analyzed using a Hemavet (Drew Scientific) automated cell counter. 40 μ L of peripheral blood, 2.5×10^4 bone marrow cells, or 1.0×10^5 splenic cells were plated in 3mL Mouse Methylcellulose Complete Media (HSC007, R&D Systems). Cultures were plated in duplicate in 60 mm petri dishes and incubated in a humidified chamber with 5% CO₂ at 37 °C. The number of colonies per dish was counted on day 7.

4.2.5. Flow cytometry

Bone marrow, spleen and peripheral blood were processed for flow cytometry as previously described²⁷⁰. Cells were analyzed on a Gallios flow cytometer (Beckman Coulter) or sorted on a Sony SY3200 “Synergy” high-speed cell sorter (Sony). Data analysis was done using FloJo version 10.0.7 software (TreeStar). The following antibodies were used for staining murine cells: Gr-1 (RB6-8C5), CD19 (1D3), CD48 (BCM1), B220 (RA3-6B2), CD3e (17A2), Ter119 (TER-119), Sca-1 (D7), CD117 (2B8), CD115 (AFS98), CD45 (30-F11), CD45.1 (A20) and CD45.2

(104) from eBiosciences; CD31 (390), F4/80 (BM8), I-A/I-E (M5/114.15.2), CD11c (N418), CD150 (TC15-12F12.2), CD169 (3D6.112), CD11b (M1/70) and XCR1 (ZET) from BioLegend.

For cell sorting, classical dendritic cells from bone marrow and spleen were both identified as CX3CR1-GFP^{high} B220⁻ Gr-1⁻ MHCII^{high} CD11c^{high} F4/80⁺ cells. Endothelial cells were identified as Lineage⁻ (CD45⁻ Ter119⁻ Gr-1⁻) CD31⁺ cells with Sca1⁺ to mark arteriolar and Sca1⁻ to mark sinusoidal endothelial cell.

For staining human bone marrow cells, the following antibodies were used: CD3 (555332), CD15 (555401), CD19 (555412) and CD11c (B-ly6) from BD Biosciences; CD13 (WM-15), CD20 (2H7) and CD56 (MEM188) from eBiosciences; CD33 (P67.6), CD1c (L161), CD14 (M5E2), CD141 (M80) and HLA-DR (L243) from BioLegend.

4.2.6. Immunostaining of bone sections

Mouse hindlimbs were processed for immunostaining as previously described¹⁹. The following antibodies were used: chicken anti-GFP (ab13970, Abcam), rat anti-MHCII (107601, BioLegend), Rat anti-Sca1 (557403, BD Biosciences), goat anti-VECadherin (AF1002, R&D Systems), and anti-B220 (12-0452-83, EBioscience); AlexaFluor 488 donkey anti-rat IgG (Invitrogen), AlexaFluor 488 donkey anti-chicken IgG (Jackson ImmunoResearch), and biotin-conjugated donkey anti-goat IgG (Jackson ImmunoResearch)]. In some cases, slides were then incubated with streptavidin-DyLight 649 (Jackson ImmunoResearch) for 30 minutes at room temperature. Finally, slides were mounted with ProLong Gold antifade reagent with DAPI (Life Technologies). Images were acquired with an LSM 700 microscope (Carl Zeiss), and images were processed using Volocity software (PerkinElmer).

4.2.7. Real-time quantitative RT-PCR

Mouse femurs were flushed with 1 mL of TRIzol reagent (Invitrogen), and RNA was isolated according to the manufacturer's instructions. Reverse transcription was performed using iScript™ cDNA Synthesis Kit (Bio-Rad) according to the manufacturer's instructions. Quantitative PCR was performed using iTaq™ Universal Probes Supermix (Bio-Rad) on a StepOne Plus Real-Time PCR System (Applied Biosystems). RNA content was normalized to mouse β -actin. Primer and probes for mouse β -actin (Mm01324804_m1), CXCL12 (Mm00445553_m1), CXCL1 (Mm04207460_m1), and CXCL2 (Mm00436450_m1) were ordered from ThermoFisher.

4.2.8. RNA expression profiling

RNA was purified from sorted classical dendritic cells (cDCs) and endothelial cells using the Qiagen RNeasy Micro Kit (74004, Qiagen). For cDC RNA samples, libraries were generated using the NuGen Pico SL kit (NuGEN Technologies, San Carlos, CA) and then hybridized to Affymetrix Mouse Gene 1.0 ST arrays (Affymetrix, Santa Clara, CA). Gene set enrichment was performed using the GSEA software (Broad Institute). Differences in gene expression were determined using Significance Analysis of Microarrays (SAM; Stanford University, Stanford, CA). Expression data has been submitted to Gene Expression Omnibus, record number.

4.2.9. *In vitro* permeability test and cell migration assay

Human Umbilical Vein Endothelial Cells (HUVECs) (S200-05N, Sigma) were cultured in Endothelial Cell Growth Medium (211-500, Sigma) at 37 °C, 5% CO₂. 2×10^5 HUVECs were pre-

cultured in the upper chamber of the Boyden Chamber system for 24 hours to form a HUVEC layer. During the same time, the HUVEC layer was pre-treated with 40ng/ml recombinant CXCL1 (453-KC-010/CF, Thermo Fisher) or PBS as control.

To test permeability of the HUVEC layer for large molecules, 400 μ l Endothelial Cell Growth Medium containing 100 μ g/ml Evan's blue was added to the upper chamber of the cell insert with 0.4 μ m pores in the membrane (141078, Thermo Fisher). 1ml of Hank balanced salt solution (H6648-500ML, Sigma) was added to the bottom chamber. After 1 hour incubation at 37 $^{\circ}$ C, 5% CO₂, Evan's blue in the bottom chamber was measured by light absorbance at 620nm using Epoch 2 microplate spectrophotometer (Biotek), and the amount of Evan's blue was calculated using a standard curve. Amount of Evan's blue in the CXCL1 treated samples were normalized to the amount in the PBS treated control samples for comparison.

To test permeability of the HUVEC layer for cell migration, 400 μ l medium containing $\sim 5 \times 10^4$ human CD34⁺ cells were added to the upper chamber of the cell insert with 3 μ m pores in the membrane (141080, Thermo Fisher). Human CD34⁺ cells were enriched from primary human bone marrow donated by healthy donors, using CD34 MicroBead Kit (130-100-453, Miltenyi Biotec) and autoMACS Pro Separator (Miltenyi Biotec). 1ml of medium containing 100ng/ml recombinant CXCL12 (578702, BioLegend) was added to the bottom chamber. Meanwhile, CXCL1 or PBS was added to the appropriate samples to continue the pre-treatment. After 24 hour incubation at 37 $^{\circ}$ C, 5% CO₂, number of cells migrated to the bottom chamber was quantified and the percentage was calculated.

4.2.10. Statistical analyses

Statistical significance was determined using Prism software (GraphPad). Unless otherwise indicated, unpaired t-test or 1/2-way ANOVA analyses were used to evaluate the significance of differences between two or multiple groups. All data are presented as mean \pm SEM.

4.3. Results

4.3.1. Classical dendritic cells (cDCs) are enriched in the perivascular region and may be functionally specific for the perivascular niche.

Dendritic cells (DCs) are a component of the innate immune system and are distributed throughout the body. DCs are professional antigen presenting cells that contribute to immune cell activation through the secretion of cytokines and chemokines. DCs display considerable phenotypic and functional heterogeneity, suggesting that DCs in specific tissues may have evolved to perform distinct functions³⁷⁻³⁹. DCs include classical DCs (cDCs) with dendritic morphology and outstanding capacity for presenting antigens and priming T cells, and plasmacytoid DCs (pDCs) which are lymphocyte-like cells specialized in the production of type I interferons^{40,41,43}. cDCs may be further divided into type 1 cDCs (cDC1s), mainly against viruses, tumors and intracellular pathogens, and type 2 cDCs (cDC2s), mainly against parasites, allergens, extracellular bacteria and fungi⁴². A prior study identified a resident population of cDCs in the bone marrow and provided evidence that these cells promote the survival of circulating mature B cells in the bone marrow⁴⁹. To better characterize BM cDCs, we developed a multicolor flow cytometry to analyze myeloid cell populations in *Cx3cr1^{gfp/+}* mice, which express high levels of green fluorescent protein (GFP) in monocytes and BM cDCs, but not in

bone marrow macrophages^{7,267}. Monocytes were identified as CX3CR1-GFP^{high} MHC II^{low} B220⁻/CD19⁻ cells (Fig. 4.1a), and, consistent with prior studies, expressed F4/80 but were mostly negative for CD11c and CD169 (Fig. 4.1b)^{271,272}. Bone marrow macrophages were identified as CX3CR1-GFP^{low}, MHC II⁺, B220⁻/CD19⁻ cells and expressed CD169 and F4/80, but little CD11c. Finally, BM cDCs were identified as CX3CR1-GFP^{high} and MHC II^{high} B220⁻/CD19⁻ cells. As expected, BM cDCs expressed a high level of CD11c and F4/80, but a low level of CD169⁵¹. cDCs represent $0.048 \pm .017\%$ of nucleated cells in mouse bone marrow compared to $0.096 \pm .047\%$ for macrophages (n = 11 mice). A prior study showed that BM cDCs are perivascular, although this study did not distinguish between venous sinusoids and arterioles⁴⁹. We show that the great majority of CX3CR1-GFP^{high} and MHC II^{high} DCs in the bone marrow are perivascular (Fig. 4.1c: iv-viii), with the majority of cells with 10 μm of a venous sinusoid or arteriole (Fig. 4.1d, e).

To further characterize mouse BM cDCs, we assessed their expression of XCR1 and CD11b, which are selectively expressed on cDC1s and cDC2s, respectively⁴². Nearly all of the cDCs express CD11b but not XCR1, suggesting that the majority of murine BM DCs are cDC2-like cells (Fig. 4.1f). We next examined bone marrow from healthy donors to determine whether cDCs also are present in human bone marrow. Indeed, the percentage of cDCs in human bone marrow ($0.076 \pm .041\%$, n = 3 donors) was similar to that seen in murine bone marrow. Moreover, the majority of cDCs in human bone marrow express CD1c but not CD141, consistent with a cDC2-like phenotype (Fig. 4.1g)⁴². RNA expression profiling was performed on sorted murine BM cDCs and compared to prior data generated using splenic cDC2 cells. Surprisingly, the patterns of gene expression for chemokines and chemokine receptors were strikingly

different, suggesting that BM cDCs may represent a unique dendritic cell population with distinct functional properties (Fig. 4.1h).

4.3.2. BM cDC ablation induces a loss of macrophage and HSPC mobilization

To assess their functional importance, BM cDCs were ablated using *CD11c^{dtr}* mice. A prior study showed that treatment with diphtheria toxin (DT) results in efficient ablation of cDCs in the bone marrow, but it is also associated with systemic toxicity leading to death^{273,274}. As reported previously²⁷⁵, to circumvent DT-induced lethality, we transplanted bone marrow from *CD11c^{dtr}* mice into irradiated wild-type congenic recipients (Supplemental Fig. 4.1a). Treatment of *CD11c^{dtr}* bone marrow chimeras with DT did not affect the number of HSPCs in the bone marrow (Fig. 2a, Supplemental Fig. 4.1b), but resulted in a modest HSPC mobilization into spleen and blood (Fig. 2b,c, Supplemental Fig. 4.1c), as quantified by CFU-C and C-kit⁺ Sca1⁺ Lin⁻ (KSL) marked HSPCs. Prior studies have shown that *CD11c^{dtr}* targets certain macrophage subsets in peripheral organs^{274,276,277}. Indeed, we observed a loss of bone marrow macrophages after 6 days treatment of DT (Fig. 4.2d). Of note, after 1 day treatment of DT, cDCs but not macrophages in the bone marrow were depleted, raising the possibility that macrophage loss is secondary to cDC loss (Fig. 4.2d).

Recent studies have identified Zbtb46 as a transcription factor that is expressed in cDCs but not in pDCs, macrophages or other myeloid or lymphoid cells^{278,279}. To confirm the specificity of Zbtb46 expression in cDCs, we analyzed *Zbtb46^{gfp}* mice, in which GFP is knocked into the *Zbtb46* locus²⁷⁹. As expected, Zbtb46-GFP was expressed at high levels in BM cDCs, but in neither bone marrow macrophages nor monocytes (Fig. 4.2e). Since endothelial cells also

express $Zbtb46^{278,279}$, we transplanted $Zbtb46^{dtr}$ bone marrow into irradiated wild-type recipients to restrict $Zbtb46^{dtr}$ to the hematopoietic lineage, thus to assess the effect of BM cDC ablation on HSPCs. DT treatment on $Zbtb46^{dtr}$ bone marrow chimeras resulted in a marked loss of BM cDCs (Fig. 4.2f). Similar to $CD11c^{dtr}$ bone marrow chimeras, we also observed a loss of bone marrow macrophages in the same mice following DT treatment, which occurred later than BM cDC ablation (Fig. 4.2f). To determine whether this loss of macrophages was cell-autonomous, we generated mixed wild-type and $Zbtb46^{dtr}$ bone marrow chimeras using similar transplantation method. As expected, DT treatment resulted in the loss of $Zbtb46^{dtr}$ derived but not wild-type derived BM cDCs (Fig. 4.2g). In contrast, DT treatment resulted in decreases of both wild-type and $Zbtb46^{dtr}$ derived bone marrow macrophages (Fig. 4.2h). Collectively, these data strongly suggest that BM cDC ablation results in a secondary and non-cell autonomous loss of bone marrow macrophages.

Ablation of bone marrow macrophages has been reported to alter the HSPC niche and induce HSPC mobilization^{7,52}. Therefore, to precisely assess the role of BM cDCs on HSPC regulation and maintenance, it was necessary to include additional macrophage ablation model and double ablation model for comparison with BM cDC ablation model. Recent studies have reported $CD169^{dtr}$ may ablate bone marrow macrophages specifically^{7,53,268,269}. Thus, we transplanted $Zbtb46^{dtr}$, $CD169^{dtr}$, or $CD169^{dtr}:Zbtb46^{dtr}$ bone marrow into irradiated wild-type recipients. 6 days of DT treatment on all three bone marrow chimeras did not induce any significant changes in bone marrow and spleen cellularity (Supplemental Fig. 4.1d,e). In the bone marrow, all three chimeras showed no significant differences of KSL cells or $CD150^+ CD48^-$ KSL (KSL-SLAM) marked HSCs (Fig. 4.2i, supplemental Fig. 4.1f), although mild increases of CFU-C were observed (Fig. 4.2l). Ablation of bone marrow macrophages in $CD169^{dtr}$ bone marrow chimeras

resulted in weak mobilization of KSL cells and CFU-C into spleen and blood, but there was little mobilization of KSL-SLAM cells into spleen (Fig. 4.2j,m). In contrast, ablation of BM cDCs in both *Zbtb46^{dtr}* and *CD169^{dtr}: Zbtb46^{dtr}* bone marrow chimeras resulted in stronger mobilizations of KSL cells, KSL-SLAM cells and CFU-C into spleen and blood (Fig. 4.2j,k,m,n).

Interestingly, there were no significant differences of HSPC mobilizations between *Zbtb46^{dtr}* and *CD169^{dtr}: Zbtb46^{dtr}* bone marrow chimeras (Fig. 4.2j,k,m,n). Overall, these data demonstrate that ablation of bone marrow macrophages only induces weak HSPC mobilization in bone marrow chimeras, and ablation of BM cDCs may induce stronger HSPC mobilization through both macrophage dependent and independent pathways.

4.3.3. BM cDC ablation affects bone marrow vascular endothelial cells

Given BM cDCs are enriched in the perivascular region, we next assessed bone marrow vascular permeability after BM cDC ablation, as it has been reported to positively affect cell mobilization in bone marrow^{280,281}. BSA-FITC was injected into *Zbtb46^{dtr}* bone marrow chimeras treated with PBS, 1 day of DT, or 6 days of DT. Mice were harvested 15 minutes later and immunofluorescent (IF) staining was performed on femurs to quantify BSA-FITC for estimating bone marrow vascular permeability (Fig. 4.3a)²⁸². We observed a trend of increasing vascular permeability along BM cDC ablation (Fig. 4.3c). In addition, we quantified the percentage of vascular endothelial cells (VECs) in whole bone marrow in the same *Zbtb46^{dtr}* bone marrow chimeras by IF staining and found the percentage of VECs increased after BM cDC ablation (Fig. 4.3b,d). Flow cytometry further confirmed that the number of bone marrow VECs increased 1 day after BM cDC ablation (Fig. 4.3e). Collectively, these data show that

ablation of BM cDCs may result in potential activation of bone marrow VECs for increased vascular permeability and angiogenesis.

4.3.4. BM cDC ablation activates sinusoidal endothelial cells and sinusoidal CXCR2 signaling

To determine potential molecular pathways involved in BM cDC ablation induced activation of bone marrow VECs, we performed gene expression analysis in endothelial cells from *Zbtb46^{dtr}* bone marrow chimeras treated with 1 day of DT or PBS. At this time point, only BM cDCs were ablated, but not bone marrow macrophages, thus the result would be specific to BM cDC ablation. Sinusoidal endothelial cells (SECs) were marked as Lin⁻ CD31⁺ Sca1⁻ cells and arteriolar endothelial cells (AECs) were marked as Lin⁻ CD31⁺ Sca1⁺ cells, and both populations were sorted using FACS. We performed RNA microarray analysis on both populations, and PCA was performed to measure and visualize differences for each population before or after BM cDC ablation. While AECs showed no significant differences between the two conditions, SECs may be activated after BM cDC ablation for differential gene expressions (Supplemental Fig. 4.2a,b). To further test this possibility, we performed RNA sequencing analysis in SECs from *Zbtb46^{dtr}* bone marrow chimeras treated with 1 day of DT or PBS. We performed t-distributed stochastic neighbor embedding (t-SNE) to measure and visualize differences between the two conditions and the result was consistent with the microarray analysis (Fig. 4.4a). SECs were activated after BM cDC ablation and there were 635 significantly differentially expressed genes with >5 fold differences, p-value < 0.05 and FDR < 0.02. To search for potential pathways activated in SECs after BM cDC ablation, gene set enrichment analysis (GSEA) was performed. The most enriched gene set showed activation of chemokines

and cytokines related pathways (Fig. 4.4b). Also, gene set for angiogenesis was highly enriched, which was consistent with the observed expansion of VECs measured by IF staining and flow cytometry (Fig. 4.3d,e and Fig. 4.4c). Among expressed chemokine receptors in SECs, CXCR2 was most highly up-regulated after BM cDC ablation (Fig. 4.4d). Importantly, recent and early studies have reported CXCR2 activation could induce vascular permeability and HSPC mobilization^{72,283-285}. We performed quantitative real-time PCR (qRT-PCR) on whole bone marrow RNAs from *Zbtb46^{dtr}* bone marrow chimeras treated with PBS, 1 day or 6 days of DT. Both ligands for CXCR2, CXCL1 (KC) and CXCL2 (Gro-β) were up-regulated following BM cDC ablation (Fig. 4.4e,f). To confirm that this observation was not due to a non-specific up-regulation of chemokines induced by acute inflammation, we measured whole bone marrow RNA level of CXCL12, a common and pro-inflammatory chemokine in the bone marrow, and found no increase after BM cDC ablation (Supplemental Fig. 4.2c). To further test whether there was an acute inflammation, we measured neutrophil numbers in blood and bone marrow^{286,287}, and found little or no increase (Supplemental Fig. 4.2d,e). Both results suggested up-regulations of CXCL1 and CXCL2 were specific to BM cDC ablation. Thus, CXCR2 is activated in SECs after BM cDC ablation, which may play an important role for regulating sinusoidal vascular permeability and HSPC mobilization.

4.3.5. CXCR2 signaling pathway is important for BM cDC ablation induced HSPC mobilization

To test our hypothesis on the role of CXCR2, we first confirmed prior studies^{11-13, 32} by testing whether activation of CXCR2 may induce vascular permeability using *in vitro* migration

assay. Human umbilical vein endothelial cells (HUVECs) were plated in the upper chamber of the Boyden chamber for migration assay to form a HUVEC layer, and treated with PBS or recombinant CXCL1 (rCXCL1) to activate CXCR2 signaling (Fig. 4.5a). To test vascular permeability of the HUVEC layer for large molecules, Evan's blue was added to the upper chamber of the Boyden chamber with 0.4 μ m pores in the membrane (Fig. 4.5a). Quantified by light absorbance, the amount of Evan's blue in the bottom chamber after 1 hour increased modestly upon CXCR2 activation, suggesting an increased permeability of the HUVEC layer (Fig. 4.5b). To test the effects of CXCR2 activation on HSPC migration, CD34⁺ cells were isolated from healthy human bone marrow and added to the upper chamber of the Boyden chamber with 3 μ m pores in the membrane, and medium containing recombinant CXCL12 was added to the bottom chamber to induce cell migration²⁸⁸⁻²⁹⁰ (Fig. 4.5a). A modest increase of cell migration through the HUVEC layer was observed after 24 hours upon CXCR2 activation (Fig. 4.5c). To test the role of CXCR2 signaling on BM cDC ablation induced HSPC mobilization, we transplanted *Zbtb46*^{dtr} bone marrow into irradiated *Cxcr2*^{-/-} recipients, restricting knock-out of CXCR2 to the stromal cells and endothelial cells in the bone marrow of these recipients. We then compared them with previous *Zbtb46*^{dtr} bone marrow chimeras in wild-type recipients, for HSPC mobilization after 6 days treatment of PBS or DT (Fig. 4.5d). BM cDC ablation did not affect bone marrow and spleen cellularity in *Zbtb46*^{dtr} *Cxcr2*^{-/-} bone marrow chimeras, and there was a mild decrease of cellularity compared to *Zbtb46*^{dtr} wild-type bone marrow chimeras with the same treatment (Supplemental Fig. 4.3a,b). In the bone marrow of *Zbtb46*^{dtr} *Cxcr2*^{-/-} bone marrow chimeras, BM cDC ablation did not induce any significant differences in KSL cells (Fig. 4.3e) and KSL-SLAM cells (Supplemental Fig. 4.3c), although there might be a trend of mild increase of CFU-C which was similar to the pattern observed in

Zbtb46^{dtr} wild-type bone marrow chimeras (Supplemental Fig. 4.3d). In the spleen of *Zbtb46^{dtr}* *Cxcr2^{-/-}* bone marrow chimeras, BM cDC ablation resulted in weaker mobilizations of KSL cells, KSL-SLAM cells and CFU-C, compared to *Zbtb46^{dtr}* wild-type bone marrow chimeras (Fig. 4.5f-h). Similar to the spleen, a weaker mobilization of CFU-C was observed in the blood of *Zbtb46^{dtr}* *Cxcr2^{-/-}* bone marrow chimeras, compared to *Zbtb46^{dtr}* wild-type bone marrow chimeras (Fig. 4.5i). Collectively, data from both *in vitro* and *in vivo* experiments support our hypothesis that CXCR2 signaling plays an important role in the regulation of HSPC mobilization induced after BM cDC ablation.

4.4. Summary

In conclusion, data from this study suggests BM cDC as a novel perivascular niche component that regulates HSPC retention and trafficking, at least in part, through its regulation of sinusoidal CXCR2 signaling and vascular permeability. This observation is consistent with the findings from our colleagues, where Dr. John Dipersio's group shows endothelial CXCR2 is important for Gro- β induced neutrophil mobilization into the blood. Our results do not provide evidence to explain how BM cDCs regulate SECs. However, as bone marrow macrophage has been reported to regulate HSPCs through indirect regulation of stromal cells^{7,52}, we suspect similar process may be involved.

4.5. Acknowledgments

This work was supported by a grant from the National Institutes of Health: RO1 HL60772 (DCL). The authors thank Dr. Daniel Littman for providing the *Cx3cr1*gfp mice, Dr. Takashi Nagasawa for providing the *Cxcl12*gfp mice, Dr. Kenneth Murphy for providing the *Zbtb46*DTR/+ and *Zbtb46*gfp mice. We thank the staff of the Siteman Cancer Center Flow Cytometry Core for their expert technical assistance. We thank Amy Schmidt for technical assistance, and Jackie Tucker-Davis for animal care.

4.6. Author Contributions

Jingzhu Zhang, Teerawit Supakordej and Daniel C. Link conceived and designed the experiments, and analyzed the data. JZ and TS contribute equally to this study. Mahil Rao performed the flow cytometry for *Cx3cr1*^{gfp} mice. Joseph Krambs helped analyzing RNA-seq data. Grazia Abou Ezzi helped generating bone marrow chimeras. Rachel Ye performed the flow cytometry for human samples. DCL supervised all of the research.

4.7. Figures

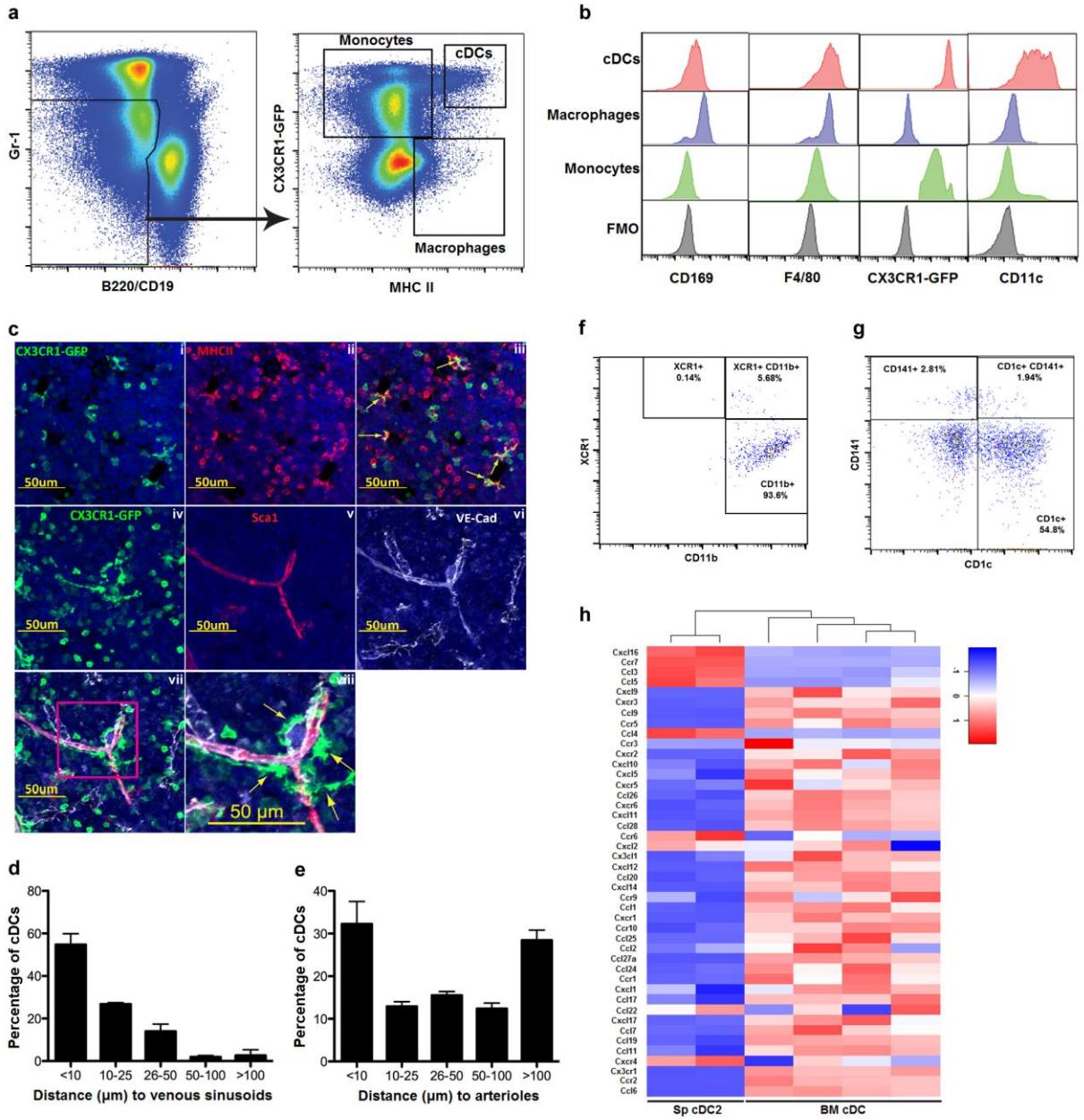


Figure 4.1. Classical dendritic cells (cDCs) are enriched in the perivascular region and may be functionally specific for the perivascular niche. (a) Representative flow plots showing the gating strategy used to identify bone marrow monocytes, macrophages, and cDCs in *Cx3cr1^{gfp/+}* mice. Gr-1^{hi} neutrophils and B220⁺/CD19⁺ B cells were excluded as shown in the left panel. Monocytes were identified as CX3CR1-GFP⁺ MHC II^{low} cells, cDCs as CX3CR1-GFP^{high} MHCII^{high} cells, and macrophages as CX3CR1-GFP^{low} MHCII⁺ B220⁻ cells. (b) The gated monocyte, macrophage, and cDC populations were profiled for expression of the indicated lineage markers. FMO, fluorescence minus one control. (c) Representative photomicrographs of femur sections from *Cx3Cr1^{gfp/+}* mice. Slides were stained with GFP (green) (i), MHC II (red) (ii) and the merge (iii). Slides were stained with GFP (green) (iv), Sca1⁺ arterioles (red) (v), VE-Cadherin⁺ venous sinusoids and arterioles (white) (vi) and merge (vii); higher magnification of boxed region (viii). Yellow arrows indicate cDCs. Counterstaining with DAPI highlights nuclei (blue). (d,e) Quantification of the distance from cDCs to the nearest venous sinusoid (d) or arteriole (e) (data pooled from n = 3 mice). (f) Representative flow plot showing the expression of two murine cDC markers, XCR1 for cDC1 and CD11b for cDC2, in murine bone marrow cDCs, gated as Gr-1⁻ B220⁻ MHCII^{high} CD11c^{high} cells. (g) Representative flow plot showing the expression of two human cDC markers, CD141 for cDC1 and CD1c for cDC2, in human bone marrow cDCs, gated as Lin⁻ CD14⁻ CD13⁺ CD33⁺ CD11c⁺ HLA-DR⁺ cells. (h) A heat map comparing the expressions of all chemokines and their receptors between mouse BM cDCs and mouse spleen (Sp) cDC2s (GSE110789, Durai V. 2018). Data represent mean ± SEM.

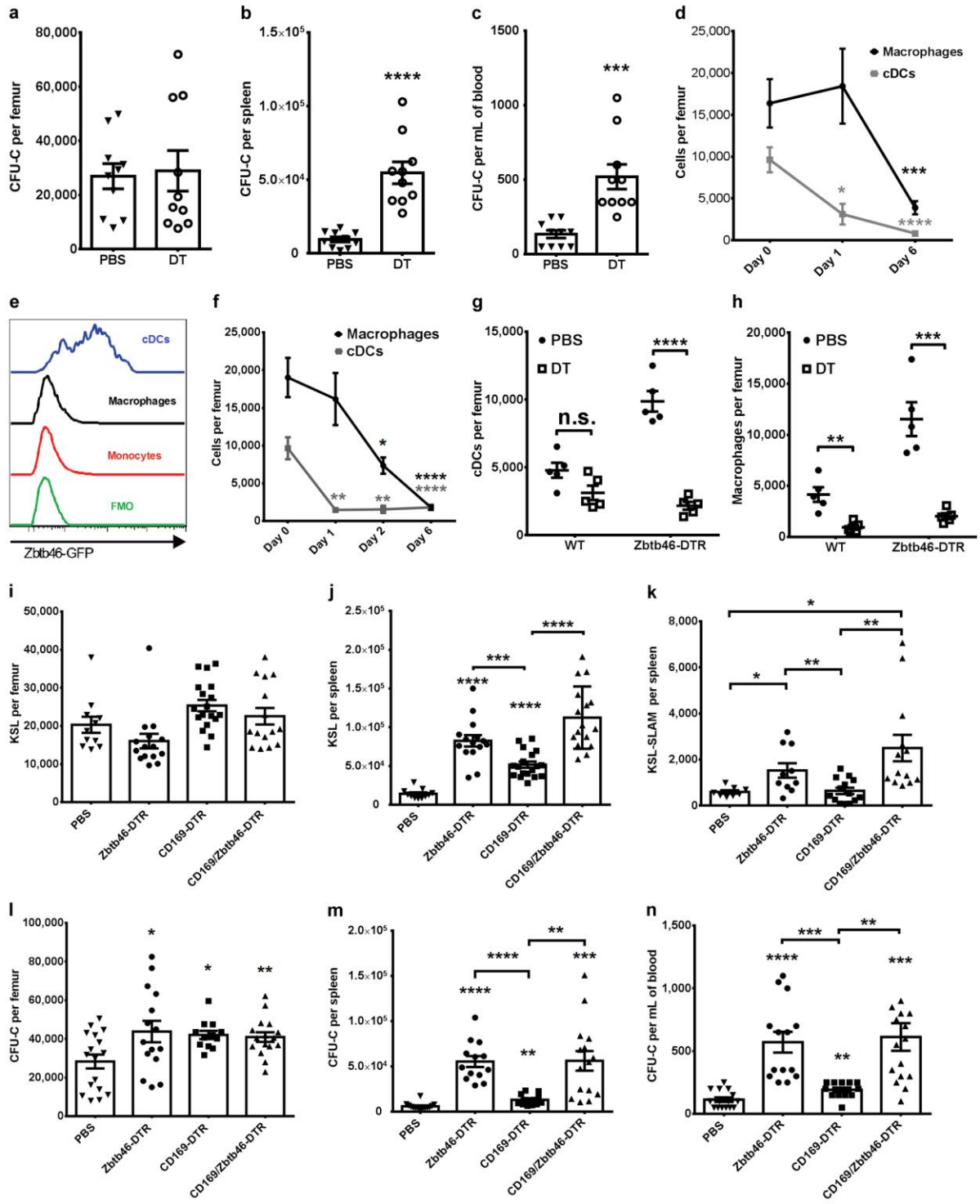


Figure 4.2. BM cDC ablation induces a loss of macrophage and HSPC mobilization. (a-d) Bone marrow from *CD11c^{dtr}* mice were transplanted into irradiated wildtype recipients and after eight weeks, the resulting chimeras were treated with PBS or DT for 6 days. The number of CFU-C in bone marrow (**a**), spleen (**b**) and blood (**c**) were quantified (n = 10 mice per cohort). (**d**) *CD11c^{dtr}* bone marrow chimeras were treated with DT for 1 day (n = 3 mice), 6 days (n = 10 mice), or with PBS (n = 10 mice), and BM cDCs and macrophages were quantified by flow cytometry. (**e**) Bone marrow monocytes (Gr-1^{low} B220⁻ CD115⁺ cells), macrophages (B220⁻ MHCII⁺ F4/80⁺ cells), and cDCs (MHCII^{high} CD11c^{high} cells) from *Zbtb46^{gfp/+}* mice were assessed for Zbtb46-GFP expression. FMO means fluorescence minus one control. (**f**) *Zbtb46^{dtr}* bone marrow chimeras were generated using same method and were treated with DT for 1 day (n = 5 mice), 2 days (n = 5 mice), 6 days (n=12 mice) or with PBS (n = 11 mice) and BM cDCs and macrophages were quantified. (**g,h**) Bone marrow from wild-type (Ly5.1) and *Zbtb46^{dtr}* (Ly5.2) mice were mixed (1:1) and transplanted into irradiated wild-type recipients (Ly5.1/5.2). The resulting wild-type and *Zbtb46^{dtr}* mixed bone marrow chimeras were treated with PBS or DT for 6 days, and the number of cDCs (**g**) and macrophages (**h**) in the bone marrow that were derived from wild-type (WT) or *Zbtb46^{dtr}* (Zbtb46-DTR) cells were quantified (n = 5 mice per cohort). (**i-n**) *Zbtb46^{dtr}* (Zbtb46-DTR), *CD169^{dtr}* (CD169-DTR) and *CD169^{dtr}:Zbtb46^{dtr}* (CD169/Zbtb46-DTR) bone marrow were transplanted into wild-type recipients. Eight weeks after transplantation, these mice were treated with PBS or DT for 6 days. The numbers of Lineage⁻ (CD45, CD31, Ter119, Gr-1) Sca1⁺ C-kit⁺ (KSL) cells in bone marrow (**i**) and spleen (**j**), the number of CD150⁺ CD48⁻ KSL (KSL-SLAM) cells in spleen (**k**), and the numbers of CFU-C in bone marrow (**l**), spleen (**m**) and blood (**n**) were quantified (n = 8-18 mice per cohort). Data represent the mean ± SEM. *P < 0.05; **P < 0.01; ***P < 0.001; ****P < 0.0001 compared with PBS-treated or day 0 mice if no top line indicating the specific comparison groups. “n.s.” means no significance.

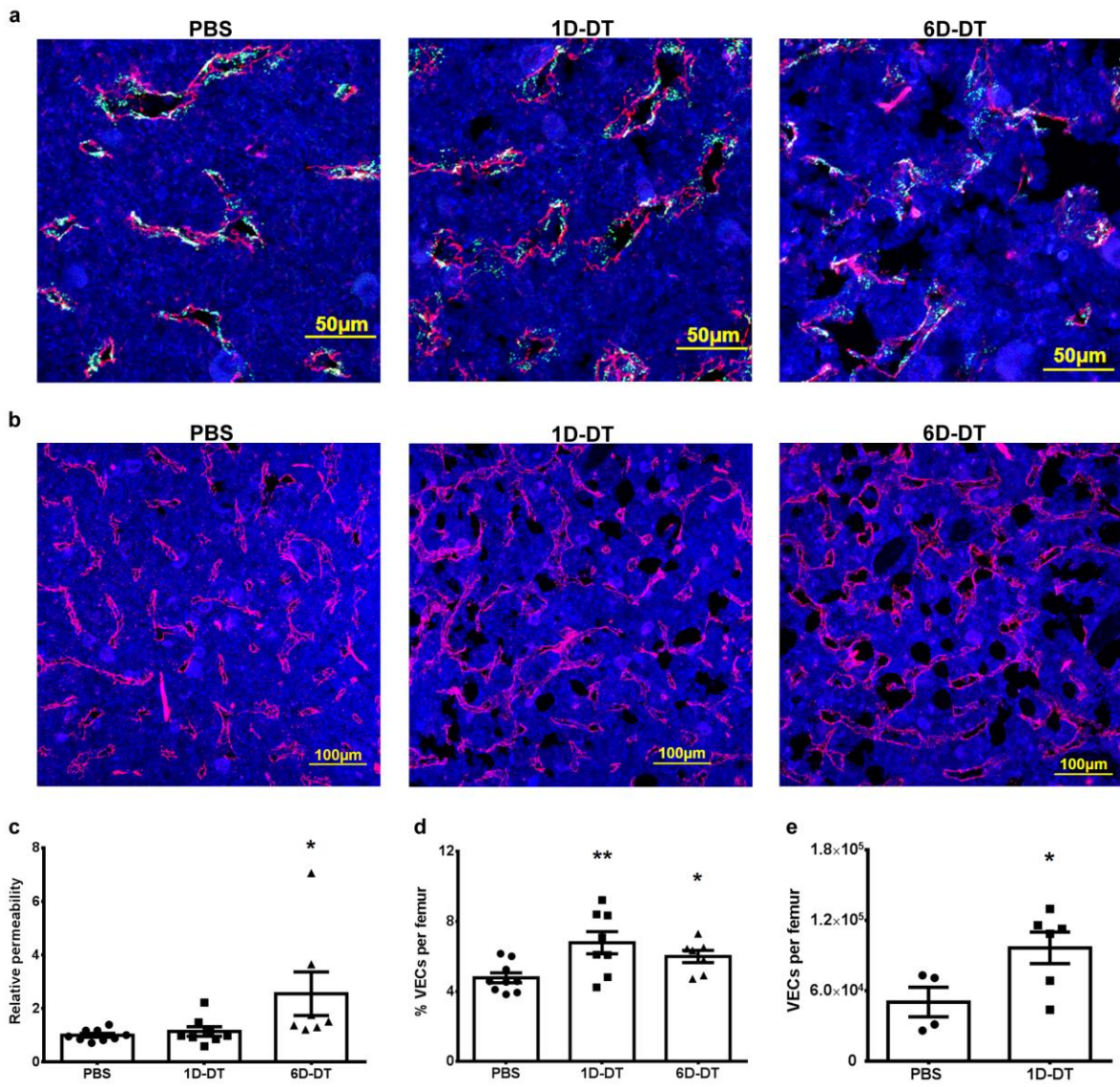


Figure 4.3. Ablation of BM cDCs affects bone marrow vascular endothelial cells (VECs).

(a,b) Representative photomicrographs of femur sections from *Zbtb46^{dtr}* bone marrow chimeras treated with PBS (left), 1 day of DT (1D-DT, middle) or 6 days of DT (6D-DT, right). (a) BSA-FITC was injected into these mice 15mins before sacrifice, and was labeled in green. Slides were stained for VE-Cadherin⁺ /CD31⁺ VECs (red). (b) Slides were stained for VE-Cadherin⁺ /CD31⁺ VECs (red). Counterstaining with DAPI highlights nuclei (blue). Original magnification, 200X.

(c) Vascular permeability in bone marrow for BSA-FITC was measured and normalized to PBS treated group. (d) Percentage of VEC volumes in the bone marrow of these mice were quantified (n = 9, 8, 7 mice for PBS, 1D-DT and 6D-DT groups). (e) Bone marrow VECs in *Zbtb46^{dtr}* bone marrow chimeras treated with PBS or 1D-DT were quantified by flow cytometry, gated as Lineage⁻ (CD45, Ter119, Gr-1) CD31⁺ cells (n = 4 or 6 mice for PBS or 1D-DT groups). Data represent the mean ± SEM. *P < 0.05; **P < 0.01 compared with PBS-treated mice.

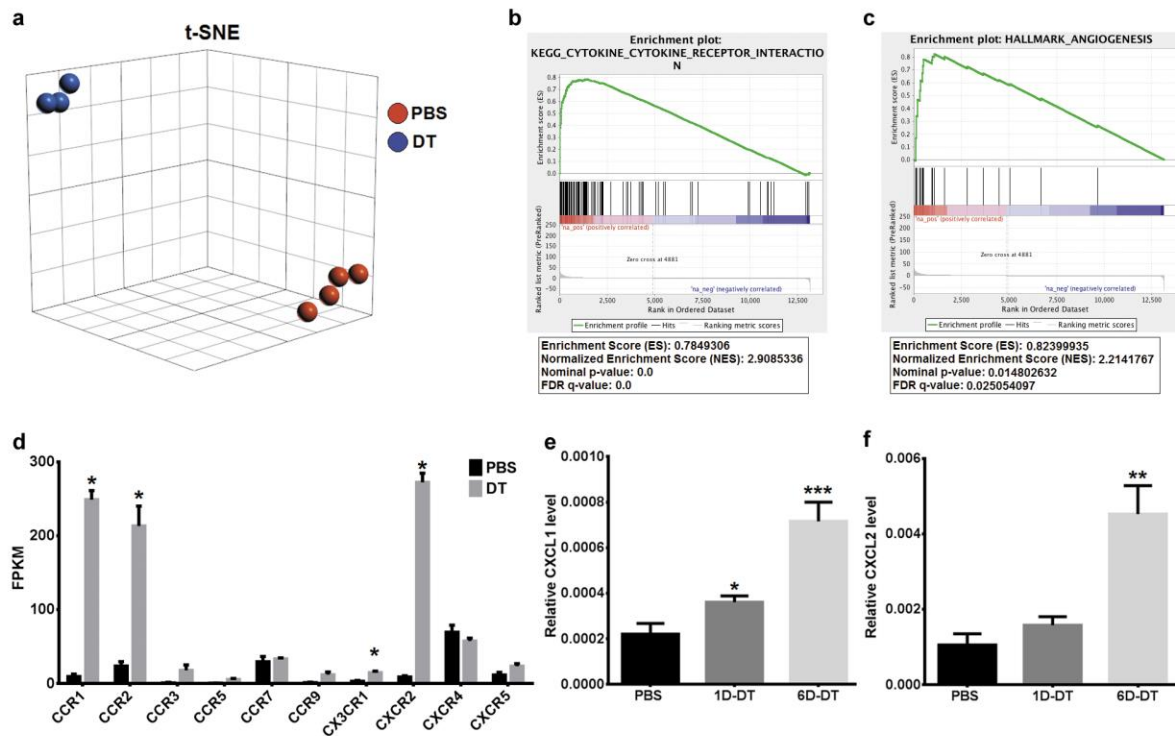


Figure 4.4. Ablation of BM cDCs activates sinusoidal endothelial cells and sinusoidal CXCR2 signaling. (a) Sinusoidal endothelial cells were sorted from *Zbtb46^{dtr}* bone marrow chimeras treated with PBS or 1D-DT, and RNA-sequencing (RNA-seq) analysis was performed in these cells. We performed t-distributed stochastic neighbor embedding (t-SNE) test to measure and visualize differences between PBS (n = 4 mice) and 1D-DT (n = 3 mice) groups. (b,c) RNA-seq data were analyzed using gene set enrichment analysis (GSEA) and two significantly enriched gene sets of interest were shown. (d) Expression levels of all expressed chemokine in sinusoidal endothelial cells. (e) CXCL1 and (f) CXCL2 expressions were analyzed by quantitative real-time PCR (qRT-PCR) in whole bone marrow from *Zbtb46^{dtr}* bone marrow chimeras treated with PBS, 1D-DT or 6D-DT (n = 6, 5, 5 mice for these groups). Data represent the mean \pm SEM. *P < 0.05; **P < 0.01; ***P < 0.001 compared with PBS-treated mice.

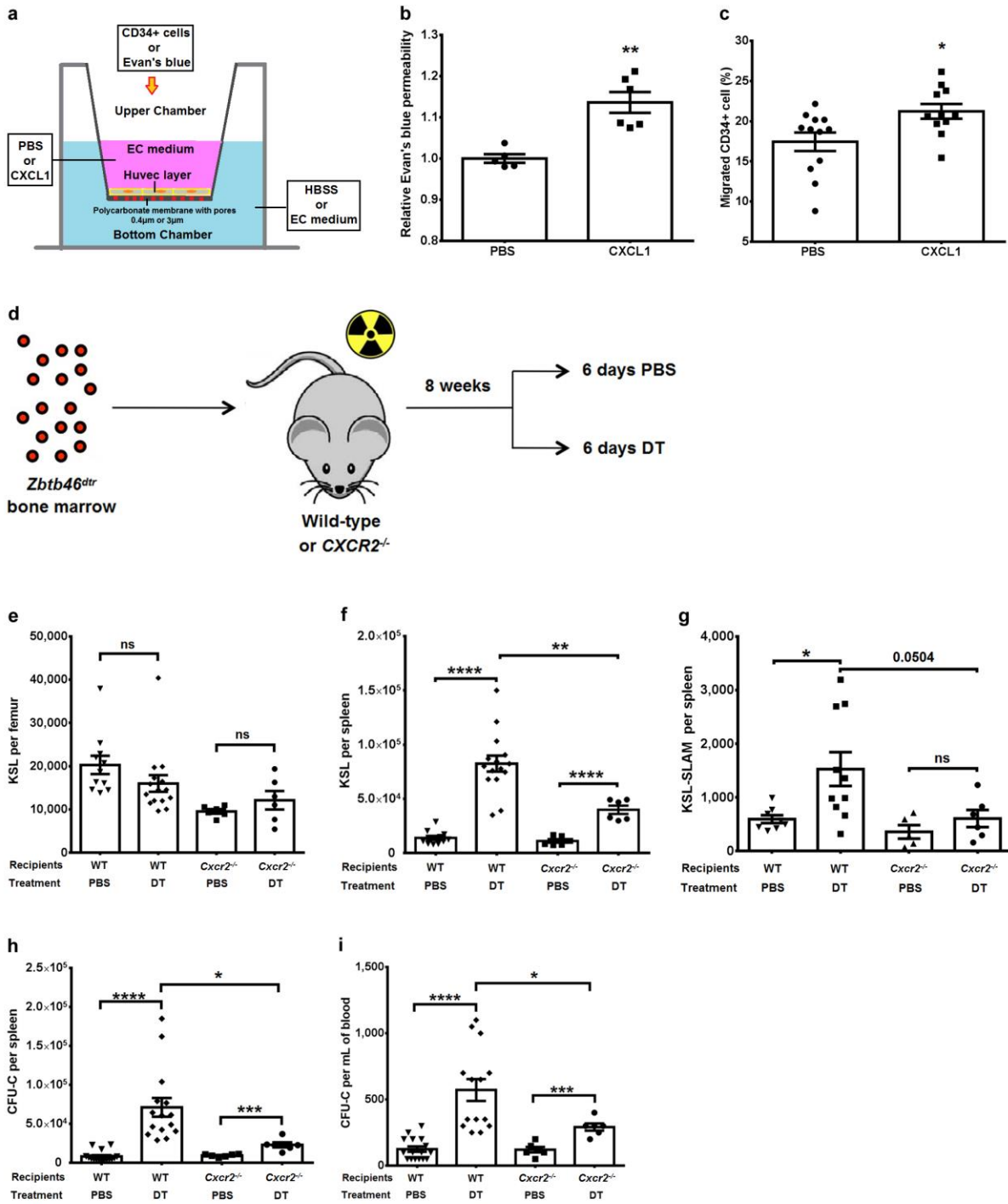
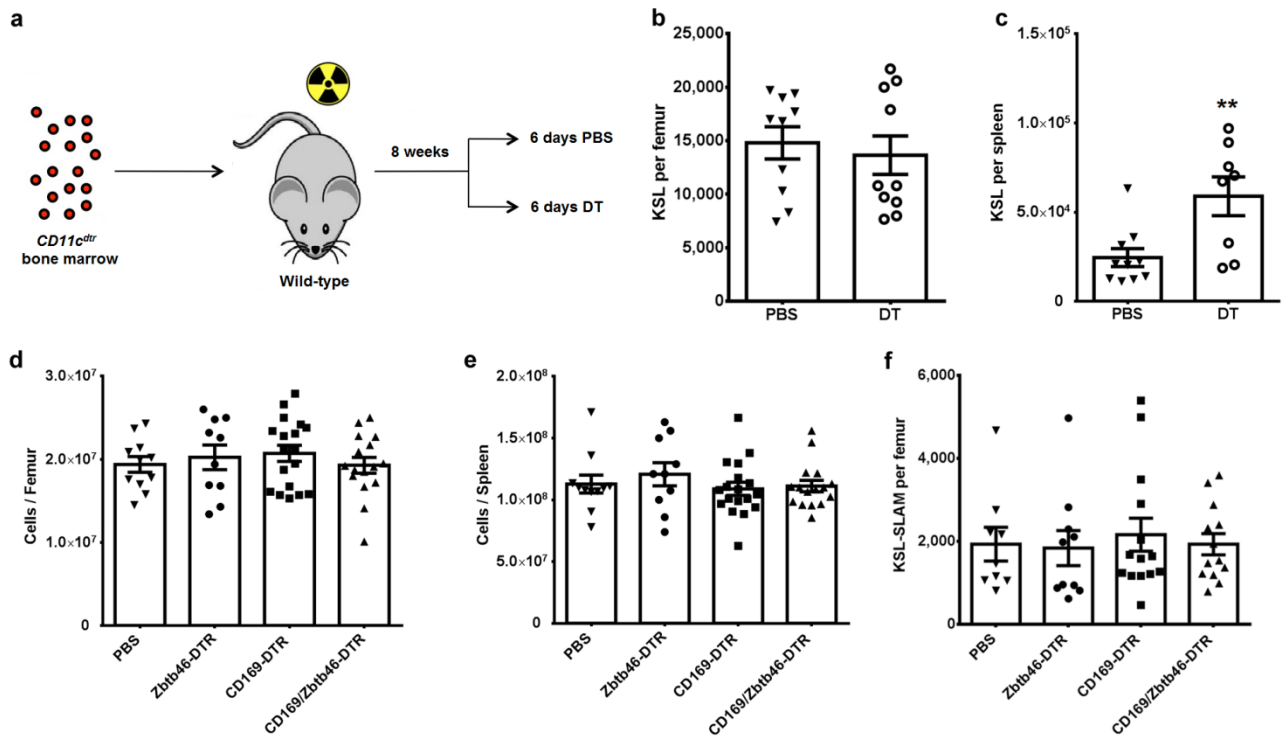


Figure 4.5. CXCR2 signaling pathway is important for BM cDC ablation induced HSPC mobilization. (a-c) Human umbilical vein endothelial cells (HUVECs) were cultured in endothelial cell (EC) medium in the upper chamber of the Boyden Chamber for migration assay. HUVECs were treated with PBS or recombinant CXCL1, incubated at 37 °C, 5% CO₂. (b) Evan's blue was added to the upper chamber with Hank's balanced salt saline (HBSS) in the bottom chamber, polycarbonate membrane pore size = 0.4 μm. After 1 hour incubation, the amount of Evan's blue in the bottom chamber was quantified by measuring light absorbance (n = 5 or 6 per group). (c) CD34⁺ human bone marrow cells from healthy donor were added to the upper chamber, with EC medium containing 100ng/mL SDF1 in the bottom chamber, polycarbonate membrane pore size = 3 μm. After 24 hours incubation, the number of migrated CD34⁺ cells in the bottom chamber was quantified by cellometer (n = 11 or 12 per group). (d) Bone marrow cells from *Zbtb46^{dtr}* mice were transplanted into irradiated wild-type (previously done in Fig 2) or *Cxcr2^{-/-}* recipients. Eight weeks after transplantation, mice were treated with PBS or DT for 6 days. (e-i) The number of KSL cells in bone marrow (e) and spleen (f), the number of KSL-SLAM cells in spleen (g), and the number of CFU-C in spleen (h) and blood (i) were quantified (n = 12, 16, 6, 6 mice for WT PBS, WT DT, *Cxcr2^{-/-}* PBS and *Cxcr2^{-/-}* DT groups). Data represent the mean ± SEM. *P < 0.05; **P < 0.01; ***P < 0.001; ****P < 0.0001 comparing to PBS-treated group if no top line indicating the specific comparing groups.

4.8. Supplemental Figures



Supplemental Figure 4.1. BM cDC ablation induces a loss of macrophage and HSPC

mobilization. (a) Bone marrow from *CD11c^{dtr}* mice were transplanted into irradiated wild-type

recipients and after eight weeks, the resulting chimeras were treated with PBS or DT for 6 days.

(b,c) KSL cells were quantified in bone marrow (b) and spleen (c) (n = 8-10 mice per cohort).

(d-f) *Zbtb46^{dtr}* (Zbtb46-DTR), *CD169^{dtr}* (CD169-DTR) and *CD169^{dtr}:Zbtb46^{dtr}* (CD169/Zbtb46-

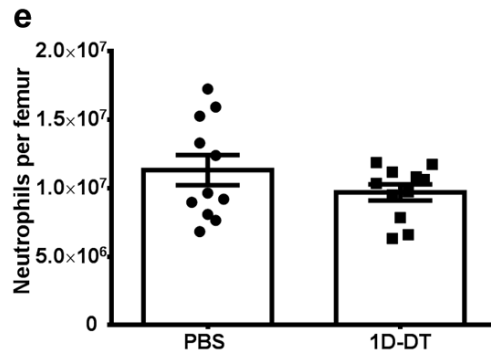
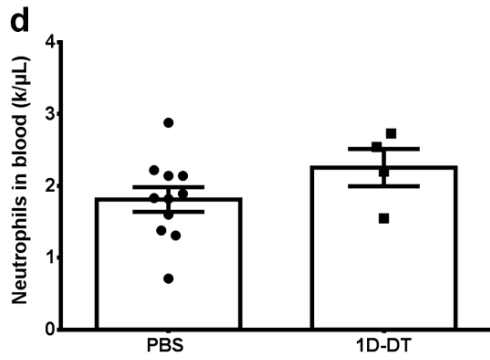
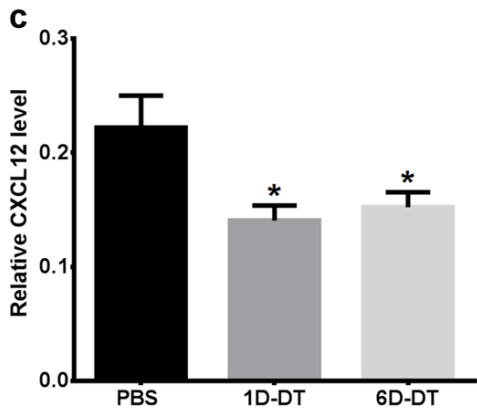
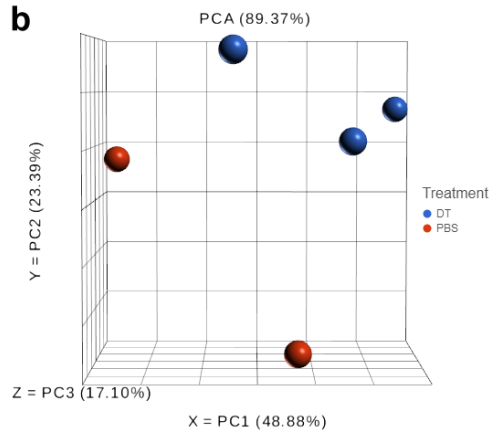
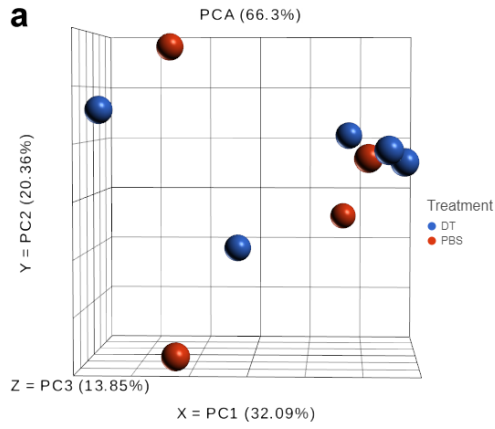
DTR) bone marrow were transplanted into wild-type recipients. Eight weeks after

transplantation, mice were treated with PBS or DT for 6 days. Total cellularity in bone marrow

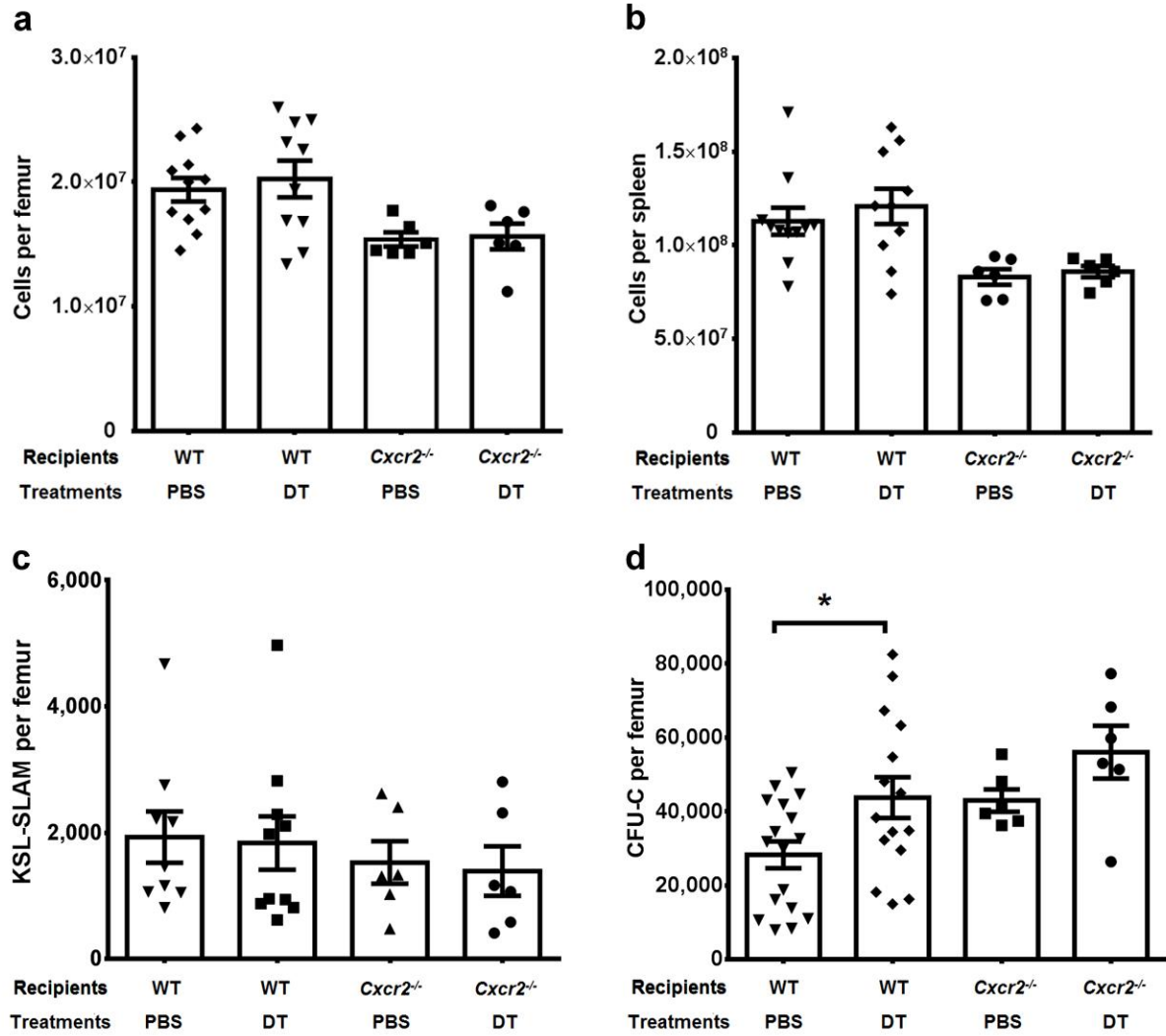
(d) and spleen (e), and KSL-SLAM cells (f) in bone marrow were quantified (n = 10-18 mice per

cohort). Data represent the mean \pm SEM. *P < 0.05; **P < 0.01 compared with PBS-treated

mice.



Supplemental Figure 4.2. Ablation of BM cDCs activated sinusoidal endothelial cells and sinusoidal CXCR2 signaling. (a,b) Arteriolar and sinusoidal endothelial cells (AECs and SECs) were sorted from *Zbtb46^{dtr}* bone marrow chimeras treated with PBS or 1 day of DT (1D-DT), and RNA microarray analyses were performed in these populations. We performed principal component analysis (PCA) to measure and visualize differences between PBS and 1D-DT groups, for (a) AECs (n = 4 or 5 mice for PBS or 1D-DT groups) and (b) SECs (n = 2 or 3 mice for PBS or 1D-DT groups). (c) CXCL12 expression was measured by quantitative real-time PCR (qRT-PCR) in whole bone marrow from *Zbtb46^{dtr}* bone marrow chimeras treated with PBS, 1D-DT or 6D-DT (n = 6, 5, 5 mice for these groups). (d,e) *Zbtb46^{dtr}* bone marrow chimeras were treated with PBS or 1 day of DT, neutrophils were quantified in blood by Hemavet Hematology Analyzer (n = 11 or 4 for each group) (d) and in bone marrow by flow cytometry, gated as Gr-1^{high} cells (n = 11 mice per group) (e). Data represent the mean \pm SEM *P < 0.05 compared with PBS-treated mice.



Supplemental Figure 4.3. CXCR2 signaling pathway is important for BM cDC ablation

induced HSPC mobilization. (a-d) Bone marrow cells from *Zbtb46*^{dtr} mice were transplanted into irradiated wild-type (previously done in Fig 2) or *Cxcr2*^{-/-} recipients. Eight weeks after transplantation, mice were treated with PBS or DT for 6 days. Total cellularity in bone marrow (a) and spleen (b), KSL-SLAM cells (c) and CFU-C (d) in bone marrow were quantified (n = 6-17 mice per cohort). Data represent the mean ± SEM. *P < 0.05.

CHAPTER 5: SUMMARY AND FUTURE DIRECTIONS

The goal of this work is to improve the overall understanding of the bone marrow perivascular niche. Here, we further characterized a known bone marrow niche component, mesenchymal stromal cells, and proposed a novel niche cell component, bone marrow classical dendritic cells (BM cDCs). In Chapter 2, we examined the heterogeneity of mesenchymal stromal cells using different transgenic *Cre* models and identified a subset of CAR cells potentially enriched for osteoprogenitors. This study further highlights the heterogeneity of mesenchymal stromal cells in the bone marrow and suggests appropriate models to interrogate this heterogeneity. In Chapter 3, we used a *Cxcl12* conditional deletion model and multiple stromal specific transgenic *Cre* models to assess the role of CXCL12 from different stromal cell populations on the regulation of B lymphopoiesis. We show that CXCL12 from *Ocn-Cre* targeted stromal cells is important in the regulation of mature naive B cells and memory B cells in the bone marrow. This study demonstrates the functional heterogeneity of stromal cells and may provide insights to the development of potential therapies for B cell related diseases. In Chapter 4, we used ablation models to assess the role of BM cDCs in the regulation of HSPCs in the bone marrow and discovered that BM cDCs serve as an important hematopoietic niche component to regulate HSPC trafficking through its regulation of sinusoidal CXCR2 signaling. These data improve our understanding of the hematopoietic niche and provide potential targets for the development of cell mobilization related treatment.

5.1. Targeting mesenchymal stromal cells with different *Cre*-recombinase transgenes

5.1.1. Summary

In Chapter 2, we characterized three *Cre*-recombinase transgenes for their targeting specificity on bone marrow stromal cells. *Ocn-Cre* has been widely used to target osteoblasts in past studies^{245,247,248}. Our data show that *Ocn-Cre* targets not only all osteoblasts, but also osteocytes, ~70% of CAR cells, and the majority of arteriolar pericytes. *Dmp1-Cre* has been widely used to target osteocytes^{250,252,266}. We show that *Dmp1-Cre* targets all osteoblasts, as well as ~30% of CAR cells. Expression profiling of these CAR cells shows higher expression of genes associated with mature osteoblasts, suggesting their potential enrichment for osteoprogenitors. We also, for the first time, characterized the bone marrow stromal cells targeted by a *Tagln-Cre* transgene, and show that *Tagln-Cre* targets all osteoblasts, ~70% of CAR cells, and both venous sinusoidal and arteriolar pericytes. Collectively, we have rigorously defined the targeting specificities in the bone marrow for the three *Cre*-recombinase transgenes. *Ocn-Cre* and *Dmp1-Cre* target broader stromal cell populations than previously appreciated, which should be considered when designing future studies. Moreover, we present *Tagln-Cre* as a new tool to efficiently target both venous sinusoidal and arteriolar pericytes in the bone marrow.

5.1.2. Are *Dmp1-Cre* targeted stromal cells truly enriched for osteoprogenitors?

Our data suggests that *Dmp1-Cre* targeted stromal cells may be enriched for osteoprogenitors. However, this hypothesis is only based on gene expression profiling using RNA microarray and further experiments are required to confirm this finding. First, quantitative real-time PCR may be used to confirm the up-regulation of genes associated with mature osteoblasts, which were detected by RNA microarray. Second, we may perform functional

assays to test the osteoprogenic capacity of *Dmp1-Cre* targeted stromal cells. We may sort these cells using the same strategy as for gene expression profiling, and culture the sorted cells *in vitro* to test their multi-lineage capacity using colony forming unit (CFU) assays for adipocytes (CFU-A), osteoblasts (CFU-Ob) and chondrocytes (CFU-Ch). Total CAR cells and *Ocn-Cre* targeted CAR cells may also be sorted and cultured to test their multi-lineage capacity. By comparing their multi-lineage capacities, especially the capacity to form osteoblasts among these different subsets of CAR cells, we will be able to confirm whether *Dmp1-Cre* targeted stromal cells are truly enriched for osteoprogenitors.

5.1.3. Further characterize the heterogeneity of CAR cells

Prior studies have discussed the heterogeneity of mesenchymal stromal cells in the bone marrow and have described different subsets of stromal cells for their specific functions, such as LepR⁺ cells and Nestin-GFP cells^{10,12}. In this study, we further identified *Dmp1-Cre* targeted stromal cells to include potential osteoprogenitors. However, it remains unanswered how many functionally different subsets of stromal cells may exist. Recent studies suggest that distinct niches may exist to regulate different types of cells, such as quiescent or more proliferative HSCs^{12,18,79}. Further dissecting the heterogeneity of stromal cells will provide insights to better characterize distinct niches with more specific functions. This will improve our understanding of the regulation of different cells in the bone marrow, providing fundamental knowledge to support future research in both basic and clinical science. For future studies, CAR cells, representing the majority of mesenchymal stromal cells, may be sorted from *Cxcl12^{gfp}* mice and analyzed by single cell RNA sequencing. Based on the gene expression profile, clustering analysis may be performed to discover more specific subsets of CAR cells. It is important to notice that due to the

overall similarity among CAR cells, clustering analysis may be inefficient to detect more specific cell subsets. Alternatively, differential gene expressions should also be analyzed and such analysis should focus on genes representing surface markers or genes with important functions in the regulation of the bone marrow niche.

5.2. CXCL12 from *Ocn-Cre* targeted mesenchymal stromal cells regulates late-stage B cell development

5.2.1. Summary

In Chapter 3, we assessed the role of CXCL12 from different stromal cells in the regulation of B cell development in the bone marrow. We show that CXCL12 from *Ocn-Cre* targeted stromal cells is specifically important for the homing and/or retention of mature naive B cells. We also show that *Dmp1-Cre* targeted stromal cells play no significant role in the regulation of B cell development, consistent with our prior study showing that *Dmp1-Cre* targeted CAR cells express low levels of IL-7¹⁹. In addition, our data suggests that CXCL12 from *Ocn-Cre* targeted stromal cells regulates memory B cells specifically in the bone marrow. Collectively, these data suggest that B cells require distinct niches at different stages of development, and *Ocn-Cre* targeted stromal cells may represent a specific niche for late-stage B cell development. Moreover, *Ocn-Cre* targeted stromal cells may also regulate memory B cells, thus potentially contributing to the regulation of B cell immune memory and humoral immunity. This study may provide insights to further understand immune memory, which in turn will contribute to improvements in the treatment of the relevant diseases.

5.2.2. Functionally characterize the role of bone marrow memory B cells in the regulation of humoral immunity

In this study, we used NP-CGG to induce NP-specific memory B cells and observed a significant reduction of these cells in the bone marrow of *Ocn-Cre:Cxcl12^{fllox/fllox}* mice compared to the *Cxcl12^{fllox/fllox}* control mice. Of notice, the number of memory B cells in the bone marrow constitutes ~40% of total memory B cells, including memory B cells from the spleen (Fig 3.5A&B), assuming one femur represents ~9% of total bone marrow cells. We observed ~50% reduction in memory B cells in the bone marrow of *Ocn-Cre:Cxcl12^{fllox/fllox}* mice, roughly representing a 20% reduction in total memory B cells. It remains questionable whether this modest reduction of memory B cells has a significant impact on memory B cell derived humoral immunity. To test this, we have an ongoing study in which a similar number of bone marrow cells containing NP-specific memory B cells from *Ocn-Cre:Cxcl12^{fllox/fllox}* or *Cxcl12^{fllox/fllox}* mice will be transferred into *IgHa/J* mice, followed by secondary immunization with NP-CGG. ELISA will be performed to quantify the NP-specific IgG1b antibodies generated by NP-specific memory B cells from the donor mice. In addition, using the same method, we could compare the function of NP-specific memory B cells from the bone marrow and the spleen.

5.2.3. How does CXCL12 ablation in *Ocn-Cre* targeted stromal cells affect other cells in the bone marrow?

Our study focused on how CXCL12 ablation in different stromal cells regulates B cell development. However, our preliminary data also suggests a significant reduction of T cells, especially CD8⁺ T cells and Foxp3⁺ regulatory T (Treg) cells in the bone marrow upon CXCL12 ablation in *Ocn-Cre* targeted stromal cells (Fig 5.1A). In contrast, no significant reduction of T

cells was observed in *Dmp1-Cre:Cxcl12^{flox/flox}* mice (Fig 5.1B). These data suggest that CD8⁺ T cells and Treg cells, as well as mature naive B cells and memory B cells, may share the same niche in the bone marrow. A recent study has suggested Foxp3⁺ regulatory T cells play an important role in the regulation of B lymphopoiesis²⁹¹. Thus, it is possible that Treg cells may be important for the regulation of mature naive B cells and memory B cells in our CXCL12 ablation model. To test this possibility, the same CXCL12 ablation model may be applied in a background of Treg cell deficient mice. The effects of CXCL12 ablation in *Ocn-Cre* targeted stromal cells on mature naive B cells and memory B cells will be assessed in the lack of Treg cells.

Moreover, prior studies have suggested CD8⁺ T cells in the bone marrow may function as memory T cells²⁹². Although this hypothesis needs further confirmation, it is important to note that two potential populations of memory B cells and memory T cells are both regulated by CXCL12 from *Ocn-Cre* targeted stromal cells. These data indicate that a unique bone marrow niche may exist to regulate memory cells, thus potentially regulating immune memory in the bone marrow. More interestingly, the fact that memory B cells and memory T cells may share the same niche suggests the potential necessity in our future research to focus on a whole system, instead of a specific cell type. This may provide a different perspective to investigators when considering and designing their future experiments.

5.2.4. Do *Ocn-Cre* targeted stromal cells regulate mature naive B cells and memory B cells through other pathways?

CXCL12 is an important bone marrow niche factor regulating hematopoiesis and B lymphopoiesis²⁰. Our prior study has suggested the critical role of CXCL12 in the regulation of

B cell development at different stages³. In this study, we show that CXCL12 from *Ocn-Cre* targeted stromal cells regulates mature naive B cells and memory B cells, suggesting these cells are potentially an important component for a specific B cell niche. As previously discussed, B cell development is a complicated process requiring the contribution from different molecular pathways. To better understand the role of *Ocn-Cre* targeted stromal cells in the regulation of B lymphopoiesis, it is necessary to further characterize these cells to test whether additional pathways are involved in their regulation of B cells.

To assess this possibility, we are currently breeding *Ocn-Cre:ROSA26^{Ai9/+}:Col2.3^{gfp}* and *Dmp1-Cre:ROSA26^{Ai9/+}:Col2.3^{gfp}* mice. The *ROSA26^{Ai9/+}* transgene allows for the identification of *Ocn-Cre* or *Dmp1-Cre* targeted cells as tdTomato⁺ cells¹⁹. The *Col2.3^{gfp}* transgene allows for the identification of osteoblasts and osteoblast progenitors as GFP⁺ cells²⁹³. In combination, we can accurately sort *Ocn-Cre* or *Dmp1-Cre* targeted tdTomato⁺ GFP⁻ stromal cells, excluding osteoblasts. We will then perform RNA sequencing analysis on these two subsets of stromal cells and compare their gene expression profiles. We will try to discover genes enriched in *Ocn-Cre* targeted stromal cells that are potentially important for the regulation of B cells, especially mature naive B cells and memory B cells. Among these genes, we will select candidates for further functional tests, potentially using transgenic ablation models depending on their availability. This future study may help improve our understanding of the heterogeneity of stromal cells and the regulation of B cell development by specific stromal cells.

5.3. Bone marrow cDCs regulate hematopoietic stem and progenitor cell trafficking

5.3.1. Summary

In Chapter 4, we assessed the role of bone marrow (BM) cDCs in the regulation of the hematopoietic niche and HSPCs. Using *Cx3cr1^{gfp}* mice, we identified cDCs in the bone marrow and show that they localize to both sinusoidal and arteriolar regions. We further discovered that the majority of these BM cDCs have a cDC2-like immunophenotype, but their gene expression profile suggests that they are functionally different from conventional cDC2s in the spleen. Interestingly, we also identified a similar population of BM cDCs in human bone marrow, emphasizing the potential clinical relevance of this study. Using ablation models, we show that the ablation of BM cDCs results in a secondary, non-cell autonomous loss of BM macrophages, which have been previously reported to regulate HSPCs⁷. In addition, we show that the ablation of BM cDCs induces HPSC mobilization, at least in part, through a macrophage independent mechanism. Since HSPC mobilization is often associated with changes in the perivascular niche, we characterized endothelial cells and discovered endothelial expansion following BM cDC ablation. We also revealed a robust up-regulation of CXCR2 in sinusoidal endothelial cells and the up-regulation of two major ligands of CXCR2 in the bone marrow, CXCL1 and CXCL2. CXCR2 activation has been reported to induce vascular permeability and HSPC mobilization⁷², thus we assessed the role of CXCR2 in the regulation of HPSC mobilization following BM cDC ablation. We show that activation of CXCR2 *in vitro* induces vascular permeability and HSPC migration. Moreover, we show that deletion of CXCR2 in non-hematopoietic cells significantly attenuates HSPC mobilization after BM cDC ablation. Collectively, these data suggest that BM cDCs play an important role in regulating HSPC trafficking, at least in part, through its regulation of sinusoidal CXCR2 signaling and vascular permeability.

5.3.2. Further assess the role of CXCR2 in endothelial cells

To examine the role of CXCR2 in the regulation of HSPC mobilization following BM cDC ablation, we transplanted *Zbtb46^{dtr}* bone marrow into irradiated *Cxcr2^{-/-}* mice. The deletion of CXCR2 is only restricted to non-hematopoietic cells in the bone marrow, including both endothelial cells and stromal cells. It is possible that the attenuated HSPC mobilization following BM cDC ablation may be a result of CXCR2 deletion in bone marrow stromal cells. To rule out this possibility, we have an ongoing experiment using *VEcad-Cre:Cxcr2^{flox/flox}* mice as the recipients for *Zbtb46^{dtr}* bone marrow transplant. This will allow us to restrict the deletion of *Cxcr2* to endothelial cells, excluding bone marrow stromal cells. We will then perform flow cytometry and CFU-C tests to assess HSPC mobilization after BM cDC ablation in these *VEcad-Cre:Cxcr2^{flox/flox}* mice.

5.3.3. How do BM cDCs regulate sinusoidal endothelial cells?

We have discovered that BM cDCs may regulate HSPC trafficking through its regulation of sinusoidal CXCR2 signaling. However, how BM cDCs regulate sinusoidal endothelial cells remains unknown. A prior study on BM macrophages suggests that they regulate HPSC trafficking through mesenchymal stromal cells⁷. BM cDCs and BM macrophages share the same myeloid origin, so we hypothesize that BM cDCs may also regulate mesenchymal stromal cells. To test this hypothesis, we performed a pilot experiment in which bone marrow stromal cells (BMSCs) were sorted from *Zbtb46^{dtr}* bone marrow chimeras treated with 1 day of DT or PBS. RNA microarray analysis on these cells suggested a potential functional change in BMSCs following BM cDC ablation (Fig. 5.2A). Expression of CXCL1 and CXCL2 were up-regulated in the whole bone marrow following BM cDC ablation to activate sinusoidal CXCR2 signaling

(Fig. 4.4E&F). Surprisingly, the expression of CXCL1, but not CXCL2, was significantly increased in BMSCs by more than 3-fold following BM cDC ablation (Fig. 5.2B&C), indicating the partial involvement of BMSCs in the regulation of sinusoidal CXCR2 signaling. Collectively, these preliminary data suggest that BM cDCs may regulate sinusoidal endothelial cells, at least in part, through their regulation of BMSCs.

While BMSCs may regulate sinusoidal endothelial cells through their up-regulation of CXCL1, it remains unknown how BM cDCs regulate BMSCs. Since the majority of BM cDCs and BMSCs are both localized to the perivascular region, it is likely that the two cell populations are in close proximity. Thus, it is possible that BM cDCs may directly regulate BMSCs through the release of intermediate molecules or direct physical interaction. To test this possibility, gene expression profiles from both cell populations will be compared to identify potential factor/receptor pairs expressed by BM cDCs and BMSCs, respectively. In addition, *Zbtb46^{gfp}:Cxcl1^{DsRed}* mice may be generated, in which BM cDCs are marked as GFP⁺ cells and BMSCs are marked as DsRed⁺ cells. Bone sections from these mice may then be imaged to check whether direct physical interaction exists between BM cDCs and BMSCs. In summary, understanding the mechanisms involved in the regulation of BMSCs and sinusoidal endothelial cells by BM cDCs will provide insights to the advancement in both basic and clinical research.

5.3.4. How do BM cDCs regulate BM macrophages?

In *Zbtb46^{dtr}* bone marrow chimeras, the ablation of BM cDCs was observed 1 day after DT treatment, and the ablation of BM macrophages was observed at day 2. Our data suggests that BM cDC ablation may induce a secondary, non-cell autonomous loss of BM macrophages. However, the mechanism involved in this regulation remains unclear. One possibility is that the

death of BM cDCs will release signaling molecules, such as chemokines and cytokines, which may induce cell death specifically in BM macrophages. Another possibility is that BM cDCs may provide critical signals to support the survival of BM macrophages through their release of survival factors or through direct physical interaction. To test these possibilities, gene expression profiles from both BM cDCs and BM macrophages will be compared to identify potential signaling pathways contributing to the survival or cell death of BM macrophages. In contrast to direct regulation, BM cDCs may regulate BM macrophages indirectly through intermediate cells, such as BMSCs. In addition to the above scenarios, BM cDCs and BM macrophages share the same myeloid origin, thus the loss of BM cDCs may affect their common progenitor to undergo a more cDC lineage committed differentiation, preventing the replenishment of BM macrophages. Future research may include characterization of myeloid progenitors, BMSCs and other cell populations in the bone marrow, before or after BM cDC ablation. Better understanding of the mechanisms involved in the secondary loss of BM macrophages will likely provide targets to the development of macrophage-depleting agents with significant clinical applicability.

5.3.5. Assess the effects of BM cDC ablation on osteoblasts

Other than sinusoidal endothelial cells, we also assessed the effects of BM cDC ablation on osteoblasts. *Zbtb46^{dtr}* bone marrow chimeras were treated with DT for 6 days and we observed a significant decrease in osteocalcin (*Bglap2*) mRNA level in the whole bone marrow (Fig. 5.3A). Osteocalcin is mainly expressed by mature osteoblasts, thus our data suggests a suppression of osteoblasts following BM cDC ablation. To test the effects of BM cDC ablation on osteoblasts, *Zbtb46^{dtr}* bone marrow was transplanted into *Col2.3^{gfp}* mice in which osteoblasts are marked as

GFP⁺ cells, followed by DT or PBS treatment 8 weeks after transplant. Using flow cytometry, we quantified and sorted GFP⁺ osteoblasts from DT or PBS treated *Zbtb46^{dtr}* bone marrow chimeras. To our surprise, no significant difference was observed in the number of osteoblasts after BM cDC ablation, compared to the control group (Fig. 5.3B). In addition, we tested the expression of osteocalcin in sorted GFP⁺ osteoblasts and observed a significant decrease in the osteocalcin mRNA level after BM cDC ablation (Fig. 5.3C). Collectively, our preliminary data suggests that osteoblasts might be functionally suppressed following BM cDC ablation.

A prior study suggested that BM macrophage ablation might induce a functional suppression of osteoblasts⁷. To test whether BM cDCs may regulate osteoblasts in a macrophage-independent pathway, we compared bone marrow chimeras transplanted with *Zbtb46^{dtr}*, *CD169^{dtr}* and *CD169^{dtr}:Zbtb46^{dtr}* bone marrow for the ablation of BM cDCs, BM macrophages and both. The whole bone marrow osteocalcin mRNA levels in these mice suggest that BM cDCs may regulate osteoblasts in a macrophage-independent pathway (Fig. 5.3D). However, large variability exists in the osteocalcin mRNA level in *CD169^{dtr}* bone marrow chimeras, and further testing is necessary to support this hypothesis. One potential experiment is to transplant *CD169^{dtr}* bone marrow into *Col2.3^{gfp}* mice and treat these chimeras with 6 days of DT to ablate BM macrophages. We can then sort GFP⁺ osteoblasts and test their expression of osteocalcin. In addition, it is more important to figure out the mechanism involved in the regulation of osteoblasts by either BM cDCs or BM macrophages. These two populations mainly localize to the perivascular region and osteoblasts localize to the endosteal region, thus intermediate cells may be involved to relay the signals for their interactions. Further characterization of osteoblasts using RNA-seq analysis before and after BM cDC ablation may help detect potential pathways driving the suppression of osteoblasts. Potential factors activating

these pathways will then be tested in whole bone marrow or specific cell populations.

Osteoblasts are a critical component for osteogenesis and understanding the suppression of osteoblasts will provide important insights to the development of potential therapies for bone related diseases.

5.4. Conclusion

In this thesis, we further characterized the roles and functions of two bone marrow niche components. In Chapter 2, we show that *Ocn-Cre*, *Dmp1-Cre* and *Tagln-Cre* transgenes target different subsets of bone marrow mesenchymal stromal cells. We revealed that *Ocn-Cre* and *Dmp1-Cre* target broader cell populations than previously appreciated, which should be incorporated in the design of future study. We also suggest that *Dmp1-Cre* targeted stromal cells may be enriched for osteoprogenitors. In Chapter 3, we tested the function of CXCL12 from different subsets of stromal cells on B lymphopoiesis. We show that CXCL12 from *Ocn-Cre* targeted stromal cells is particularly important for the regulation of mature naive B cells and memory B cells, potentially through the regulation of their homing and/or retention. In Chapter 4, we assessed the role of BM cDCs in the regulation of the HSPCs. We show that BM cDC ablation results in a secondary, non-cell autonomous loss of BM macrophages. We also discovered that BM cDCs may regulate HSPC trafficking in a macrophage independent pathway, at least in part, through its regulation of sinusoidal CXCR2 signaling and vascular permeability. Collectively, this thesis study helps improve our understanding of the heterogeneity of stromal cells and the regulation of B lymphopoiesis by different stromal cells. In addition, we propose a novel bone marrow niche component that regulates HSPC trafficking. Although future research is required to mechanistically study the stromal cells and BM cDCs, the results generated from

this study provide insights that are important for the advancement in both basic and clinical biology.

5.5. Figures

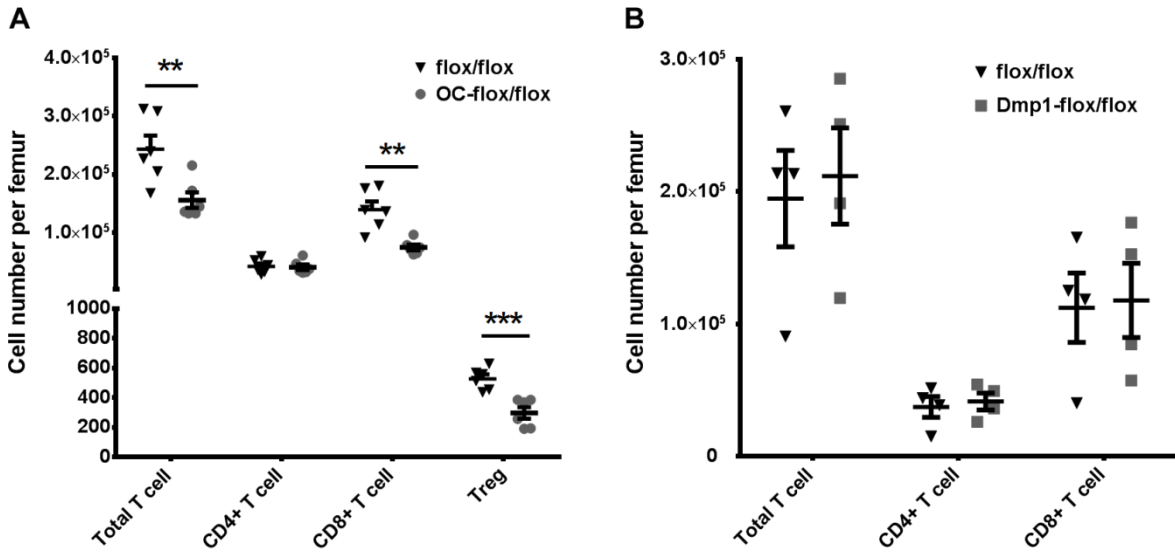


Figure 5.1. CXCL12 expression in *Ocn-Cre* targeted stromal cells is important for the regulation of T cells. A&B. Femurs were harvested from *Ocn-Cre:Cxcl12^{flox/flox}* mice (**A**), *Dmp1-Cre:Cxcl12^{flox/flox}* mice (**B**), and *Cxcl12^{flox/flox}* control mice (**A&B**). Bone marrow was then analyzed using flow cytometry to quantify the number of different T cells, gated as T cell receptor (TCR)⁺ cells. Sample size, n = 4-6 mice per group in all experiments. Data represent the mean ± SEM, **P < 0.01; ***P < 0.001.

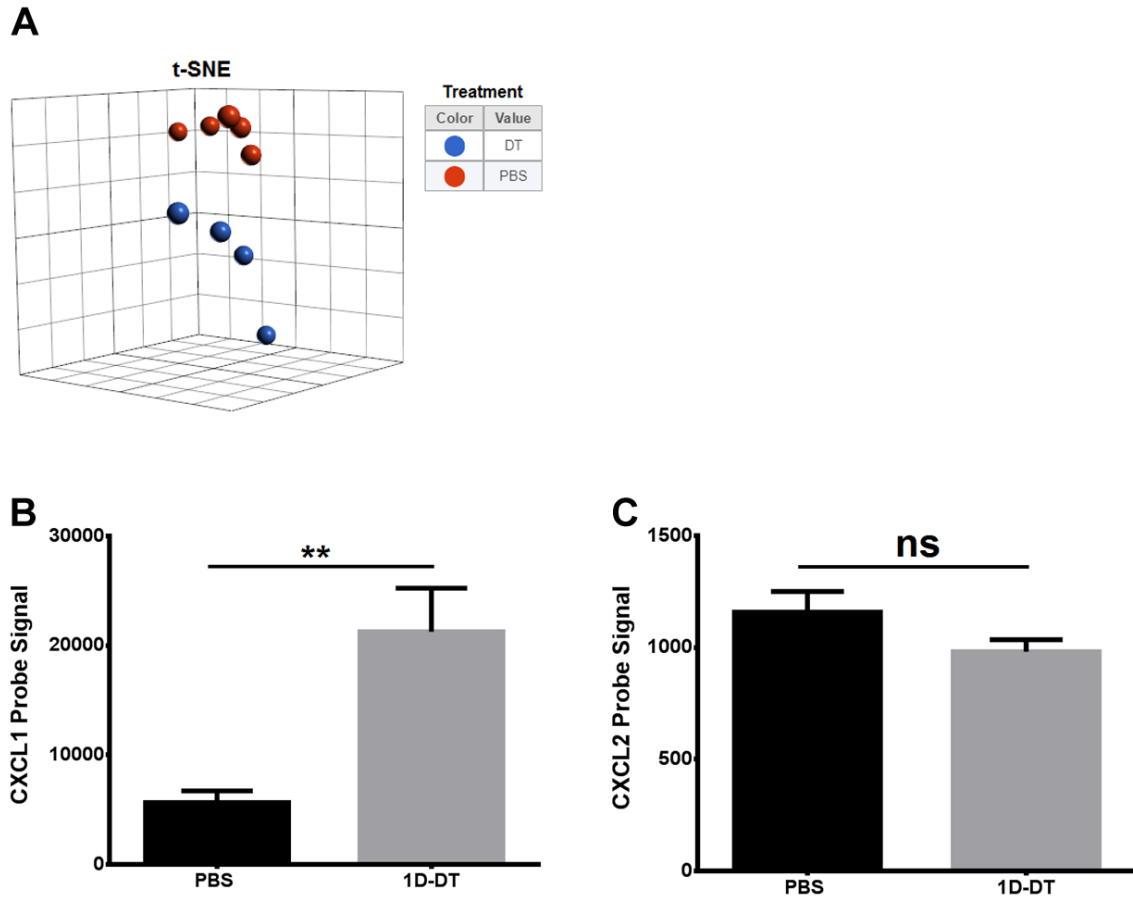


Figure 5.2. The effects of BM cDC ablation on bone marrow stromal cells (BMSCs). Bone marrow stromal cells were FACS sorted from *Zbtb46^{dlr}* bone marrow chimeras treated with 1 day of DT or PBS (n = 4 or 5 mice, respectively). Sorted cells were then used for RNA microarray analysis. **A.** Gene expression profiles from the two conditions were compared and visualized using t-Distributed Stochastic Neighbor Embedding (tSNE) analysis. **B.** The expression level of CXCL1 mRNA in BMSCs was quantified by probe signal. **C.** The expression level of CXCL2 mRNA in BMSCs was quantified by probe signal. Data represent the mean \pm SEM, **P < 0.01; “ns” means no significant difference.

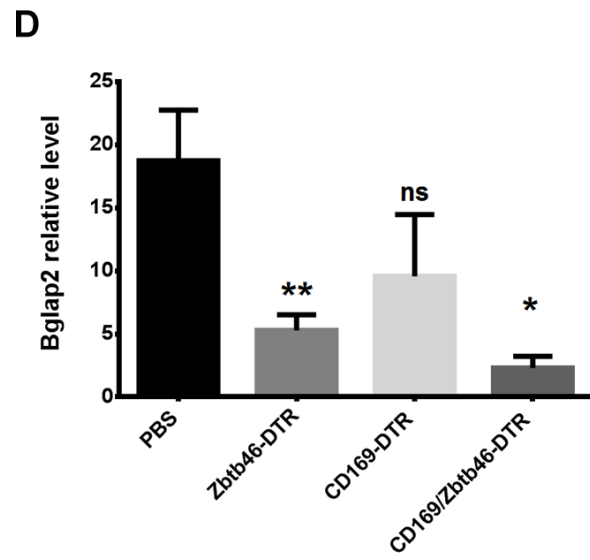
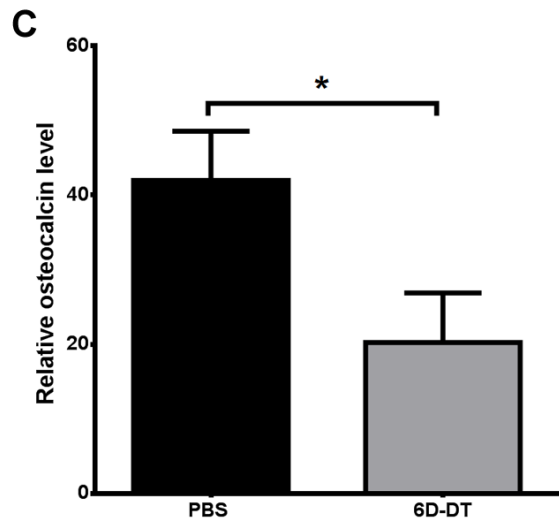
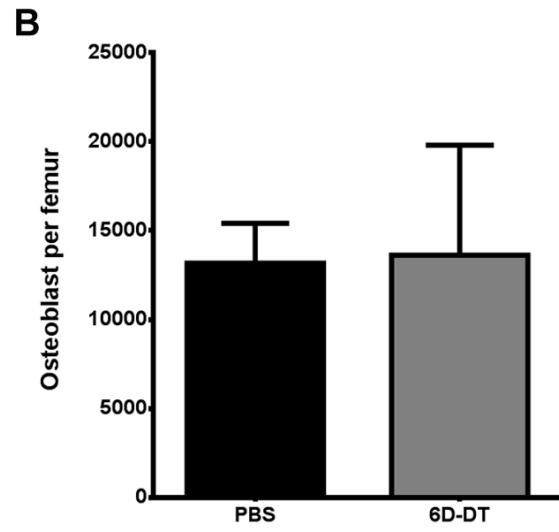
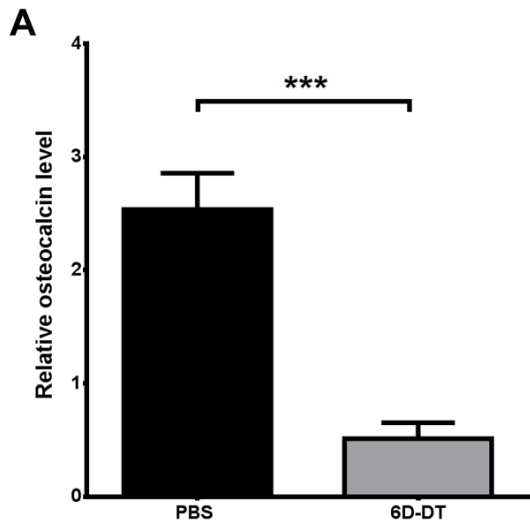


Figure 5.3. The effects of BM cDC ablation on osteoblasts. **A.** The mRNA level of osteocalcin (*Bglap2*) in whole bone marrow of *Zbtb46^{dtr}* bone marrow chimeras, measured by RT-qPCR and was normalized to the expression level of β -actin (n = 5 mice for both groups). *Zbtb46^{dtr}* bone marrow was transplanted into irradiated *Col2.3^{gfp}* mice. After 8 weeks, these chimeras were treated with DT or PBS for 6 days. **B.** The number of GFP⁺ osteoblasts was measured by flow cytometry (n = 4 or 5 mice, respectively). **C.** GFP⁺ osteoblasts were sorted by FACS and their mRNA level of osteocalcin was measured by RT-qPCR (n = 4 or 5 mice, respectively). *Zbtb46^{dtr}*, *CD169^{dtr}* and *CD169^{dtr}:Zbtb46^{dtr}* bone marrow was transplanted into irradiated wildtype recipient mice. After 8 weeks, these recipient mice were treated with 6 days of DT or PBS. **D.** The mRNA levels of osteocalcin in whole bone marrow of these mice were measured by RT-qPCR (n = 6,6,5,4 mice respectively). Data represent the mean \pm SEM, *P<0.05; **P < 0.01; ***P < 0.001; “ns” means no significant difference. Samples were compared to PBS control group unless otherwise indicated.

REFERENCES

1. Doulatov, S., Notta, F., Laurenti, E. & Dick, J.E. Hematopoiesis: a human perspective. *Cell stem cell* **10**, 120-136 (2012).
2. Jagannathan-Bogdan, M. & Zon, L.I. Hematopoiesis. *Development* **140**, 2463-2467 (2013).
3. Greenbaum, A., *et al.* CXCL12 in early mesenchymal progenitors is required for haematopoietic stem-cell maintenance. *Nature* **495**, 227-230 (2013).
4. Calvi, L.M. & Link, D.C. Cellular complexity of the bone marrow hematopoietic stem cell niche. *Calcified tissue international* **94**, 112-124 (2014).
5. Morrison, S.J. & Scadden, D.T. The bone marrow niche for haematopoietic stem cells. *Nature* **505**, 327-334 (2014).
6. Zhao, M., *et al.* Megakaryocytes maintain homeostatic quiescence and promote post-injury regeneration of hematopoietic stem cells. *Nature medicine* **20**, 1321-1326 (2014).
7. Chow, A., *et al.* Bone marrow CD169+ macrophages promote the retention of hematopoietic stem and progenitor cells in the mesenchymal stem cell niche. *The Journal of experimental medicine* **208**, 261-271 (2011).
8. Schofield, R. The relationship between the spleen colony-forming cell and the haemopoietic stem cell. *Blood cells* **4**, 7-25 (1978).
9. Dexter, T.M., Allen, T.D. & Lajtha, L.G. Conditions controlling the proliferation of haemopoietic stem cells in vitro. *Journal of cellular physiology* **91**, 335-344 (1977).
10. Ding, L., Saunders, T.L., Enikolopov, G. & Morrison, S.J. Endothelial and perivascular cells maintain haematopoietic stem cells. *Nature* **481**, 457-462 (2012).
11. Ding, L. & Morrison, S.J. Haematopoietic stem cells and early lymphoid progenitors occupy distinct bone marrow niches. *Nature* **495**, 231-235 (2013).
12. Kunisaki, Y., *et al.* Arteriolar niches maintain haematopoietic stem cell quiescence. *Nature* **502**, 637-643 (2013).
13. Inra, C.N., *et al.* A perisinusoidal niche for extramedullary haematopoiesis in the spleen. *Nature* **527**, 466-471 (2015).
14. Skoda, R.C. Thrombocytosis. *Hematology. American Society of Hematology. Education Program*, 159-167 (2009).
15. Khodadi, E., Asnafi, A.A., Shahrabi, S., Shahjahani, M. & Saki, N. Bone marrow niche in immune thrombocytopenia: a focus on megakaryopoiesis. *Annals of hematology* **95**, 1765-1776 (2016).
16. Bowman, R.L., Busque, L. & Levine, R.L. Clonal Hematopoiesis and Evolution to Hematopoietic Malignancies. *Cell stem cell* **22**, 157-170 (2018).
17. Valderrabano, R.J. & Wu, J.Y. Bone and blood interactions in human health and disease. *Bone* (2018).
18. Acar, M., *et al.* Deep imaging of bone marrow shows non-dividing stem cells are mainly perisinusoidal. *Nature* **526**, 126-+ (2015).
19. Zhang, J. & Link, D.C. Targeting of Mesenchymal Stromal Cells by Cre-Recombinase Transgenes Commonly Used to Target Osteoblast Lineage Cells. *Journal of bone and mineral research : the official journal of the American Society for Bone and Mineral Research* **31**, 2001-2007 (2016).

20. Sugiyama, T., Kohara, H., Noda, M. & Nagasawa, T. Maintenance of the hematopoietic stem cell pool by CXCL12-CXCR4 chemokine signaling in bone marrow stromal cell niches. *Immunity* **25**, 977-988 (2006).
21. Mendez-Ferrer, S., *et al.* Mesenchymal and haematopoietic stem cells form a unique bone marrow niche. *Nature* **466**, 829-834 (2010).
22. Murphy, K., Travers, P., Walport, M. & Janeway, C. *Janeway's immunobiology*, (Garland Science, New York, 2012).
23. Cooper, M.D. The early history of B cells. *Nature Reviews Immunology* **15**, 191-197 (2015).
24. Pelanda, R. & Torres, R.M. Central B-Cell Tolerance: Where Selection Begins. *Csh Perspect Biol* **4**(2012).
25. Inlay, M.A., *et al.* Ly6d marks the earliest stage of B-cell specification and identifies the branchpoint between B-cell and T-cell development. *Genes & development* **23**, 2376-2381 (2009).
26. Hardy, R.R., Carmack, C.E., Shinton, S.A., Kemp, J.D. & Hayakawa, K. Resolution and Characterization of Pro-B and Pre-Pro-B Cell Stages in Normal Mouse Bone-Marrow. *Journal of Experimental Medicine* **173**, 1213-1225 (1991).
27. Hardy, R.R., *et al.* B-cell commitment, development and selection. *Immunological reviews* **175**, 23-32 (2000).
28. Hardy, R.R., Hayakawa, K., Haaijman, J. & Herzenberg, L.A. B-cell subpopulations identified by two-colour fluorescence analysis. *Nature* **297**, 589-591 (1982).
29. Monroe, J.G. & Dorshkind, K. Fate decisions regulating bone marrow and peripheral B lymphocyte development. *Advances in immunology* **95**, 1-50 (2007).
30. LeBien, T.W. & Tedder, T.F. B lymphocytes: how they develop and function. *Blood* **112**, 1570-1580 (2008).
31. Cariappa, A., Chase, C., Liu, H.Y., Russell, P. & Pillai, S. Naive recirculating B cells mature simultaneously in the spleen and bone marrow. *Blood* **109**, 2339-2345 (2007).
32. Yoshida, T., *et al.* Memory B and memory plasma cells. *Immunological reviews* **237**, 117-139 (2010).
33. Tokoyoda, K., Zehentmeier, S., Chang, H.D. & Radbruch, A. Organization and maintenance of immunological memory by stroma niches. *European journal of immunology* **39**, 2095-2099 (2009).
34. Shenoy, G.N., *et al.* Recruitment of memory B cells to lymph nodes remote from the site of immunization requires an inflammatory stimulus. *Journal of immunology* **189**, 521-528 (2012).
35. Ochsnein, A.F., *et al.* Protective long-term antibody memory by antigen-driven and T help-dependent differentiation of long-lived memory B cells to short-lived plasma cells independent of secondary lymphoid organs. *Proceedings of the National Academy of Sciences of the United States of America* **97**, 13263-13268 (2000).
36. Paramithiotis, E. & Cooper, M.D. Memory B lymphocytes migrate to bone marrow in humans. *Proceedings of the National Academy of Sciences of the United States of America* **94**, 208-212 (1997).
37. Geissmann, F., *et al.* Development of monocytes, macrophages, and dendritic cells. *Science* **327**, 656-661 (2010).
38. Hashimoto, D., Miller, J. & Merad, M. Dendritic cell and macrophage heterogeneity in vivo. *Immunity* **35**, 323-335 (2011).

39. Merad, M., Sathe, P., Helft, J., Miller, J. & Mortha, A. The dendritic cell lineage: ontogeny and function of dendritic cells and their subsets in the steady state and the inflamed setting. *Annual review of immunology* **31**, 563-604 (2013).
40. Reizis, B. Classical dendritic cells as a unique immune cell lineage. *Journal of Experimental Medicine* **209**, 1053-1056 (2012).
41. Steinman, R.M. Decisions About Dendritic Cells: Past, Present, and Future. *Annual Review of Immunology, Vol 30* **30**, 1-22 (2012).
42. Collin, M. & Bigley, V. Human dendritic cell subsets: an update. *Immunology* **154**, 3-20 (2018).
43. Mildner, A. & Jung, S. Development and Function of Dendritic Cell Subsets. *Immunity* **40**, 642-656 (2014).
44. Geissmann, F., *et al.* Development of Monocytes, Macrophages, and Dendritic Cells. *Science* **327**, 656-661 (2010).
45. Naik, S.H., *et al.* Development of plasmacytoid and conventional dendritic cell subtypes from single precursor cells derived in vitro and in vivo. *Nature immunology* **8**, 1217-1226 (2007).
46. Onai, N., *et al.* Identification of clonogenic common Flt3(+) M-CSFR+ plasmacytoid and conventional dendritic cell progenitors in mouse bone marrow. *Nature immunology* **8**, 1207-1216 (2007).
47. Naik, S.H., *et al.* Intrasplenic steady-state dendritic cell precursors that are distinct from monocytes. *Nature immunology* **7**, 663-671 (2006).
48. Liu, K., *et al.* In Vivo Analysis of Dendritic Cell Development and Homeostasis. *Science* **324**, 392-397 (2009).
49. Sapozhnikov, A., *et al.* Perivascular clusters of dendritic cells provide critical survival signals to B cells in bone marrow niches. *Nature immunology* **9**, 388-395 (2008).
50. Sindhava, V.J., *et al.* Bone marrow dendritic cell-mediated regulation of TLR and B cell receptor signaling in B cells. *Journal of immunology* **189**, 3355-3367 (2012).
51. Jiao, J., *et al.* Central role of conventional dendritic cells in regulation of bone marrow release and survival of neutrophils. *Journal of immunology* **192**, 3374-3382 (2014).
52. Winkler, I.G., *et al.* Bone marrow macrophages maintain hematopoietic stem cell (HSC) niches and their depletion mobilizes HSCs. *Blood* **116**, 4815-4828 (2010).
53. Chow, A., *et al.* CD169(+) macrophages provide a niche promoting erythropoiesis under homeostasis and stress. *Nature medicine* **19**, 429-436 (2013).
54. Park, D., *et al.* Endogenous bone marrow MSCs are dynamic, fate-restricted participants in bone maintenance and regeneration. *Cell stem cell* **10**, 259-272 (2012).
55. Van Vlasselaer, P., Falla, N., Snoeck, H. & Mathieu, E. Characterization and purification of osteogenic cells from murine bone marrow by two-color cell sorting using anti-Sca-1 monoclonal antibody and wheat germ agglutinin. *Blood* **84**, 753-763 (1994).
56. Koide, Y., *et al.* Two distinct stem cell lineages in murine bone marrow. *Stem cells* **25**, 1213-1221 (2007).
57. Crisan, M., *et al.* A perivascular origin for mesenchymal stem cells in multiple human organs. *Cell stem cell* **3**, 301-313 (2008).
58. Morikawa, S., *et al.* Prospective identification, isolation, and systemic transplantation of multipotent mesenchymal stem cells in murine bone marrow. *The Journal of experimental medicine* **206**, 2483-2496 (2009).

59. Pinho, S., *et al.* PDGFRalpha and CD51 mark human nestin+ sphere-forming mesenchymal stem cells capable of hematopoietic progenitor cell expansion. *The Journal of experimental medicine* **210**, 1351-1367 (2013).
60. Roberts, E.W., *et al.* Depletion of stromal cells expressing fibroblast activation protein-alpha from skeletal muscle and bone marrow results in cachexia and anemia. *The Journal of experimental medicine* **210**, 1137-1151 (2013).
61. Tran, E., *et al.* Immune targeting of fibroblast activation protein triggers recognition of multipotent bone marrow stromal cells and cachexia. *The Journal of experimental medicine* **210**, 1125-1135 (2013).
62. Wright, D.E., Wagers, A.J., Gulati, A.P., Johnson, F.L. & Weissman, I.L. Physiological migration of hematopoietic stem and progenitor cells. *Science* **294**, 1933-1936 (2001).
63. Li, W., Johnson, S.A., Shelley, W.C. & Yoder, M.C. Hematopoietic stem cell repopulating ability can be maintained in vitro by some primary endothelial cells. *Experimental hematology* **32**, 1226-1237 (2004).
64. Butler, J.M., *et al.* Endothelial cells are essential for the self-renewal and repopulation of Notch-dependent hematopoietic stem cells. *Cell stem cell* **6**, 251-264 (2010).
65. Kobayashi, H., *et al.* Angiocrine factors from Akt-activated endothelial cells balance self-renewal and differentiation of haematopoietic stem cells. *Nature cell biology* **12**, 1046-1056 (2010).
66. Kopp, H.G., Avecilla, S.T., Hooper, A.T. & Rafii, S. The bone marrow vascular niche: home of HSC differentiation and mobilization. *Physiology* **20**, 349-356 (2005).
67. Rafii, S., Butler, J.M. & Ding, B.S. Angiocrine functions of organ-specific endothelial cells. *Nature* **529**, 316-325 (2016).
68. Dar, A., *et al.* Chemokine receptor CXCR4-dependent internalization and resecretion of functional chemokine SDF-1 by bone marrow endothelial and stromal cells. *Nature immunology* **6**, 1038-1046 (2005).
69. Sipkins, D.A., *et al.* In vivo imaging of specialized bone marrow endothelial microdomains for tumour engraftment. *Nature* **435**, 969-973 (2005).
70. Ponomaryov, T., *et al.* Induction of the chemokine stromal-derived factor-1 following DNA damage improves human stem cell function. *The Journal of clinical investigation* **106**, 1331-1339 (2000).
71. Winkler, I.G., *et al.* Vascular niche E-selectin regulates hematopoietic stem cell dormancy, self renewal and chemoresistance. *Nature medicine* **18**, 1651-1657 (2012).
72. Hoggatt, J., *et al.* Rapid Mobilization Reveals a Highly Engraftable Hematopoietic Stem Cell. *Cell* **172**, 191-204 e110 (2018).
73. Kusumbe, A.P., *et al.* Age-dependent modulation of vascular niches for haematopoietic stem cells. *Nature* **532**, 380-384 (2016).
74. Ramasamy, S.K. Structure and Functions of Blood Vessels and Vascular Niches in Bone. *Stem cells international* **2017**, 5046953 (2017).
75. Kopp, H.G., Hooper, A.T., Avecilla, S.T. & Rafii, S. Functional heterogeneity of the bone marrow vascular niche. *Annals of the New York Academy of Sciences* **1176**, 47-54 (2009).
76. Nombela-Arrieta, C., *et al.* Quantitative imaging of haematopoietic stem and progenitor cell localization and hypoxic status in the bone marrow microenvironment. *Nature cell biology* **15**, 533-543 (2013).

77. Kusumbe, A.P., Ramasamy, S.K. & Adams, R.H. Coupling of angiogenesis and osteogenesis by a specific vessel subtype in bone. *Nature* **507**, 323-328 (2014).
78. Ramasamy, S.K., Kusumbe, A.P., Wang, L. & Adams, R.H. Endothelial Notch activity promotes angiogenesis and osteogenesis in bone. *Nature* **507**, 376-380 (2014).
79. Itkin, T., *et al.* Distinct bone marrow blood vessels differentially regulate haematopoiesis (vol 532, pg 323, 2016). *Nature* **538**, 274-274 (2016).
80. Pacios, S., *et al.* Osteoblast Lineage Cells Play an Essential Role in Periodontal Bone Loss Through Activation of Nuclear Factor-Kappa B. *Scientific reports* **5**(2015).
81. Palumbo, C., Palazzini, S., Zaffe, D. & Marotti, G. Osteocyte Differentiation in the Tibia of Newborn Rabbit - an Ultrastructural-Study of the Formation of Cytoplasmic Processes. *Acta Anat* **137**, 350-358 (1990).
82. Bellido, T. Osteocyte-Driven Bone Remodeling. *Calcified tissue international* **94**, 25-34 (2014).
83. Taichman, R.S. & Emerson, S.G. Human Osteoblasts Support Hematopoiesis through the Production of Granulocyte-Colony-Stimulating Factor. *Journal of Experimental Medicine* **179**, 1677-1682 (1994).
84. Taichman, R.S., Reilly, M.J. & Emerson, S.G. Human osteoblasts support human hematopoietic progenitor cells in in vitro bone marrow cultures. *Blood* **87**, 518-524 (1996).
85. Visnjic, D., *et al.* Conditional ablation of the osteoblast lineage in Col2.3 Delta tk transgenic mice. *Journal of Bone and Mineral Research* **16**, 2222-2231 (2001).
86. Visnjic, D., *et al.* Hematopoiesis is severely altered in mice with an induced osteoblast deficiency. *Blood* **103**, 3258-3264 (2004).
87. Adams, G.B., *et al.* Therapeutic targeting of a stem cell niche (vol 25, pg 238, 2007). *Nature biotechnology* **25**, 944-944 (2007).
88. Calvi, L.M., *et al.* Osteoblastic cells regulate the haematopoietic stem cell niche. *Nature* **425**, 841-846 (2003).
89. Bromberg, O., *et al.* Osteoblastic N-cadherin is not required for microenvironmental support and regulation of hematopoietic stem and progenitor cells. *Blood* **120**, 303-313 (2012).
90. Lymperi, S., *et al.* Strontium can increase some osteoblasts without increasing hematopoietic stem cells. *Blood* **111**, 1173-1181 (2008).
91. Ma, Y.D., *et al.* Defects in osteoblast function but no changes in long-term repopulating potential of hematopoietic stem cells in a mouse chronic inflammatory arthritis model. *Blood* **114**, 4402-4410 (2009).
92. Nakamura, Y., *et al.* Isolation and characterization of endosteal niche cell populations that regulate hematopoietic stem cells. *Blood* **116**, 1422-1432 (2010).
93. Calvi, L.M., *et al.* Osteoblastic expansion induced by parathyroid hormone receptor signaling in murine osteocytes is not sufficient to increase hematopoietic stem cells. *Blood* **119**, 2489-2499 (2012).
94. Ogawa, M. Differentiation and Proliferation of Hematopoietic Stem-Cells. *Blood* **81**, 2844-2853 (1993).
95. Nakorn, T.N., Miyamoto, T. & Weissman, I.L. Characterization of mouse clonogenic megakaryocyte progenitors. *Proceedings of the National Academy of Sciences of the United States of America* **100**, 205-210 (2003).

96. Norozi, F., Shahrabi, S., Hajizamani, S. & Saki, N. Regulatory role of Megakaryocytes on Hematopoietic Stem Cells Quiescence by CXCL4/PF4 in Bone Marrow Niche. *Leukemia research* **48**, 107-112 (2016).
97. Junt, T., *et al.* Dynamic visualization of thrombopoiesis within bone marrow. *Science* **317**, 1767-1770 (2007).
98. Olson, T.S., *et al.* Megakaryocytes promote murine osteoblastic HSC niche expansion and stem cell engraftment after radioablative conditioning. *Blood* **121**, 5238-5249 (2013).
99. Domingues, M.J., Cao, H.M., Heazlewood, S.Y., Cao, B. & Nilsson, S.K. Niche Extracellular Matrix Components and Their Influence on HSC. *J Cell Biochem* **118**, 1984-1993 (2017).
100. Qian, H., *et al.* Critical role of thrombopoietin in maintaining adult quiescent hematopoietic stem cells. *Cell stem cell* **1**, 671-684 (2007).
101. Nakamura-Ishizu, A., Takubo, K., Fujioka, M. & Suda, T. Megakaryocytes are essential for HSC quiescence through the production of thrombopoietin. *Biochemical and biophysical research communications* **454**, 353-357 (2014).
102. Bruns, I., *et al.* Megakaryocytes regulate hematopoietic stem cell quiescence through CXCL4 secretion. *Nature medicine* **20**, 1315-1320 (2014).
103. Heazlewood, S.Y., *et al.* Megakaryocytes co-localise with hemopoietic stem cells and release cytokines that up-regulate stem cell proliferation. *Stem Cell Res* **11**, 782-792 (2013).
104. Verschoor, C.P., Puchta, A. & Bowdish, D.M. The macrophage. *Methods in molecular biology* **844**, 139-156 (2012).
105. Gordon, S. & Taylor, P.R. Monocyte and macrophage heterogeneity. *Nature Reviews Immunology* **5**, 953-964 (2005).
106. Gordon, S. Pattern recognition receptors: Doubling up for the innate immune response. *Cell* **111**, 927-930 (2002).
107. Mosser, D.M. & Edwards, J.P. Exploring the full spectrum of macrophage activation. *Nature Reviews Immunology* **8**, 958-969 (2008).
108. Benoit, M., Desnues, B. & Mege, J.L. Macrophage polarization in bacterial infections. *Journal of immunology* **181**, 3733-3739 (2008).
109. Edwards, J.P., Zhang, X., Frauwirth, K.A. & Mosser, D.M. Biochemical and functional characterization of three activated macrophage populations. *J Leukocyte Biol* **80**, 1298-1307 (2006).
110. Martinez, F.O., Helming, L. & Gordon, S. Alternative Activation of Macrophages: An Immunologic Functional Perspective. *Annual review of immunology* **27**, 451-483 (2009).
111. Stein, M., Keshav, S., Harris, N. & Gordon, S. Interleukin-4 Potently Enhances Murine Macrophage Mannose Receptor Activity - a Marker of Alternative Immunological Macrophage Activation. *Journal of Experimental Medicine* **176**, 287-292 (1992).
112. Randolph, G.J., Beaulieu, S., Lebecque, S., Steinman, R.M. & Muller, W.A. Differentiation of monocytes into dendritic cells in a model of transendothelial trafficking. *Science* **282**, 480-483 (1998).
113. Robbins, C.S. & Swirski, F.K. The multiple roles of monocyte subsets in steady state and inflammation. *Cell Mol Life Sci* **67**, 2685-2693 (2010).
114. Jenkins, S.J., *et al.* Local Macrophage Proliferation, Rather than Recruitment from the Blood, Is a Signature of T(H)2 Inflammation. *Science* **332**, 1284-1288 (2011).
115. Randolph, G.J. No Need to Coax Monocytes. *Science* **332**, 1268-1269 (2011).

116. Dorger, M., Munzing, S., Allmeling, A.M., Messmer, K. & Krombach, F. Phenotypic and functional differences between rat alveolar, pleural, and peritoneal macrophages. *Exp Lung Res* **27**, 65-76 (2001).
117. Itoh, K., *et al.* Lipopolysaccharide promotes the survival of osteoclasts via Toll-like receptor 4, but cytokine production of osteoclasts in response to lipopolysaccharide is different from that of macrophages. *Journal of immunology* **170**, 3688-3695 (2003).
118. Bretongorius, J., *et al.* Association between Leukemic Erythroid Progenitors and Bone-Marrow Macrophages. *Blood cells* **17**, 127-146 (1991).
119. Kaur, S., *et al.* Role of bone marrow macrophages in controlling homeostasis and repair in bone and bone marrow niches. *Semin Cell Dev Biol* **61**, 12-21 (2017).
120. Bessis, M. [Erythroblastic island, functional unity of bone marrow]. *Revue d'hematologie* **13**, 8-11 (1958).
121. Lifshitz, L., Tabak, G., Gassmann, M., Mittelman, M. & Neumann, D. Macrophages as novel target cells for erythropoietin. *Haematol-Hematol J* **95**, 1823-1831 (2010).
122. Rich, I.N., Vogt, C. & Pentz, S. Erythropoietin gene expression in vitro and in vivo detected by in situ hybridization. *Blood cells* **14**, 505-520 (1988).
123. Vogt, C., Pentz, S. & Rich, I.N. A role for the macrophage in normal hemopoiesis: III. In vitro and in vivo erythropoietin gene expression in macrophages detected by in situ hybridization. *Experimental hematology* **17**, 391-397 (1989).
124. Tonkin, J., *et al.* Monocyte/Macrophage-derived IGF-1 Orchestrates Murine Skeletal Muscle Regeneration and Modulates Autocrine Polarization. *Molecular therapy : the journal of the American Society of Gene Therapy* **23**, 1189-1200 (2015).
125. Sawada, K., Krantz, S.B., Dessypris, E.N., Koury, S.T. & Sawyer, S.T. Human Colony-Forming Units-Erythroid Do Not Require Accessory Cells, but Do Require Direct Interaction with Insulin-Like Growth Factor-I and or Insulin for Erythroid Development. *Journal of Clinical Investigation* **83**, 1701-1709 (1989).
126. Liu, M., *et al.* Macrophages Support Splenic Erythropoiesis in 4T1 Tumor-Bearing Mice. *PloS one* **10**(2015).
127. Leimberg, M.J., Prus, E., Konijn, A.M. & Fibach, E. Macrophages function as a ferritin iron source for cultured human erythroid precursors. *J Cell Biochem* **103**, 1211-1218 (2008).
128. Kawane, K., *et al.* Requirement of DNase II for definitive erythropoiesis in the mouse fetal liver. *Science* **292**, 1546-1549 (2001).
129. Toda, S., Segawa, K. & Nagata, S. MerTK-mediated engulfment of pyrenocytes by central macrophages in erythroblastic islands. *Blood* **123**, 3963-3971 (2014).
130. Sinder, B.P., Pettit, A.R. & McCauley, L.K. Macrophages: Their Emerging Roles in Bone. *Journal of Bone and Mineral Research* **30**, 2140-2149 (2015).
131. Chang, M.K., *et al.* Osteal tissue macrophages are intercalated throughout human and mouse bone lining tissues and regulate osteoblast function in vitro and in vivo. *Journal of immunology* **181**, 1232-1244 (2008).
132. Cho, S.W., *et al.* Osteal macrophages support physiologic skeletal remodeling and anabolic actions of parathyroid hormone in bone. *Proceedings of the National Academy of Sciences of the United States of America* **111**, 1545-1550 (2014).
133. Schindeler, A., McDonald, M.M., Bokko, P. & Little, D.G. Bone remodeling during fracture repair: The cellular picture. *Semin Cell Dev Biol* **19**, 459-466 (2008).

134. Forbes, S.J. & Rosenthal, N. Preparing the ground for tissue regeneration: from mechanism to therapy. *Nature medicine* **20**, 857-869 (2014).
135. Chang, K.H., *et al.* p62 Is Required for Stem Cell/Progenitor Retention through Inhibition of IKK/NF-kappa B/Ccl4 Signaling at the Bone Marrow Macrophage-Osteoblast Niche. *Cell reports* **9**, 2084-2097 (2014).
136. Hur, J., *et al.* CD82/KAI1 Maintains the Dormancy of Long- Term Hematopoietic Stem Cells through Interaction with DARC- Expressing Macrophages. *Cell stem cell* **18**, 508-521 (2016).
137. Joshi, A., *et al.* Technical Advance: Transcription factor, promoter, and enhancer utilization in human myeloid cells. *J Leukocyte Biol* **97**, 985-995 (2015).
138. Christopher, M.J., Rao, M., Liu, F., Woloszynek, J.R. & Link, D.C. Expression of the G-CSF receptor in monocytic cells is sufficient to mediate hematopoietic progenitor mobilization by G-CSF in mice. *Journal of Experimental Medicine* **208**, 251-260 (2011).
139. To, L.B., Levesque, J.P. & Herbert, K.E. How I treat patients who mobilize hematopoietic stem cells poorly. *Blood* **118**, 4530-4540 (2011).
140. Winkler, I.G., *et al.* Mobilization of hematopoietic stem cells with highest self-renewal by G-CSF precedes clonogenic cell mobilization peak. *Experimental hematology* **44**, 303-314 (2016).
141. Mendez-Ferrer, S., Lucas, D., Battista, M. & Frenette, P.S. Haematopoietic stem cell release is regulated by circadian oscillations. *Nature* **452**, 442-U444 (2008).
142. Katayama, Y., *et al.* Signals from the sympathetic nervous system regulate hematopoietic stem cell egress from bone marrow. *Cell* **124**, 407-421 (2006).
143. Mendez-Ferrer, S., *et al.* Mesenchymal and haematopoietic stem cells form a unique bone marrow niche. *Nature* **466**, 829-U859 (2010).
144. Yamazaki, S., *et al.* Nonmyelinating Schwann Cells Maintain Hematopoietic Stem Cell Hibernation in the Bone Marrow Niche. *Cell* **147**, 1146-1158 (2011).
145. Yamazaki, S., *et al.* TGF-beta as a candidate bone marrow niche signal to induce hematopoietic stem cell hibernation. *Blood* **113**, 1250-1256 (2009).
146. Barker, J.E. Early transplantation to a normal microenvironment prevents the development of Steel hematopoietic stem cell defects. *Experimental hematology* **25**, 542-547 (1997).
147. Ara, T., *et al.* Long-term hematopoietic stem cells require stromal cell-derived factor-1 for colonizing bone marrow during ontogeny. *Immunity* **19**, 257-267 (2003).
148. Tokoyoda, K., Egawa, T., Sugiyama, T., Choi, B.I. & Nagasawa, T. Cellular niches controlling B lymphocyte behavior within bone marrow during development. *Immunity* **20**, 707-718 (2004).
149. Omatsu, Y., *et al.* The Essential Functions of Adipo-osteogenic Progenitors as the Hematopoietic Stem and Progenitor Cell Niche. *Immunity* **33**, 387-399 (2010).
150. Clark, M.R., Mandal, M., Ochiai, K. & Singh, H. Orchestrating B cell lymphopoiesis through interplay of IL-7 receptor and pre-B cell receptor signalling. *Nature Reviews Immunology* **14**, 69-80 (2014).
151. Vonfredejeffry, U., *et al.* Lymphopenia in Interleukin (Il)-7 Gene-Deleted Mice Identifies Il-7 as a Nonredundant Cytokine. *Journal of Experimental Medicine* **181**, 1519-1526 (1995).
152. Peschon, J.J., *et al.* Early Lymphocyte Expansion Is Severely Impaired in Interleukin-7 Receptor-Deficient Mice. *Journal of Experimental Medicine* **180**, 1955-1960 (1994).

153. Dias, S., Silva, H., Cumano, A. & Vieira, P. Interleukin-7 is necessary to maintain the B cell potential in common lymphoid progenitors. *Journal of Experimental Medicine* **201**, 971-979 (2005).
154. Gomes, A.C., *et al.* Hematopoietic Stem Cell Niches Produce Lineage-Instructive Signals to Control Multipotent Progenitor Differentiation. *Immunity* **45**, 1219-1231 (2016).
155. Zhou, B.O., Yue, R., Murphy, M.M., Peyer, J.G. & Morrison, S.J. Leptin-Receptor-Expressing Mesenchymal Stromal Cells Represent the Main Source of Bone Formed by Adult Bone Marrow. *Cell stem cell* **15**, 154-168 (2014).
156. Crane, G.M., Jeffery, E. & Morrison, S.J. Adult haematopoietic stem cell niches. *Nature Reviews Immunology* **17**, 573-590 (2017).
157. Asada, N., Takeishi, S. & Frenette, P.S. Complexity of bone marrow hematopoietic stem cell niche. *Int J Hematol* **106**, 45-54 (2017).
158. Omatsu, Y., Seike, M., Sugiyama, T., Kume, T. & Nagasawa, T. Foxc1 is a critical regulator of haematopoietic stem/progenitor cell niche formation. *Nature* **508**, 536-+ (2014).
159. Acar, M., *et al.* Deep imaging of bone marrow shows non-dividing stem cells are mainly perisinusoidal. *Nature* **526**, 126-130 (2015).
160. Mignone, J.L., Kukekov, V., Chiang, A.S., Steindler, D. & Enikolopov, G. Neural stem and progenitor cells in nestin-GFP transgenic mice. *J Comp Neurol* **469**, 311-324 (2004).
161. Asada, N., *et al.* Differential cytokine contributions of perivascular haematopoietic stem cell niches. *Nature cell biology* **19**, 214-223 (2017).
162. Isern, J., *et al.* The neural crest is a source of mesenchymal stem cells with specialized hematopoietic stem-cell-niche function. *eLife* **3**(2014).
163. Ono, N., *et al.* Vasculature-Associated Cells Expressing Nestin in Developing Bones Encompass Early Cells in the Osteoblast and Endothelial Lineage. *Developmental cell* **29**, 330-339 (2014).
164. Nagasawa, T., Kikutani, H. & Kishimoto, T. Molecular-Cloning and Structure of a Pre-B-Cell Growth-Stimulating Factor. *Proceedings of the National Academy of Sciences of the United States of America* **91**, 2305-2309 (1994).
165. Nagasawa, T., *et al.* Defects of B-cell lymphopoiesis and bone-marrow myelopoiesis in mice lacking the CXC chemokine PBSF/SDF-1. *Nature* **382**, 635-638 (1996).
166. Ma, Q., *et al.* Impaired B-lymphopoiesis, myelopoiesis, and derailed cerebellar neuron migration in CXCR4- and SDF-1-deficient mice. *Proceedings of the National Academy of Sciences of the United States of America* **95**, 9448-9453 (1998).
167. Zou, Y.R., Kottmann, A.H., Kuroda, M., Taniuchi, I. & Littman, D.R. Function of the chemokine receptor CXCR4 in haematopoiesis and in cerebellar development. *Nature* **393**, 595-599 (1998).
168. Egawa, T., *et al.* The earliest stages of B cell development require a chemokine stromal cell-derived factor/pre-B cell growth-stimulating factor. *Immunity* **15**, 323-334 (2001).
169. Mellado, M., Rodriguez-Frade, J.M., Manes, S. & Martinez, C. Chemokine signaling and functional responses: The role of receptor dimerization and TK pathway activation. *Annual review of immunology* **19**, 397-421 (2001).
170. Vlahakis, S.R., *et al.* G protein-coupled chemokine receptors induce both survival and apoptotic signaling pathways. *Journal of immunology* **169**, 5546-5554 (2002).

171. Onai, N., *et al.* Impairment of lymphopoiesis and myelopoiesis in mice reconstituted with bone marrow-hematopoietic progenitor cells expressing SDF-1-intrakine. *Blood* **96**, 2074-2080 (2000).
172. Kawabata, K., *et al.* A cell-autonomous requirement for CXCR4 in long-term lymphoid and myeloid reconstitution. *Proceedings of the National Academy of Sciences of the United States of America* **96**, 5663-5667 (1999).
173. Ma, Q., Jones, D. & Springer, T.A. The chemokine receptor CXCR4 is required for the retention of B lineage and granulocytic precursors within the bone marrow microenvironment. *Immunity* **10**, 463-471 (1999).
174. Fagraeus, A. The plasma cellular reaction and its relation to the formation of antibodies in vitro. *Journal of immunology* **58**, 1-13 (1948).
175. O'Connor, B.P., Cascalho, M. & Noelle, R.J. Short-lived and long-lived bone marrow plasma cells are derived from a novel precursor population. *Journal of Experimental Medicine* **195**, 737-745 (2002).
176. DiLillo, D.J., *et al.* Maintenance of long-lived plasma cells and serological memory despite mature and memory B cell depletion during CD20 immunotherapy in mice. *Journal of immunology* **180**, 361-371 (2008).
177. Coffman, R.L. & Cohn, M. The class of surface immunoglobulin on virgin and memory B lymphocytes. *Journal of immunology* **118**, 1806-1815 (1977).
178. Black, S.J., Vanderloo, W., Loken, M.R. & Herzenberg, L.A. Expression of Igd by Murine Lymphocytes - Loss of Surface Igd Indicates Maturation of Memory B-Cells. *Journal of Experimental Medicine* **147**, 984-996 (1978).
179. Klein, U., Rajewsky, K. & Kuppers, R. Human immunoglobulin (Ig)M(+)IgD(+) peripheral blood B cells expressing the CD27 cell surface antigen carry somatically mutated variable region genes: CD27 as a general marker for somatically mutated (memory) B cells. *Journal of Experimental Medicine* **188**, 1679-1689 (1998).
180. Kobata, T., *et al.* Cd27-Cd70 Interactions Regulate B-Cell Activation by T-Cells. *Proceedings of the National Academy of Sciences of the United States of America* **92**, 11249-11253 (1995).
181. Agematsu, K., *et al.* Cd27/Cd70 Interaction Directly Drives B-Cell Igg and Igm Synthesis. *European journal of immunology* **25**, 2825-2829 (1995).
182. Jacquot, S., Kobata, T., Iwata, S., Morimoto, C. & Schlossman, S.F. CD154/CD40 and CD70/CD27 interactions have different and sequential functions in T cell-dependent B cell responses - Enhancement of plasma cell differentiation by CD27 signaling. *Journal of immunology* **159**, 2652-2657 (1997).
183. Agematsu, K., *et al.* Generation of plasma cells from peripheral blood memory B cells: Synergistic effect of interleukin-10 and CD27/CD70 interaction. *Blood* **91**, 173-180 (1998).
184. Klein, U., Kuppers, R. & Rajewsky, K. Evidence for a large compartment of IgM-expressing memory B cells in humans. *Blood* **89**, 1288-1298 (1997).
185. Tangye, S.G., Liu, Y.J., Aversa, G., Phillips, J.H. & de Vries, J.E. Identification of functional human splenic memory B cells by expression of CD148 and CD27. *The Journal of experimental medicine* **188**, 1691-1703 (1998).
186. Fecteau, J.F., Cote, G. & Neron, S. A new memory CD27-IgG+ B cell population in peripheral blood expressing VH genes with low frequency of somatic mutation. *Journal of immunology* **177**, 3728-3736 (2006).

187. Wirths, S. & Lanzavecchia, A. ABCB1 transporter discriminates human resting naive B cells from cycling transitional and memory B cells. *European journal of immunology* **35**, 3433-3441 (2005).
188. Xiao, Y.L., Hendriks, J., Langerak, P., Jacobs, H. & Borst, J. CD27 is acquired by primed B cells at the centroblast stage and promotes germinal center formation. *Journal of immunology* **172**, 7432-7441 (2004).
189. Jash, A., *et al.* ZBTB32 Restricts the Duration of Memory B Cell Recall Responses. *Journal of immunology* **197**, 1159-1168 (2016).
190. Crotty, S., *et al.* Cutting edge: Long-term B cell memory in humans after smallpox vaccination. *Journal of immunology* **171**, 4969-4973 (2003).
191. Gray, D. & Skarvall, H. B-Cell Memory Is Short-Lived in the Absence of Antigen. *Nature* **336**, 70-73 (1988).
192. Maruyama, M., Lam, K.P. & Rajewsky, K. Memory B-cell persistence is independent of persisting immunizing antigen. *Nature* **407**, 636-642 (2000).
193. Mamani-Matsuda, M., *et al.* The human spleen is a major reservoir for long-lived vaccinia virus-specific memory B cells. *Blood* **111**, 4653-4659 (2008).
194. Martinez-Gamboa, L., *et al.* Role of the spleen in peripheral memory B-cell homeostasis in patients with autoimmune thrombocytopenia purpura. *Clin Immunol* **130**, 199-212 (2009).
195. MacDonald, K.P.A., *et al.* Characterization of human blood dendritic cell subsets. *Blood* **100**, 4512-4520 (2002).
196. Dzionek, A., *et al.* BDCA-2, BDCA-3 and BDCA-4: Three markers for distinct subsets of dendritic cells in human peripheral blood. *Journal of immunology* **165**, 6037-6046 (2000).
197. Murphy, T.L., *et al.* Transcriptional Control of Dendritic Cell Development. *Annual Review of Immunology, Vol 34* **34**, 93-119 (2016).
198. Williams, M., *et al.* Unsupervised High-Dimensional Analysis Aligns Dendritic Cells across Tissues and Species. *Immunity* **45**, 669-684 (2016).
199. Heidkamp, G.F., *et al.* Human lymphoid organ dendritic cell identity is predominantly dictated by ontogeny, not tissue microenvironment. *European journal of immunology* **47**, 158-159 (2017).
200. Granot, T., *et al.* Dendritic Cells Display Subset and Tissue-Specific Maturation Dynamics over Human Life. *Immunity* **46**, 504-515 (2017).
201. Ziegler-Heitbrock, L., *et al.* Nomenclature of monocytes and dendritic cells in blood. *Blood* **116**, E74-E80 (2010).
202. Crozat, K., *et al.* The XC chemokine receptor 1 is a conserved selective marker of mammalian cells homologous to mouse CD8 alpha(+) dendritic cells. *Journal of Experimental Medicine* **207**, 1283-1292 (2010).
203. Tamura, T., Kurotaki, D. & Koizumi, S. Regulation of myelopoiesis by the transcription factor IRF8. *Int J Hematol* **101**, 342-351 (2015).
204. Bigley, V., *et al.* Biallelic interferon regulatory factor 8 mutation: A complex immunodeficiency syndrome with dendritic cell deficiency, monocytopenia, and immune dysregulation. *The Journal of allergy and clinical immunology* (2017).
205. Hambleton, S., *et al.* IRF8 mutations and human dendritic-cell immunodeficiency. *The New England journal of medicine* **365**, 127-138 (2011).

206. Tailor, P., Tamura, T., Morse, H.C. & Ozato, K. The BXH2 mutation in IRF8 differentially impairs dendritic cell subset development in the mouse. *Blood* **111**, 1942-1945 (2008).
207. Haniffa, M., *et al.* Human tissues contain CD141hi cross-presenting dendritic cells with functional homology to mouse CD103+ nonlymphoid dendritic cells. *Immunity* **37**, 60-73 (2012).
208. Poulin, L.F., *et al.* Characterization of human DNGR-1+ BDCA3+ leukocytes as putative equivalents of mouse CD8alpha+ dendritic cells. *The Journal of experimental medicine* **207**, 1261-1271 (2010).
209. Jongbloed, S.L., *et al.* Human CD141(+) (BDCA-3)(+) dendritic cells (DCs) represent a unique myeloid DC subset that cross-presents necrotic cell antigens. *Journal of Experimental Medicine* **207**, 1247-1260 (2010).
210. Bachem, A., *et al.* Superior antigen cross-presentation and XCR1 expression define human CD11c(+)CD141(+) cells as homologues of mouse CD8(+) dendritic cells. *Journal of Experimental Medicine* **207**, 1273-1281 (2010).
211. Cohn, L., *et al.* Antigen delivery to early endosomes eliminates the superiority of human blood BDCA3(+) dendritic cells at cross presentation. *Journal of Experimental Medicine* **210**, 1049-1063 (2013).
212. Ahrens, S., *et al.* F-Actin Is an Evolutionarily Conserved Damage-Associated Molecular Pattern Recognized by DNGR-1, a Receptor for Dead Cells. *Immunity* **36**, 635-645 (2012).
213. Zhang, J.G., *et al.* The Dendritic Cell Receptor Clec9A Binds Damaged Cells via Exposed Actin Filaments. *Immunity* **36**, 646-657 (2012).
214. Schreiber, G., *et al.* The C-type lectin receptor CLEC9A mediates antigen uptake and (cross-)presentation by human blood BDCA3(+) myeloid dendritic cells. *Blood* **119**, 2284-2292 (2012).
215. Li, J., *et al.* Antibodies targeting Clec9A promote strong humoral immunity without adjuvant in mice and non-human primates. *European journal of immunology* **45**, 854-864 (2015).
216. Yoshio, S., *et al.* Human Blood Dendritic Cell Antigen 3 (BDCA3)(+) Dendritic Cells Are a Potent Producer of Interferon-lambda in Response to Hepatitis C Virus. *Hepatology* **57**, 1705-1715 (2013).
217. Williams, M., *et al.* Skin-draining lymph nodes contain dermis-derived CD103(-) dendritic cells that constitutively produce retinoic acid and induce Foxp3(+) regulatory T cells. *Blood* **115**, 1958-1968 (2010).
218. Idoyaga, J., *et al.* Specialized role of migratory dendritic cells in peripheral tolerance induction. *Journal of Clinical Investigation* **123**, 844-854 (2013).
219. Yin, X.Y., *et al.* Human Blood CD1c(+) Dendritic Cells Encompass CD5(high) and CD5(low) Subsets That Differ Significantly in Phenotype, Gene Expression, and Functions. *Journal of immunology* **198**, 1553-1564 (2017).
220. Villani, A.C., *et al.* Single-cell RNA-seq reveals new types of human blood dendritic cells, monocytes, and progenitors. *Science* **356**(2017).
221. Collin, M., Dickinson, R. & Bigley, V. Haematopoietic and immune defects associated with GATA2 mutation. *British journal of haematology* **169**, 173-187 (2015).

222. Scott, C.L., *et al.* The transcription factor Zeb2 regulates development of conventional and plasmacytoid DCs by repressing Id2. *Journal of Experimental Medicine* **213**, 897-911 (2016).
223. Briseno, C.G., *et al.* Deficiency of transcription factor RelB perturbs myeloid and DC development by hematopoietic-extrinsic mechanisms. *Proceedings of the National Academy of Sciences of the United States of America* **114**, 3957-3962 (2017).
224. Sichier, D., *et al.* IRF8 Transcription Factor Controls Survival and Function of Terminally Differentiated Conventional and Plasmacytoid Dendritic Cells, Respectively. *Immunity* **45**, 626-640 (2016).
225. Van Rhijn, I., Ly, D. & Moody, D.B. CD1a, CD1b, and CD1c in immunity against mycobacteria. *Advances in experimental medicine and biology* **783**, 181-197 (2013).
226. Lundberg, K., *et al.* Transcriptional profiling of human dendritic cell populations and models--unique profiles of in vitro dendritic cells and implications on functionality and applicability. *PloS one* **8**, e52875 (2013).
227. Harman, A.N., *et al.* Identification of lineage relationships and novel markers of blood and skin human dendritic cells. *Journal of immunology* **190**, 66-79 (2013).
228. Sittig, S.P., *et al.* A Comparative Study of the T Cell Stimulatory and Polarizing Capacity of Human Primary Blood Dendritic Cell Subsets. *Mediators of inflammation* **2016**, 3605643 (2016).
229. Nizzoli, G., *et al.* IL-10 promotes homeostatic proliferation of human CD8(+) memory T cells and, when produced by CD1c(+) DCs, shapes naive CD8(+) T-cell priming. *European journal of immunology* **46**, 1622-1632 (2016).
230. Di Blasio, S., *et al.* Human CD1c(+) DCs are critical cellular mediators of immune responses induced by immunogenic cell death. *Oncoimmunology* **5**, e1192739 (2016).
231. Grouard, G., *et al.* The enigmatic plasmacytoid T cells develop into dendritic cells with interleukin (IL)-3 and CD40-ligand. *Journal of Experimental Medicine* **185**, 1101-1111 (1997).
232. Siegal, F.P., *et al.* The nature of the principal type 1 interferon-producing cells in human blood. *Science* **284**, 1835-1837 (1999).
233. Schmitz, J., *et al.* BDCA-2, a novel plasmacytoid dendritic cell-specific C-type lectin type II transmembrane protein: Molecular cloning and functional characterization. *Journal of Investigative Dermatology* **117**, 1009-1009 (2001).
234. Ju, X., Zenke, M., Hart, D.N. & Clark, G.J. CD300a/c regulate type I interferon and TNF-alpha secretion by human plasmacytoid dendritic cells stimulated with TLR7 and TLR9 ligands. *Blood* **112**, 1184-1194 (2008).
235. Bao, M. & Liu, Y.J. Regulation of TLR7/9 signaling in plasmacytoid dendritic cells. *Protein & cell* **4**, 40-52 (2013).
236. Tussiwand, R. & Gautier, E.L. Transcriptional regulation of mononuclear phagocyte development. *Frontiers in immunology* **6**(2015).
237. Spits, H., Couwenberg, F., Bakker, A.Q., Weijer, K. & Uttenbogaart, C.H. Id2 and id3 inhibit development of CD34(+) stem cells into predendritic cell (Pre-DC)2 but not into Pre-DC1: Evidence for a lymphoid origin of Pre-DC2. *Journal of Experimental Medicine* **192**, 1775-1783 (2000).
238. Swiecki, M. & Colonna, M. The multifaceted biology of plasmacytoid dendritic cells. *Nature Reviews Immunology* **15**, 471-485 (2015).

239. Lande, R., *et al.* Neutrophils Activate Plasmacytoid Dendritic Cells by Releasing Self-DNA-Peptide Complexes in Systemic Lupus Erythematosus. *Science translational medicine* **3**(2011).
240. Ganguly, D., *et al.* Self-RNA-antimicrobial peptide complexes activate human dendritic cells through TLR7 and TLR8. *Journal of Experimental Medicine* **206**, 1983-1994 (2009).
241. Berggren, O., *et al.* IFN-alpha production by plasmacytoid dendritic cell associations with polymorphisms in gene loci related to autoimmune and inflammatory diseases. *Hum Mol Genet* **24**, 3571-3581 (2015).
242. Froidure, A., Vandenplas, O., D'Alpaos, V. & Pilette, C. Defects in Plasmacytoid Dendritic Cell Expression of Inducible Costimulator Ligand and IFN-alpha Are Associated in Asthma with Disease Persistence. *American journal of respiratory and critical care medicine* **192**, 392-395 (2015).
243. Pritchard, A.L., *et al.* Innate IFNs and Plasmacytoid Dendritic Cells Constrain Th2 Cytokine Responses to Rhinovirus: A Regulatory Mechanism with Relevance to Asthma. *Journal of immunology* **188**, 5898-5905 (2012).
244. Ghirelli, C., *et al.* Breast Cancer Cell-Derived GM-CSF Licenses Regulatory Th2 Induction by Plasmacytoid Predendritic Cells in Aggressive Disease Subtypes. *Cancer Res* **75**, 2775-2787 (2015).
245. Brennan-Speranza, T.C. & Conigrave, A.D. Osteocalcin: an osteoblast-derived polypeptide hormone that modulates whole body energy metabolism. *Calcified tissue international* **96**, 1-10 (2015).
246. Lee, N.K., *et al.* Endocrine regulation of energy metabolism by the skeleton. *Cell* **130**, 456-469 (2007).
247. Burgers, T.A., *et al.* Mice lacking pten in osteoblasts have improved intramembranous and late endochondral fracture healing. *PloS one* **8**, e63857 (2013).
248. Zhong, Z., *et al.* Wntless functions in mature osteoblasts to regulate bone mass. *Proceedings of the National Academy of Sciences of the United States of America* **109**, E2197-2204 (2012).
249. Qin, C., D'Souza, R. & Feng, J.Q. Dentin matrix protein 1 (DMP1): new and important roles for biomineralization and phosphate homeostasis. *Journal of dental research* **86**, 1134-1141 (2007).
250. Kalajzic, I., *et al.* In vitro and in vivo approaches to study osteocyte biology. *Bone* **54**, 296-306 (2013).
251. Kalajzic, I., *et al.* Dentin matrix protein 1 expression during osteoblastic differentiation, generation of an osteocyte GFP-transgene. *Bone* **35**, 74-82 (2004).
252. Xiao, Z., *et al.* Osteocyte-specific deletion of Fgfr1 suppresses FGF23. *PloS one* **9**, e104154 (2014).
253. Xiong, J., *et al.* Matrix-embedded cells control osteoclast formation. *Nature medicine* **17**, 1235-1241 (2011).
254. Madisen, L., *et al.* A robust and high-throughput Cre reporting and characterization system for the whole mouse brain. *Nature neuroscience* **13**, 133-140 (2010).
255. Zhang, J., *et al.* Generation of an adult smooth muscle cell-targeted Cre recombinase mouse model. *Arteriosclerosis, thrombosis, and vascular biology* **26**, e23-24 (2006).

256. Zhang, M., *et al.* Osteoblast-specific knockout of the insulin-like growth factor (IGF) receptor gene reveals an essential role of IGF signaling in bone matrix mineralization. *The Journal of biological chemistry* **277**, 44005-44012 (2002).
257. Ara, T., *et al.* A role of CXC chemokine ligand 12/stromal cell-derived factor-1/pre-B cell growth stimulating factor and its receptor CXCR4 in fetal and adult T cell development in vivo. *Journal of immunology* **170**, 4649-4655 (2003).
258. Lu, Y., *et al.* DMP1-targeted Cre expression in odontoblasts and osteocytes. *Journal of dental research* **86**, 320-325 (2007).
259. Umans, L., *et al.* Inactivation of Smad5 in endothelial cells and smooth muscle cells demonstrates that Smad5 is required for cardiac homeostasis. *The American journal of pathology* **170**, 1460-1472 (2007).
260. Assinder, S.J., Stanton, J.A. & Prasad, P.D. Transgelin: an actin-binding protein and tumour suppressor. *The international journal of biochemistry & cell biology* **41**, 482-486 (2009).
261. El-Bizri, N., *et al.* SM22alpha-targeted deletion of bone morphogenetic protein receptor 1A in mice impairs cardiac and vascular development, and influences organogenesis. *Development* **135**, 2981-2991 (2008).
262. Eash, K.J., Greenbaum, A.M., Gopalan, P.K. & Link, D.C. CXCR2 and CXCR4 antagonistically regulate neutrophil trafficking from murine bone marrow. *The Journal of clinical investigation* **120**, 2423-2431 (2010).
263. Omatsu, Y., *et al.* The essential functions of adipo-osteogenic progenitors as the hematopoietic stem and progenitor cell niche. *Immunity* **33**, 387-399 (2010).
264. Tokoyoda, K., Egawa, T., Sugiyama, T., Choi, B.I. & Nagasawa, T. Cellular niches controlling B lymphocyte behavior within bone marrow during development. *Immunity* **20**, 707-718 (2004).
265. Sugiyama, T., Kohara, H., Noda, M. & Nagasawa, T. Maintenance of the hematopoietic stem cell pool by CXCL12-CXCR4 chemokine signaling in bone marrow stromal cell niches. *Immunity* **25**, 977-988 (2006).
266. Komori, T. Mouse models for the evaluation of osteocyte functions. *Journal of bone metabolism* **21**, 55-60 (2014).
267. Jung, S., *et al.* Analysis of fractalkine receptor CX(3)CR1 function by targeted deletion and green fluorescent protein reporter gene insertion. *Molecular and cellular biology* **20**, 4106-4114 (2000).
268. Saito, M., *et al.* Diphtheria toxin receptor-mediated conditional and targeted cell ablation in transgenic mice. *Nature biotechnology* **19**, 746-750 (2001).
269. Miyake, Y., *et al.* Critical role of macrophages in the marginal zone in the suppression of immune responses to apoptotic cell-associated antigens. *The Journal of clinical investigation* **117**, 2268-2278 (2007).
270. Richards, M.K., Liu, F., Iwasaki, H., Akashi, K. & Link, D.C. Pivotal role of granulocyte colony-stimulating factor in the development of progenitors in the common myeloid pathway. *Blood* **102**, 3562-3568 (2003).
271. Pillai, M.M., Hayes, B. & Torok-Storb, B. Inducible transgenes under the control of the hCD68 promoter identifies mouse macrophages with a distribution that differs from the F4/80 - and CSF-1R-expressing populations. *Experimental hematology* **37**, 1387-1392 (2009).

272. Christopher, M.J., Rao, M., Liu, F., Woloszynek, J.R. & Link, D.C. Expression of the G-CSF receptor in monocytic cells is sufficient to mediate hematopoietic progenitor mobilization by G-CSF in mice. *The Journal of experimental medicine* **208**, 251-260 (2011).
273. Jung, S., *et al.* In vivo depletion of CD11c⁺ dendritic cells abrogates priming of CD8⁺ T cells by exogenous cell-associated antigens. *Immunity* **17**, 211-220 (2002).
274. Probst, H.C., *et al.* Histological analysis of CD11c-DTR/GFP mice after in vivo depletion of dendritic cells. *Clinical and experimental immunology* **141**, 398-404 (2005).
275. Bar-On, L. & Jung, S. Defining in vivo dendritic cell functions using CD11c-DTR transgenic mice. *Methods in molecular biology* **595**, 429-442 (2010).
276. Bradford, B.M., Sester, D.P., Hume, D.A. & Mabbott, N.A. Defining the anatomical localisation of subsets of the murine mononuclear phagocyte system using integrin alpha X (Itgax, CD11c) and colony stimulating factor 1 receptor (Csf1r, CD115) expression fails to discriminate dendritic cells from macrophages. *Immunobiology* **216**, 1228-1237 (2011).
277. Landsman, L. & Jung, S. Lung macrophages serve as obligatory intermediate between blood monocytes and alveolar macrophages. *J Immunol* **179**, 3488-3494 (2007).
278. Meredith, M.M., *et al.* Expression of the zinc finger transcription factor zDC (Zbtb46, Btbd4) defines the classical dendritic cell lineage. *The Journal of experimental medicine* **209**, 1153-1165 (2012).
279. Satpathy, A.T., *et al.* Zbtb46 expression distinguishes classical dendritic cells and their committed progenitors from other immune lineages. *The Journal of experimental medicine* **209**, 1135-1152 (2012).
280. Levesque, J.P., *et al.* Hematopoietic progenitor cell mobilization results in hypoxia with increased hypoxia-inducible transcription factor-1 alpha and vascular endothelial growth factor A in bone marrow. *Stem cells* **25**, 1954-1965 (2007).
281. Itkin, T., *et al.* Distinct bone marrow blood vessels differentially regulate haematopoiesis. *Nature* **532**, 323-328 (2016).
282. Petri, B., *et al.* Endothelial LSP1 is involved in endothelial dome formation, minimizing vascular permeability changes during neutrophil transmigration in vivo. *Blood* **117**, 942-952 (2011).
283. Kohler, A., *et al.* G-CSF-mediated thrombopoietin release triggers neutrophil motility and mobilization from bone marrow via induction of Cxcr2 ligands. *Blood* **117**, 4349-4357 (2011).
284. Reutershan, J., *et al.* Critical role of endothelial CXCR2 in LPS-induced neutrophil migration into the lung. *The Journal of clinical investigation* **116**, 695-702 (2006).
285. Lei, X., Hossain, M., Qadri, S.M. & Liu, L. Different microvascular permeability responses elicited by the CXC chemokines MIP-2 and KC during leukocyte recruitment: role of LSP1. *Biochemical and biophysical research communications* **423**, 484-489 (2012).
286. Metcalf, D., Robb, L., Dunn, A.R., Mifsud, S. & Di Rago, L. Role of granulocyte-macrophage colony-stimulating factor and granulocyte colony-stimulating factor in the development of an acute neutrophil inflammatory response in mice. *Blood* **88**, 3755-3764 (1996).

287. Wengner, A.M., Pitchford, S.C., Furze, R.C. & Rankin, S.M. The coordinated action of G-CSF and ELR + CXC chemokines in neutrophil mobilization during acute inflammation. *Blood* **111**, 42-49 (2008).
288. Fukuda, S., Broxmeyer, H.E. & Pelus, L.M. Flt3 ligand and the Flt3 receptor regulate hematopoietic cell migration by modulating the SDF-1alpha(CXCL12)/CXCR4 axis. *Blood* **105**, 3117-3126 (2005).
289. Wendel, C., *et al.* CXCR4/CXCL12 participate in extravasation of metastasizing breast cancer cells within the liver in a rat model. *PloS one* **7**, e30046 (2012).
290. Dmitriev, P., *et al.* Dux4 controls migration of mesenchymal stem cells through the Cxcr4-Sdf1 axis. *Oncotarget* **7**, 65090-65108 (2016).
291. Pierini, A., *et al.* Foxp3(+) regulatory T cells maintain the bone marrow microenvironment for B cell lymphopoiesis. *Nature communications* **8**, 15068 (2017).
292. Di Rosa, F. Two Niches in the Bone Marrow: A Hypothesis on Life-long T Cell Memory. *Trends in immunology* **37**, 503-512 (2016).
293. Kalajzic, I., *et al.* Use of type I collagen green fluorescent protein transgenes to identify subpopulations of cells at different stages of the osteoblast lineage. *Journal of Bone and Mineral Research* **17**, 15-25 (2002).